LULEÅ UNIVERSITY OF TECHNOLOGY

2001:328 CIV

MASTER'S THESIS

Concrete Slabs Designed with Finite Element Methods

Modelling Parameters, Crack Analyses and Reinforcement Design

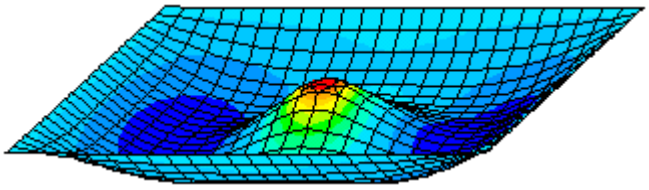

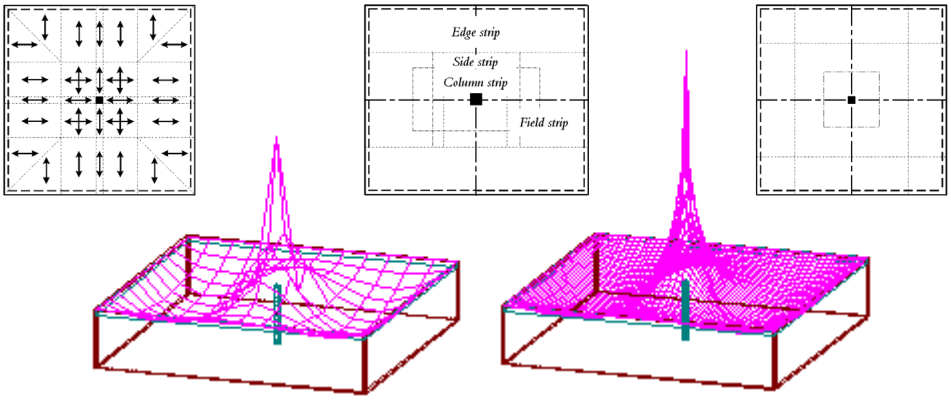

OLA ENOCHSSON and PETER DUFVENBERG

MASTER OF SCIENCE PROGRAMME

Department of Civil and Mining Engineering
Division of Structural Engineering

2001:328 CIV • ISSN: 1402 - 1617 • ISRN: LTU - EX - - 01/328 - - SE

ENOCHSSON/DUFVENBERG Concrete Slabs Designed with Finite Element Methods

LULEÅ
UNIVERSITY
OF TECHNOLOGY

MASTER'S THESIS 2001:328 CIV

Concrete Slabs Designed with Finite Element Methods

Modelling Parameters, Crack Analyses and Reinforcement Design

Ola Enochsson
Peter Dufvenberg

Division of Structural Engineering
Department of Civil and Mining Engineering
Luleå University of Technology
SE - 971 87 Luleå
Sweden

Preface

The present thesis is mainly based on work done between November 2000 and August 2001 at the Division of Structural Engineering, the Department of Civil and Mining Engineering at Luleå University of Technology (LTU). The thesis is performed for SKANSKA IT Solutions in Malmö, Sweden, as a reference material in design of flat slab floors based on a linear elastic FE-analysis, with the emphasis to their FE-software program FEM-Design.

First we want to thank our examiner Prof. Tech Dr Thomas Olofsson for all help with computers, software programs and much more, and also our supervisor Stefan Åberg at SKANSKA IT Solutions for his big patience. Further we want to thank Tech Dr Milan Veljkovic, Ass Prof. Tech Dr Jan-Erik Jonasson and Tech Dr Robert Tano.

We want to give a special gratitude to Designer Mr Dick Lundell SKANSKA Teknik Malmö for his contribution in consideration of practical design and the head of the Division Prof. Tech Dr Lennart Elfgren for his help with the historical background of plate theory and the belonging references.

Furthermore we want to thank the head of SKANSKA IT Solutions Paul Rehn and his staff and all the programmers and Hungarian authorities in FEM for their engagement.

Finally we want to thank our families who have put up with us spending all of our time this Christmas and summer with the work of the thesis.

LULEÅ in October 2001

Ola Enochsson and Peter Dufvenberg

Abstract

Powerful numerical calculation methods like the Finite Element Method (FEM) are not recommended in design handbooks for design of slabs. In contrary, its distribution of reinforcement is considered to be unsuitable for practical use, see e.g. Hillerborg *et al (1990), (1996)*. Most FE-programs are also more adapted for analyses than for design.

SKANSKA IT Solutions in Malmö, Sweden, has developed a FE-based design program called FEM-Design. The program handles e.g. FE-analyses and designs of frames, trusses, beams, shear walls and plates.

The thesis main objectives were to:

- Propose a method to deal with the in FE-analyses common problem of extreme-value of moments in centre of interior columns/walls in flat slab floors.
- Verify FEM-Design's crack analysis and calculated effects of actions and required reinforcement.
- Propose a practical method to distribute the reinforcement quantities.

Simple structures of flat slab floors are used for the FE-analyses. Anchor- or joint lengths and required top or anchor reinforcement in corners are not considered in reinforcement design.

Chapter 2 Modelling parameters - The FE-analyses show that the mesh density and the modelling of the column stiffness mainly affects the size of the support moments, whereas the field moments is almost independent of all modelling parameters. FEM-Design's automatically generated mesh gave good results with respect to the size of the support moments. However, the result of moment distribution or actually the reinforcement distribution can be improved by distributing the column stiffness over one plate element. The multi spring concept is also suggested for interior walls wider than 0.2 m.

Chapter 3 Crack analyses – FEM-Design's iterative nonlinear crack analysis is found to be adequate for design, despite that the crack propagation differs quite much in comparison with Abaqus/Explicit smeared crack approach. FEM-Design's load-displacement curve shows better agreement with an experimental test, McNiece *(1978)*, than Abaqus/Explicit. The difference depends on the implemented crack theory i.e. when a crack is considered to be a crack.

Chapter 4 Design of reinforcement – The traditionally design methods, the strip method and the yield line theory, distribute moments with the same size in a certain area, whereas FEM-Design calculates moments according to the theory of elasticity at each node. This means that FEM-Design's design moments or the required reinforcement have to be chosen at certain points and redistributed by a design method.

Chapter 5 FE-based analyses and design – A FE-based design method is developed with respect to the capabilities of FEM-Design and the FE-analyses performed with the traditionally distributed reinforcement from chapter 4. Comparisons between the three methods show that the FE-based reinforcement design method (FED) distributes less total amount of reinforcement than the two traditional methods with respect of both bending- and final design.

Chapter 6 Conclusions – FE-analyses can be used to get a practical reinforcement design in concrete slabs in contradiction to Hillerborg's statement *et al (1990), (1996)* – if the reinforcement like other methods are redistributed in appropriate areas/strips.

FEM-Design has been tested against Abaqus with respect to analyses and crack propagation, and compared to hand calculation methods with respect to design. For all cases tested, FEM-Design has proven to give reliable analyses and designs. Actually, very few arguments arise against the use of FE-based design, especially since FEM-Design's plate module is found to be a very user-friendly design tool. However, the following improvements would make the program even better:

- The multi spring concept for interior columns/walls – *gives a more realistic response of support moments at designs*.
- A more available and clear input check option – *gives a much faster control and more reliable calculations*.
- Distribution method(s) for reinforcement – *enables a much faster and more exactly determination and application of user defined reinforcement*.

The distribution method (FED), proposed in chapter 5 is suggested as one suitable method to implement, because it combines FE-theory with theories behind traditional design methods.

Sammanfattning

Kraftfulla numeriska beräkningsmetoder som Finita Element Metoden (FEM), rekommenderas aldrig för dimensionering av plattor i handböcker. Tvärtom, anses dess armeringsfördelningen vara direkt olämplig för praktiskt bruk, se t.ex. Hillerborg *et al (1990), (1996)*. De flesta femprogram är dessutom mer avsedda för rena analyser, istället för dimensionering.

SKANSKA IT solutions i Malmö har utvecklat det fembaserade dimensioneringsprogrammet FEM-Design. Programmet hanterar t.ex. fem-analyser och dimensionering av ramar, fackverk, balkar, skjuvväggar och plattor.

Rapportens huvudsakliga mål var att:

- Föreslå en metod att hantera det vanligt förekommande extremvärdes-problemet för moment i centrum av innerpelare/väggar i pelardäck.
- Verifiera FEM-Designs sprickanalys och beräkning av lasteffekter och erforderlig (dimensionerande) armering.
- Föreslå en praktisk metod som fördelar armeringsmängder.

Enkla pelardäcksmodeller är använda vid femanalyserna. Förankrings- eller skarvlängder är inte beaktade vid armeringsdimensioneringen, ej heller erforderlig mängd överkants- eller förankringsarmering i hörnen.

Kapitel 2 Modelleringsparametrar - FE-analyserna visar att nättätheten och modelleringen av pelarstyvheten huvudsakligen påverkar storleken på stödmomenten, medan fältmomenten visade sig vara i det närmaste oberoende av samtliga modelleringsparametrar. FEM-Designs automatiskt genererade nät har visat sig ge goda resultat i avseende på stödmomentets storlek. Emellertid kan moment- och armeringsfördelningen förbättras genom att pelarstyvheten fördelas med ett plattelement, istället för som nu appliceras i en nod. En fördelad styvhet, eller det s.k. flerfjäderskonceptet föreslås även för innerväggar grövre än 0.2 m.

Kapitel 3 Sprickanalyser – FEM-Designs iterativa icke linjära sprickanalys anses vara adekvat ifråga om dimensionering, trots att dess uppsprickning skiljer sig relativt mycket i jämförelse med Abaqus/Explicits sprickmodell "smeared cracks". Detta p.g.a. att FEM-Designs last-förskjutningskurva visar bättre överensstämmelse med ett experimentellt försök, McNiece *(1978)*, än Abaqus/Explicit. Skillnaden anses bero på olika sprickteorier d.v.s. när en spricka betraktas som en spricka.

Kapitel 4 Dimensionering av armering – De traditionella dimensioneringsmetoderna, strimlemetoden och brottlinjeteori, fördelar moment med konstant storlek i ett och samma område, medan FEM-Design beräknar moment enligt elasticitetsteori för varje nod. Detta innebär att dimensionerande moment, eller erforderlig armering måste väljas i särskilt utvalda punkter och omfördelas enligt en passande dimensioneringsmetod.

Kapitel 5 FE-baserade analyser och dimensionering – En FE-baserad dimensioneringsmetod är utvecklad med hänsyn till möjligheterna i FEM-Design och de FE-analyser som utfördes med den traditionellt fördelade armeringen i kapitel 4. Jämförelser mellan de tre metoderna visar att den FE-baserade metoden (FED) fördelar mindre mängd armering än de två traditionella metoderna både med hänsyn till böjning och slutlig dimensionering.

Kapitel 6 Slutsatser – FE-analyser kan användas för att erhålla en praktisk armeringsdimensionering i betongplattor i motsats till Hillerborgs uttalande *et al (1990), (1996)* – ifall armeringsmängderna, likasom för andra metoder, omfördelas till lämpliga områden/strimlor.

FEM-Design har testats gentemot Abaqus i avseende på analyser och sprick propagering. I samtliga testade fall, har FEM-Design visats sig ge pålitliga analyser och dimensionering. Faktum är att det framkommer väldigt få argument emot användandet av FE-baserad dimensionering, speciellt sedan FEM-Designs plattmodul visat sig vara ett mycket användarvänligt dimensioneringsverktyg. Dock, kan följande implementeringar göra FEM-Design ännu bättre:

- Flerfjäderkoncept (fördelad styvhet) för innerpelare/väggar – *ger en mer realistisk respons av stödmoment vid dimensionering.*
- En mer tillgänglig och överskådlig kontrollfunktion av indata – *ger en betydligt snabbare kontroll, samt en mer tillförlitlig beräkning.*
- Fördelningsmetod(er) för armering – *tillåter en mycket snabbare samt en mer exakt bestämning och applicering av användardefinierad armering.*

Fördelningsmetoden (FED), föreslagen i kapitel 5, betraktas som en lämplig metod att implementera, eftersom den kombinerar FE-teori med teorier bakom traditionella dimensioneringsmetoder.

Table of Contents

Notations and Abbreviations

Explanations in the text of notations and abbreviations in direct conjunction to their appearance have preference to what is treated here.

Roman upper case letters

A	Area, [m^2]
A_s	Area reinforcement steel, [m^2/m]
E	Youngs modulus, [Pa]
G_f	Fracture energy, [Nm/m^2]
H	Height, [m]
L	Length, [m]
M_x	Bending moment in x-direction, [Nm]
M_y	Bending moment in y-direction, [Nm]
M_f	Bending field moment, [Nm]
M_s	Bending support moment, [Nm]
P	Point load, [N]
P_c	Column load, [N]
V	Shear force, [N]

Roman lower case letters

b	Width, [m]
c	Length to zero shear, [m]
	Length/width of strip, [m]
d	Effective height of cross-section, [m]
f	Strength value, [Pa]
k	Structural stiffness, [N/m]

l	Length, [m]
m	Distributed bending moment, [Nm/m]
$\overline{m}$	Relative moment, [-]
$\overline{m}_{bal}$	Balanced relative moment, [-]
n	Eccentricity factor, [-]
q	Distributed load, [N/m^2]
s	Space between reinforcement bars, [m]
u	Displacement, [m]
	Punching perimeter, [m]
w	Deflection, [m]

Greek lower case letters

α	Control parameter, [-]
β	Moment distribution factor, [-]
ε	Strain, [-]
ϕ	Diameter [m]
ν	Poissons ratio, [-]
ω	Mechanical reinforcement ratio, [-]
ω_{bal}	Balanced mechanical reinforcement ratio, [-]

Sub- or superscripts

c	Compression, concrete
d	Design value
f	Field
k	Characteristic
s	Steel, support
t	Tension
u	Ultimate limit
y	Yield limit

Abbreviations

DOF	Degrees of Freedom
FE(M)	Finite Element (Method)
FD	FEM-Design
SM	Strip Method
YL	Yield Line Theory

1 Introduction

1.1 Background and identification of problems

Design calculations in building projects are guided by design rules based on hand calculation methods. Today, when time for projecting a building gets shorter, there is a need for general and fast computer aided designing tools.

There is a large amount of design programs available on the market today. They are all based on different theories and methods, some of the programs are based on the Finite Element Method (FEM). Most FEM-programs are complicated and demands time and skilled users to perform a correct FE-analysis i.e. they are more of an analytical tool than a tool to be used in design.

Preprocessing is crucial for the use of FE-analyses. Unfortunately, there are often translation problems between modern CAD and FEM-programs, which means that modelling and definitions of input data becomes time consuming. Linear elastic FE-analyses can be deceiving if not the modelling is correct in consideration of e.g. element types, mesh dense, stiffness of supports and material behaviour and give unreasonable results of for example internal forces.

SKANSKA IT Solution in Malmö Sweden has developed the design program FEM-Design in order to remedy some of these problems. FEM-Design is a user friendly FEM-program, built on a CAD-program with pull down menus, a wizard for easy preprocessing, dialog boxes to create load cases and load combinations according to several European design codes. The program handle e.g. FE-analyses of frames, trusses, beams, shear walls and plates.

Purchasers and users of FEM-Design have asked for some sort of verification of the calculations of internal forces, crack propagation and particularly, the influence of the modelled mesh on the size of the support moment at interior columns in flat slab floors.

In design handbooks it is often told that a consistent and correct calculation according to linear elastic theory for the most slabs in principle is impossible. Of course, it is possible to use a numerical method like FEM, but unrealistic assumptions have to be made such as isotropic or orthotropic material behaviour of the plate. Even if the calculations should succeeds the results will led to such an unpractical distribution of reinforcement that the result is untimely for practical use. Therefore, design of reinforcement based on FE-analyses is not recommended to be used, see e.g. Hillerborg *et al (1990)* or Hillerborg *(1996)*.

1.2 Aim and scope

The main aims of this thesis are to verify calculations performed by the design program FEM-Design, develop a concept to apply the stiffness of an interior column to a flat slab floor and to propose a practical design method for reinforcement. The following main tasks are set up:

- Investigate the influence of the modelling mainly on the size of the support moments at interior columns, but also on the size of the field moments in flat slab floors.
- Determinate the best way to apply an interior column to the model with respect of realistic response in consideration of the distribution of moments and displacements.
- Verify FEM-Design's calculation of internal forces and crack propagation.
- Comparisons of reinforcement design between FEM-Design and traditionally design methods.
- Derive and establish a design method with respect of today available results in FEM-Design.
- Demonstrate the possibilities and power of FE-based design.

The work is concentrated on the plate module of FEM-Design and simple structures are used for the analyses. Anchors or joints lengths are not considered in design of reinforcement, nor required top or anchor reinforcement in corners.

1.3 Content

In *Chapter* 2, two base models are used to analyse the column stiffness i.e. applied at one node and at several nodes. The FE-results are discussed in terms of mesh density, element types, column widths and modelling of column stiffness. A modelling concept is discussed in order to get more realistic distribution of moments and displacements in models with interior columns i.e. in flat slab floors.

In *Chapter* 3, an experiment by McNeice (1978) is compared with results from non-linear FE-analyses performed by ABAQUS/Explicit and FEM-Design.

In *Chapter* 4, a flat slab floor is designed according to the yield line theory and the strip method. The results of the moment distribution are compared with FEM-design's distribution of moments.

In *Chapter* 5, the traditionally designed reinforcement from chapter 4 are analysed using FEM-Design with respect to crack widths, punching and deformations. A design method for reinforcement is derived and substantiated with the results from the FE-analyses and the capability of FEM-Design. The method redistributes the reinforcement areas in appropriate strips considering crack widths, punching and deformations.

Finally, in *Chapter* 6, general conclusions and suggestions for further research are made.

1.4 Briefly historical background of plate theory

The theory of elasticity for plates was developed by Navier *(1785-1836)*, Gustave Robert Kirchoff *(1824-1887)* and Maurice Lévy *(1838-1910)*, see e.g. Timoshenko *(1953)*. A classic textbook on elastic plates is Stephen P.Timoshenko and S. Woinowsky-Krieger *(1959)*.

The theory of plasticity was applied to plates by K W Johansson in Denmark *(1943)*. He developed the yield line theory, which is an upper bound kinematic method, see also Jones and Wood *(1967)*. A lower bound equilibrium method, the strip method, was developed by Arne Hillerborg in Sweden *(1956, 1969, 1996)*.

The Swedish standard method for design of slabs was developed by Hillerborg *et al (1957, 1963)*. Punching has been studied by Henrik Nylander and Sven Kinnunen *(1959, 1960, 1963)*. Slabs on soil have been studied by Anders Losberg *(1960)*.

Classical Swedish handbook chapters on concrete slabs are e.g. Bengtsson *et al (1969)* and Hillerborg *et al (1990)*.

2 Modelling parameters

2.1 Introduction

A major problem during all design calculations of continuous slabs based on the FE-theory is to determine the size of the representative maximum support moment in the area of an interior column or an interior wall. In this thesis, only the influence of an interior column is considered.

It is well known that the size of the intermediate support moment among other things depends on the modelling parameters, such as:

- Mesh density.
- Element type.
- Column width.
- Modelling of the column stiffness.

A concept to reduce the extreme value of the support moment at the column centre is discussed in terms of a Multi Spring Concept.

2.2 Methods

Two principle base models are used, based on the modelling of the column stiffness:

1. Applied at a single node.
2. Distributed over several nodes.

The first type is modelled with different element types, varying element lengths and column widths, see *Figure* 2.3 and *Table* 2.2.

The second type is modelled with varying column widths and with the stiffness of the column applied at varying number of nodes, see *Figure* 2.4 and *Table* 2.3.

All models are loaded with a uniformly distributed load of the same size. The stresses σ_x, moments M_x and the displacement u_z at the same node position along a line in x-direction are tabulated. The results of the moment distribution are plotted as functions of the distance from the column centre, towards the edge of the slab. The plotted graphs are then compared and the effects of each type of modelling are discussed. In addition, the results from FEM-Design and Abaqus are compared, whenever it is possible.

2.3 Modelling principles

2.3.1 General

The base model is composed of a symmetrical continuous concrete slab with a thickness of $t = 0.2\ m$. The model is freely supported along its all four edges by walls with the thickness $b_W = 0.15\ m$, and in centre by a single quadratic column with the cross-section $b_C \times b_C$, see e.g. *Figure* 2.3. Both the walls and the single column have the height $H = 2.5\ m$. The slab is loaded with a constant distributed load $q = 9\ kN/m^2$.

Young's Modulus, E [GPa]	**Poisson's ratio, ν**	**Tensile strength, f_{ctk} [MPa]**	**Compressive strength, f_{cck} [MPa]**
30	0.2	1.6	21.5

Table 2.1 Material characteristics.

The Abaqus models are preprocessed by FEMGV, exported as an Abaqus input file and then analysed and postprocessed by Abaqus/Standard. The FEM-Design models are easily preprocessed, analysed and postprocessed in the same interface.

Model no.	Element types in Abaqus	Element length, L_{el} [m]	Column width, b_c [m]	Column stiffness applied at no. of nodes	No. of elements along the slab sides
1	Shell	1.00	0.20	1	12
2	Shell	0.50	0.20	1	24
3	Shell	0.10	0.20	1	120
4	Solid	1.00	0.20	1	12
5	Solid	0.50	0.20	1	24
6	Shell	0.50	0.40	1	24
7	Shell	0.50	0.60	1	24

Table 2.2 The modelling parameters in Abaqus for the different models when the column stiffness is applied at one node.

Model no.	Element types in Abaqus	Element length, L_{el} [m]	Column width, b_c [m]	No. of elements to model the column	No. of nodes with applied column stiffness	No. of elements along the slab sides
8	Shell	0.50	0.20	1	8	24
9	Shell	0.50	0.40	1	8	24
10	Shell	0.50	0.60	1	8	24
11	Shell	0.50	0.20	4	21	24
12	Shell	0.50	0.40	4	21	24
13	Shell	0.50	0.60	4	21	24
14	Shell	0.50	0.20	9	40	24
15	Shell	0.50	0.40	9	40	24
16	Shell	0.50	0.60	9	40	24
17	Solid	0.50	0.20	1	8	24
18	Solid	0.50	0.40	1	8	24
19	Solid	0.50	0.60	1	8	24

Table 2.3 The modelling parameters in Abaqus for the different models when the column stiffness is distributed over several nodes.

Model no.	Element length, L_{el} [m]	Column width, b_c [m]	Column stiffness applied at no. of nodes
1	1.00	0.20	1
2	0.50	0.20	1
20	0.25	0.20	1
6	0.50	0.40	1
7	0.50	0.60	1
21	1.68 (auto)	0.20	1
22	1.68 (auto)	0.40	1
23	1.68 (auto)	0.60	1
24	Sparse mesh	0.20	8
25	Sparse mesh	0.40	8
26	Sparse mesh	0.60	8

Table 2.4 The modelling parameters in FEM-Design for the different models.

The concept of structural stiffness

The total stiffness of the walls or the column is calculated according to the generally and familiar definition of the spring constant *k*

$$F = k \cdot \Delta L \qquad 2.1$$

This constant *k* represents the force *F* required to produce a unit deflection, see *Figure* 2.1. Therefore, for an axially loaded specimen of length *L* and constant cross section area *A*, the stiffness can be formulated as

$$k = \frac{AE}{L} \qquad 2.2$$

where k is the stiffness constant [N/m]
A is the total area of the cross section [m^2]
E is the Young's modulus [Pa]
L is the height H of the wall or the column [m]

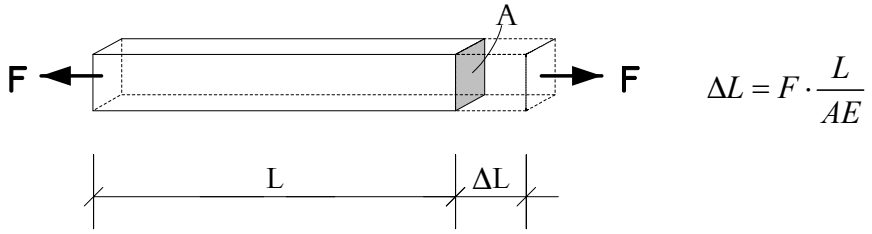

Figure 2.1 The concept of structural stiffness.

The modelling of the walls stiffness

The total stiffness of the wall has to be divided into the so-called node part of the stiffness, when a stiffness have to be prescribed to every node in each element along the wall side. Therefore, when the numbers of elements are symmetrically modelled along the slab sides, *Equation* 2.2 can be reformulated as

$$k_w = \frac{AE}{H(n-1)} \qquad 2.3$$

where n is the number of nodes along the slab side with applied wall stiffness.

The wall stiffness for the Abaqus models are given in *Table* 2.5 and the number of modelled elements are found in *Table* 2.2 and *Table* 2.3.

Model number	**Node part of the wall stiffness, k_w [MN/m]**
1,4	900
2, 5, 6, 7, 8, 9, 10, 11, 12, 13, 14, 15, 16, 17, 18 and 19	450
3	90

Table 2.5 Wall stiffness for the Abaqus models.

The element types

Four different element types are used to model the mesh in the Abaqus models. Spring elements are used to model the stiffness of the walls and the columns, see *Figure* 2.2. The element types are chosen with respect to the two types of plate elements used in FEM-Design i.e. corresponding to a eight-node quadratic plate element and a six-node triangular plate element.

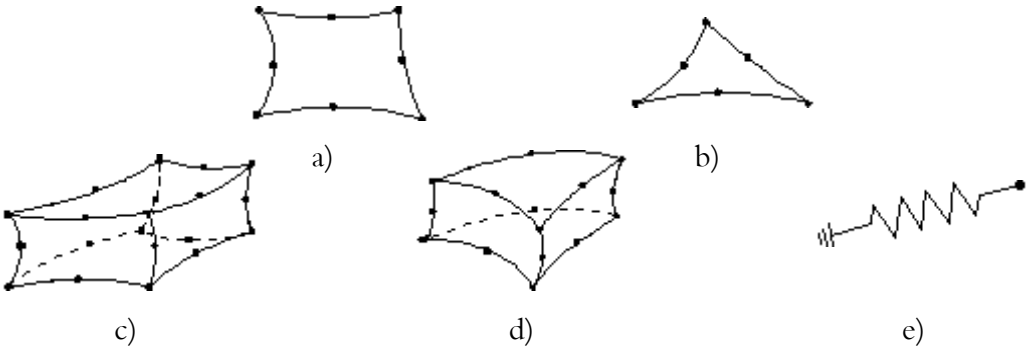

Figure 2.2 *The elements used in Abaqus*. 3D Shell Elements: *a) 8-node quadratic shell element with 5 dofs/node (S8R), b) 6-node triangular shell element with 5 dofs/node (STRI65).* 3D Solid Elements: *c) 20-node quadratic brick element with 3 dofs/node (C3D20), d) 15-node quadratic triangular prism element with 3 dofs/node (C3D15).* Spring Element: *e) Spring element between a node and ground with 6 possible dofs (SPRING1).*

2.3.2 Column stiffness applied at a single node

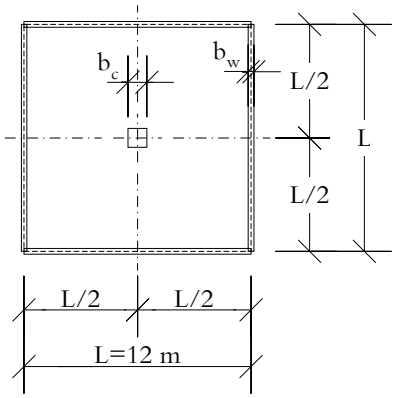

Figure 2.3 *The principle geometry of the model when the column stiffness is applied at one node.*

In this case, the models analysed by both Abaqus and FEM-Design are equal, apart from the fact that shell elements or solid elements are used in Abaqus, whereas plate elements are used in FEM-Design.

In Abaqus, the column stiffness is modelled as spring elements applied at one node. The stiffness is calculated according to *Equation* 2.2 and the values are tabulated in *Table* 2.6. In FEM-Design the column stiffness is modelled with the built in definition tool. The tool draws a visible column with the chosen cross section and material characteristics, but the stiffness is in principle modelled by the program in the same way as described above for Abaqus.

Column width, b_c [m]	**Column stiffness, k_c [MN/m]**
0.20	480
0.40	1920
0.60	4320

Table 2.6 The column stiffness when it is applied at one node in Abaqus.

2.3.3 Column stiffness distributed over several nodes

The FE-mesh in FEM-Design is generated by a automatic mesh-generator non-symmetrically. In Abaqus the mesh is modelled by hand i.e. the mesh of FEM-Design and Abaqus is not completely equal.

The model in Abaqus is divided into two different areas, area *A* and *B*, see *Figure* 2.4. Area *A* have the same element length $L_{el} = 0.5\ m$, in all the models in order to get comparable results between the different models at the same node position. In the centre of area B the column is modelled with both different column size and number of elements. The remaining area of *B* is a so-called level out area, to fulfil the mesh compatibility between area *A* and *B*, according to the following principles:

1. Two adjacent elements have nearly the same size.
2. Triangular elements are close to an equilateral-triangle.

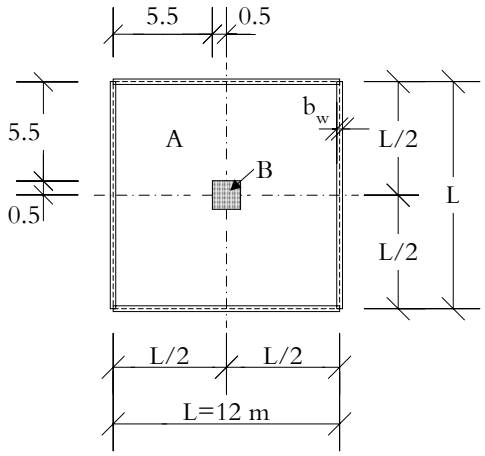

Figure 2.4 *The principle geometry of the model when the column stiffness is applied at varying number of nodes.*

Figures 2.5-2.7 shows the set up of the elements in area *B*. The first figure, *Figure* 2.5 illustrate the mesh when the column stiffness is based on the column widths 0.2 *m*, 0.4 *m* and 0.6 *m*, using only one eight-node element. The applied node part of the column stiffness is symbolically marked in one of the figures for each figure. The stiffness is given in *Table* 2.7.

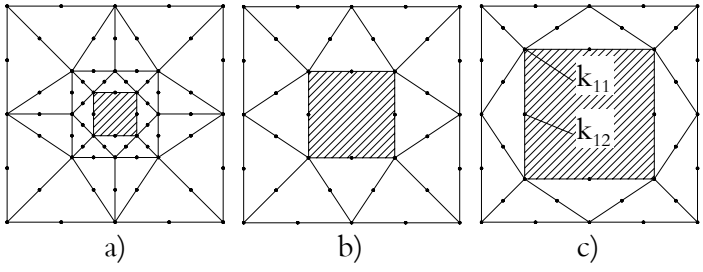

Figure 2.5 *The modelling of area B when <u>one</u> eight-node element is used to model the column stiffness, for the column width: a) b_c = 0.2 m, b) b_c = 0.4 m and c) b_c = 0.6 m.*

Figure 2.6 illustrates the mesh when four eight-node elements are used. The applied stiffness is given in *Table* 2.8.

The last figure, *Figure* 2.7 shows the mesh when nine eight-node elements are used. The applied stiffness is given in *Table* 2.9.

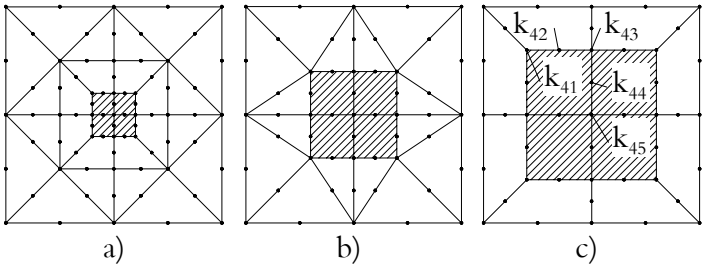

Figure 2.6 *The modelling of area B when four eight-node element is used to model the column stiffness, for the column width: a) b_c = 0.2 m, b) b_c = 0.4 m and c) b_c = 0.6 m.*

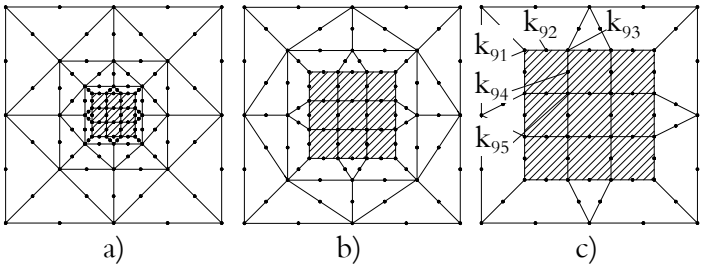

Figure 2.7 *The modelling of area B when nine eight-node element is used to model the column stiffness, for the column width: a) b_c = 0.2 m, b) b_c = 0.4 m and c) b_c = 0.6 m.*

Column stiffness

In Abaqus the column stiffness is modelled with spring elements as for the previous models, and is applied at varying number of nodes.

In FEM-Design the column stiffness is modelled in the same way as described in *Section* 2.3.2 with the built in definition tool, but is instead applied as several columns with varying areas of quadratic cross sections. The column's total area of the cross section is divided into a number of columns, which corresponds to the respectively Abaqus model.

In the Abaqus models the node part of the column stiffness is calculated according to

$$k_{ci} = C_i \frac{k_c}{n} \tag{2.4}$$

where k_{ci} is the node part of the total column stiffness, k_c [N/m].
C_i is a factor depending on the node part of the total element stiffness i.e. of the total element area.
k_c is the total column stiffness [N/m].
n is the number of elements used to model the column.
i is a index where the first number depends on the number of elements used to model the column and the second number is a number of order.

And for the FEM-Design models the corresponding node part of the total cross section area is calculated as

$$A_{ci} = C_i \frac{A_c}{n} \tag{2.5}$$

where A_{ci} is the node part of the column's total cross section area, A_c [m^2].
C_i is a factor depending on the node part of the column's total cross section area.
A_c is the column's total cross section area [m^2].
n is the number of elements used to model the column.
i is a index where the first number depends on the number of elements used to model the column and the second number is a number of order.

Column width, b_c [m]	Index, i	Node factor, C_i	Column stiffness applied in Abaqus, k_{ci} [MN/m]	Column area applied in FEM-Design, A_{ci} [m^2]
0.2	**11**	1/12	40	1/300
	12	1/6	80	2/300
0.4	**11**	1/12	160	4/300
	12	1/6	320	8/300
0.6	**11**	1/12	360	9/300
	12	1/6	720	18/300

Table 2.7 The column stiffness when the column is modelled with one element i.e. divided and applied at eight nodes.

Column width, b_c [m]	Index, i	Node factor, C_i	Column stiffness applied in Abaqus, k_{ci} [MN/m]	Column area applied in FEM-Design, A_{ci} [m^2]
0.2	**41**	1/12	10	-
	42	1/6	20	-
	43	1/6	20	-
	44	1/3	40	-
	45	1/3	40	-
0.4	**41**	1/12	40	-
	42	1/6	80	-
	43	1/6	80	-
	44	1/3	160	-
	45	1/3	160	-
0.6	**41**	1/12	90	-
	42	1/6	180	-
	43	1/6	180	-
	44	1/3	360	-
	45	1/3	360	-

Table 2.8 The column stiffness when the column is modelled with four elements i.e. divided and applied at twenty-one nodes.

Column width, b_c [m]	Index, i	Node factor, C_i	Column stiffness applied in Abaqus, k_{ci} [MN/m]	Column area applied in FEM-Design, A_{ci} [m^2]
0.2	**91**	1/12	40/9	-
	92	1/6	80/9	-
	93	1/6	80/9	-
	94	1/3	160/9	-
	95	1/3	160/9	-
0.4	**91**	1/12	160/9	-
	92	1/6	320/9	-
	93	1/6	320/9	-
	94	1/3	640/9	-
	95	1/3	640/9	-
0.6	**91**	1/12	40	-
	92	1/6	80	-
	93	1/6	80	-
	94	1/3	160	-
	95	1/3	160	-

Table 2.9 The column stiffness when the column is modelled with nine elements i.e. divided and applied at forty nodes.

Control of the distributed column stiffness

A control of the chosen distribution of the column stiffness is performed with a model existing of spring elements applied at every node of a shell element. The model is statically analysed with a continuous distributed load, $q = 1$ N/m^2.
The controlled size of the displacement u_{z1} and u_{z2}, which shall be equal in this case, shows a very small difference due to the numerics, see *Figure* 2.8.

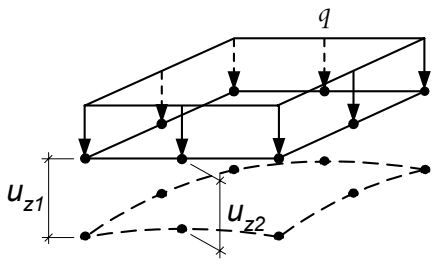

$k_{c1} = 40$ MN/m
$k_{c2} = 80$ MN/m

$\Delta u_z = u_{z2} - u_{z1} = 1{,}5 \cdot 10^{-12} \approx 0$ m

Figure 2.8 The model of the distributed column stiffness.

2.4 Results of the FE-analyses

The modelling dependencies are analysed from a total of 19 Abaqus models and 11 FEM-Design models. The results of the analyses are presented in this section by graphs and the corresponding tables can be found in *Appendix* A.

2.4.1 Mesh density

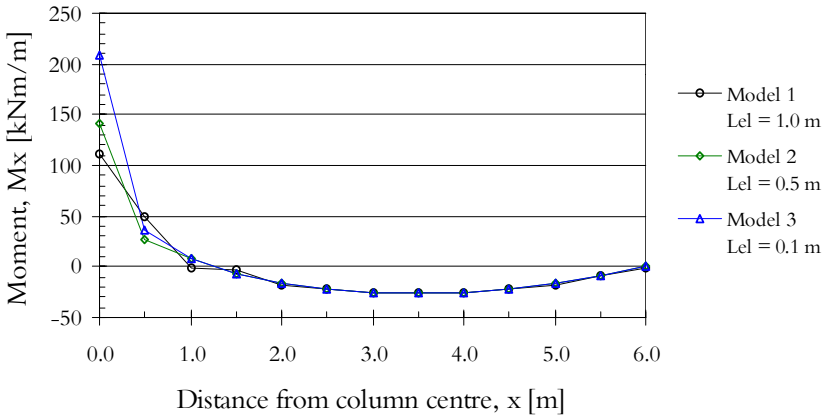

Figure 2.9 The distribution of moments M_x in the x-direction, for different mesh densities in Abaqus.

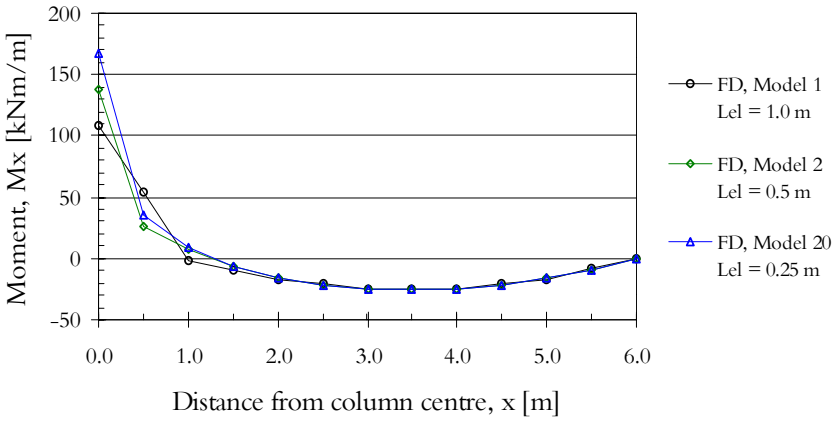

Figure 2.10 The distribution of moments M_x in the x-direction, for different mesh densities in FEM-Design.

2.4.2 Element type

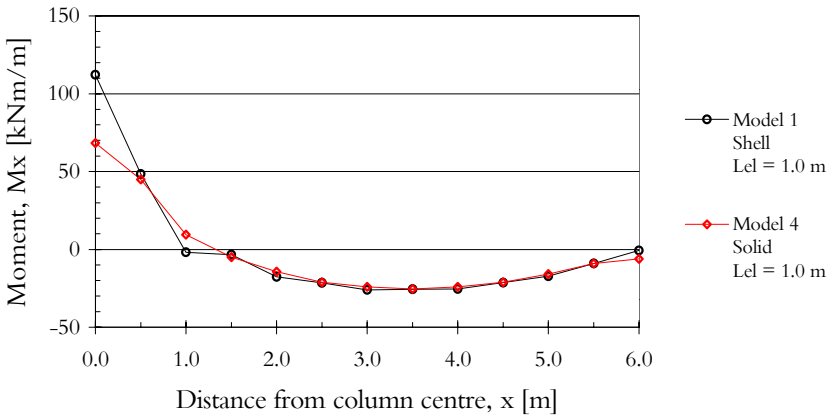

Figure 2.11 The distribution of moments M_x in the x-direction, for different element types in Abaqus, L_{el} = 1.0 m.

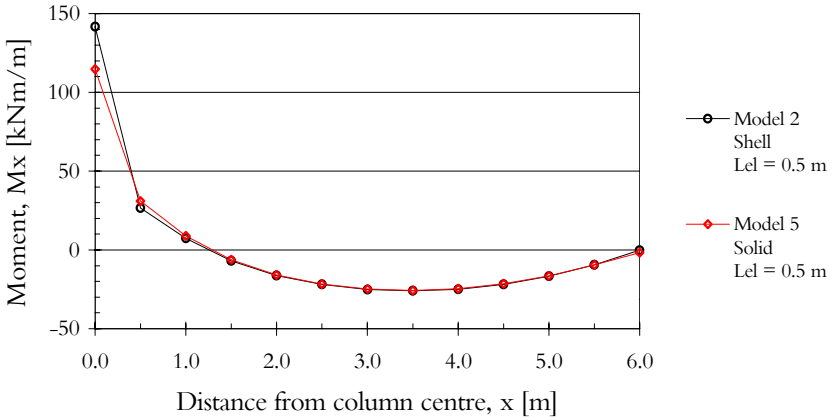

Figure 2.12 The distribution of moments M_x in the x-direction, for different element types in Abaqus, L_{el} = 0.5 m.

2.4.3 Column width

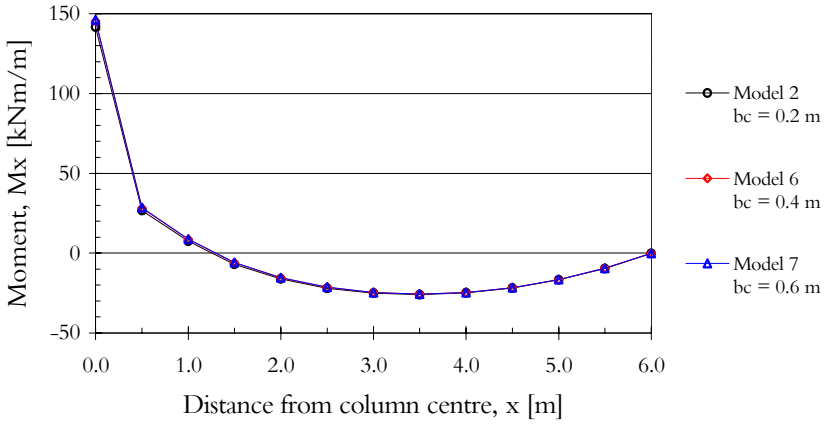

Figure 2.13 The distribution of moments M_x in the x-direction, for different column widths in Abaqus. The column stiffness is applied at 1 node.

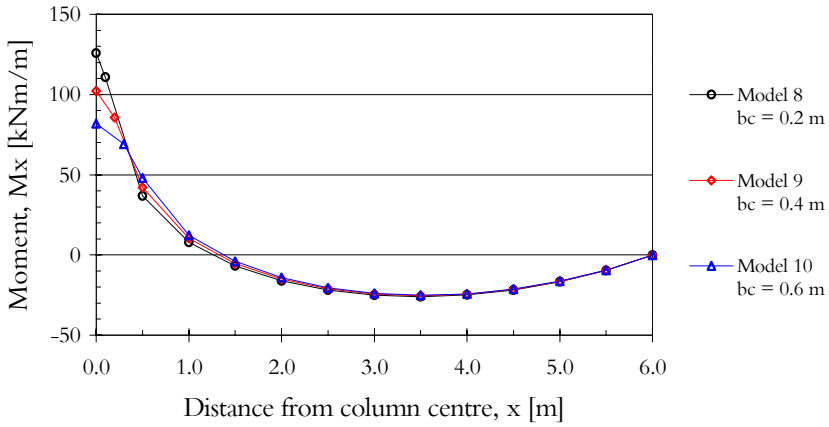

Figure 2.14 The distribution of moments M_x in the x-direction, for different column widths in Abaqus. The column stiffness is applied at 8 nodes.

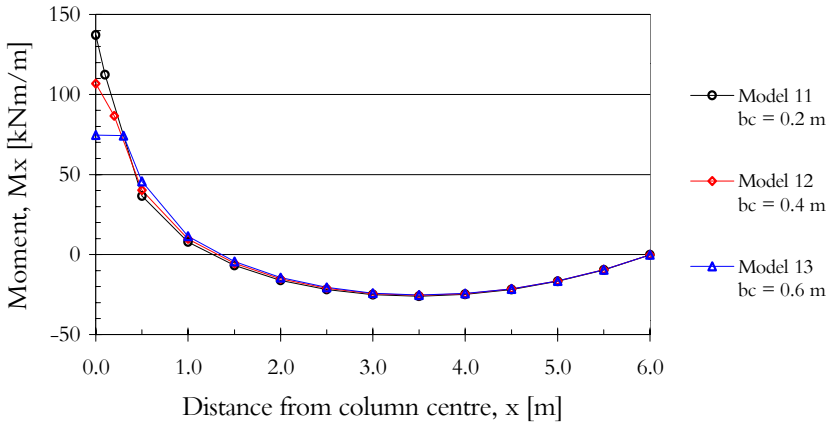

Figure 2.15 The distribution of moments M_x in the x-direction, for different column widths in Abaqus. The column stiffness is applied at 21 nodes.

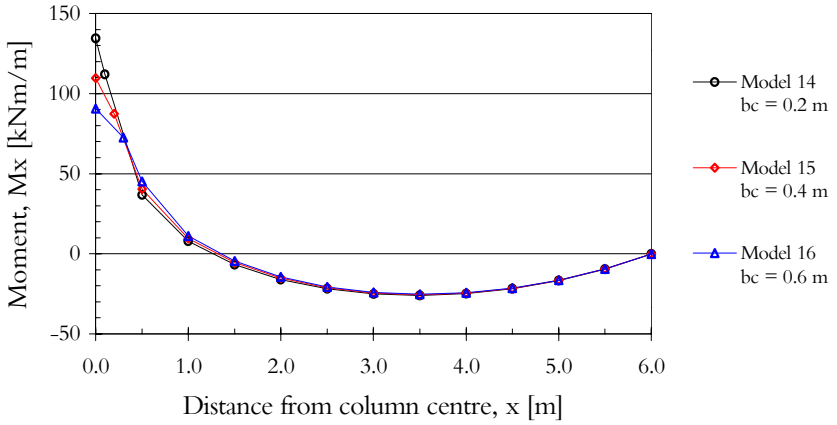

Figure 2.16 The distribution of moments M_x in the x-direction, for different column widths in Abaqus. The column stiffness is applied at 40 nodes.

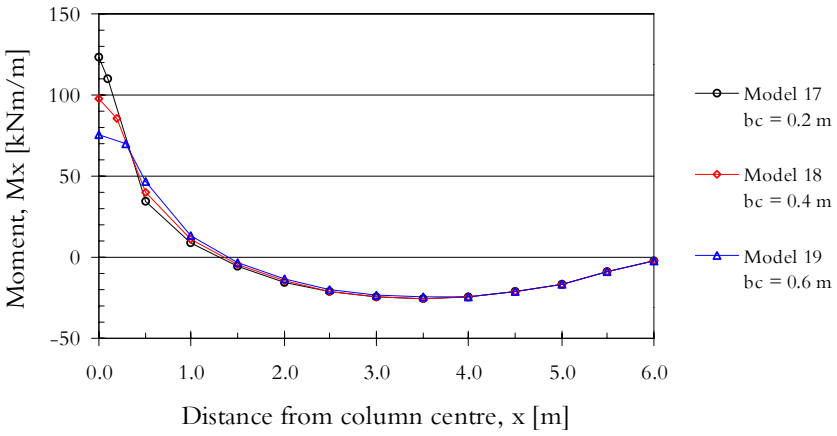

Figure 2.17 The distribution of moments M_x in the x-direction, for different column widths in Abaqus. The column stiffness is applied at 8 nodes and the element type is solid.

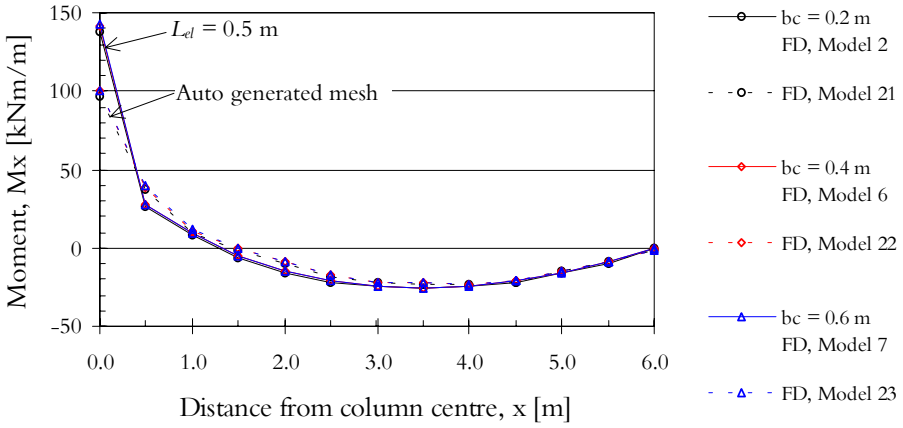

Figure 2.18 The distribution of moments M_x in the x-direction, for different column widths in FEM-Design. The column stiffness is applied at 1 node and the averaged element lenght is 0.5 m chosen automatically by the program.

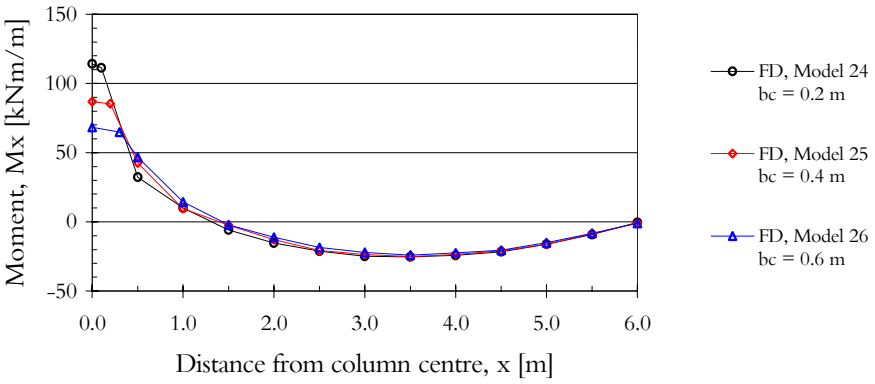

Figure 2.19 *The distribution of moments M_x in the x-direction, for different column widths in FEM-Design. The column stiffness is applied at 8 nodes and the mesh is automatically generetated as sparse as possible outwards from the column elements.*

2.4.4 Modelling of the column stiffness

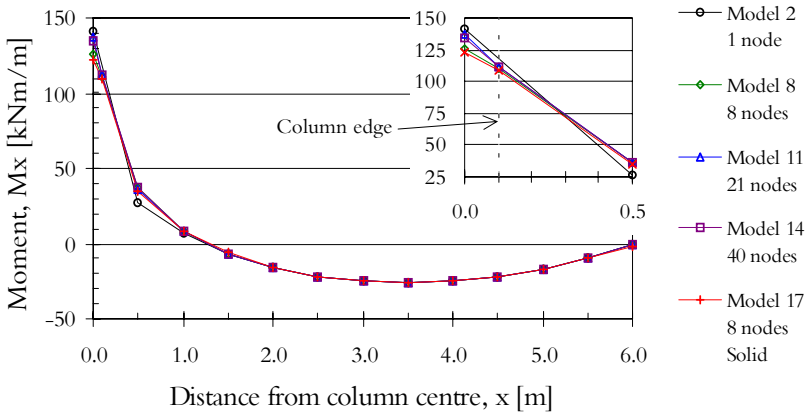

Figure 2.20 *The distribution of moments M_x in the x-direction, for different number of nodes with applied column stiffness in Abaqus. The column width b_c = 0.2 m.*

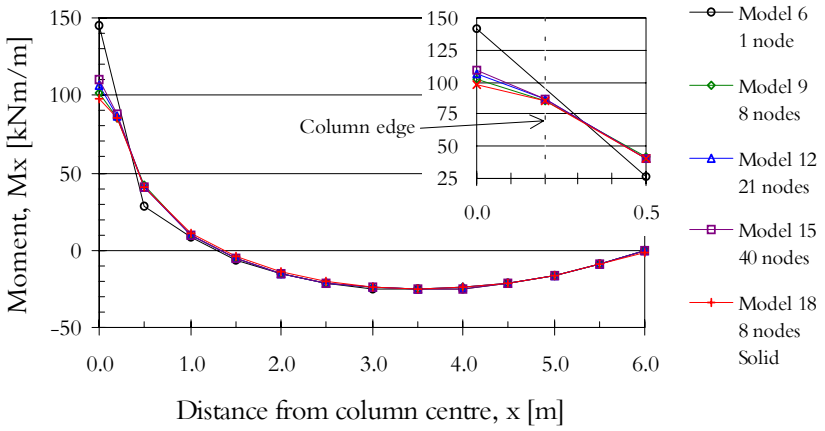

Figure 2.21 The distribution of moments M_x in the x-direction, for different number of nodes with applied column stiffness in Abaqus. The column width b_c = 0.4 m.

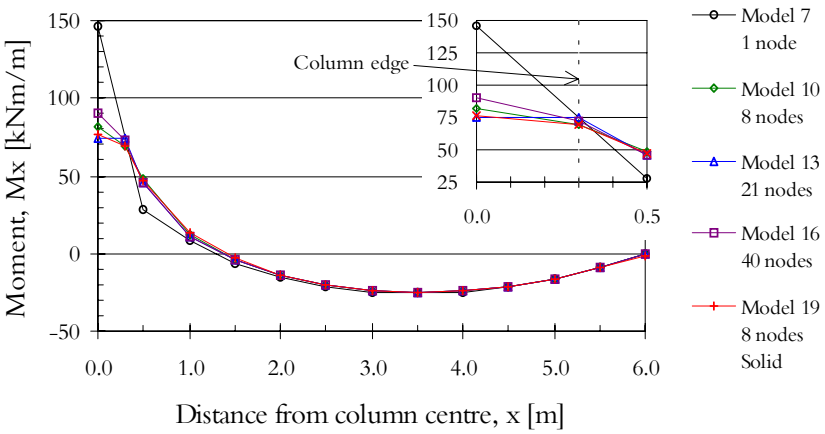

Figure 2.22 The distribution of moments M_x in the x-direction, for different number of nodes with applied column stiffness in Abaqus. The column width b_c = 0.6 m.

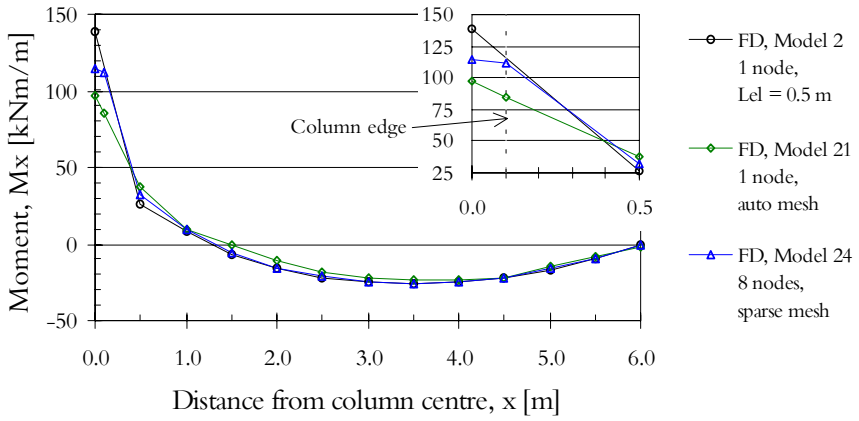

Figure 2.23 The distribution of moments M_x in the x-direction, for different number of nodes with applied column stiffness in FEM-Design. The column width b_c = 0.2 m.

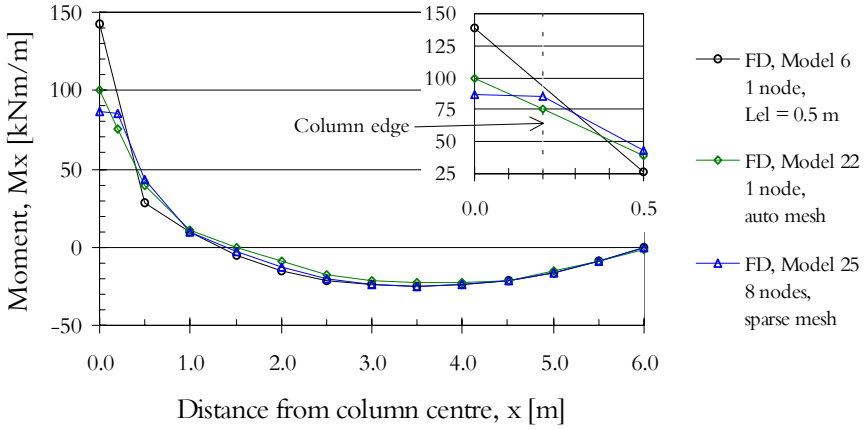

Figure 2.24 The distribution of moments M_x in the x-direction, for different number of nodes with applied column stiffness in FEM-Design. The column width b_c = 0.4 m.

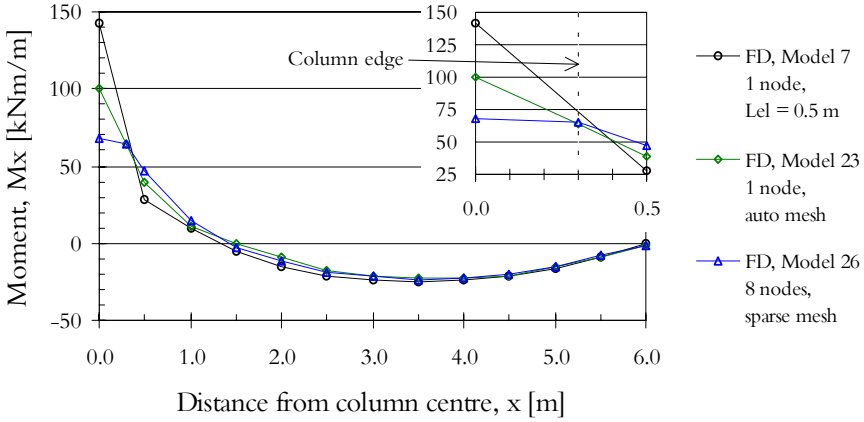

Figure 2.25 The distribution of moments M_x in the x-direction, for different number of nodes with applied column stiffness in FEM-Design. The column width b_c = 0.6 m.

2.4.5 Error estimations of the linear extrapolation

The Abaqus models modelled with the column stiffness applied at 8 nodes and 41 nodes does not have a node at the column centre. Therefore, the moment M_x is linearly extrapolated from the outer edge of area *B* and the column edge towards the centre of the column to be able to compare the maximum support moment with the other models. The extrapolation uses the slope of the moment curve in y-direction instead of the x-direction, because it gives a lower error as seen in the analyses.

The errors are estimated in order to assure that the support moment is equal to or bigger than the real value. The errors are estimated from the model with a column centre node and the column stiffness applied at 21 nodes, see *Table* 2.10 and *Figure* 2.26.

Model no	Distance, *x* [m]	Real moment[1], [kNm/m]	Extrapolated moment, [kNm/m]	Error, [kNm/m]
11	0.1	137,15	138,58	1,43
12	0.2	106,86	117,74	10,88
13	0.3	74,69	87,76	13,07

Table 2.10 The estimated errors of the extrapolated maximum support moments. Note 1: Value from model with 21 nodes.

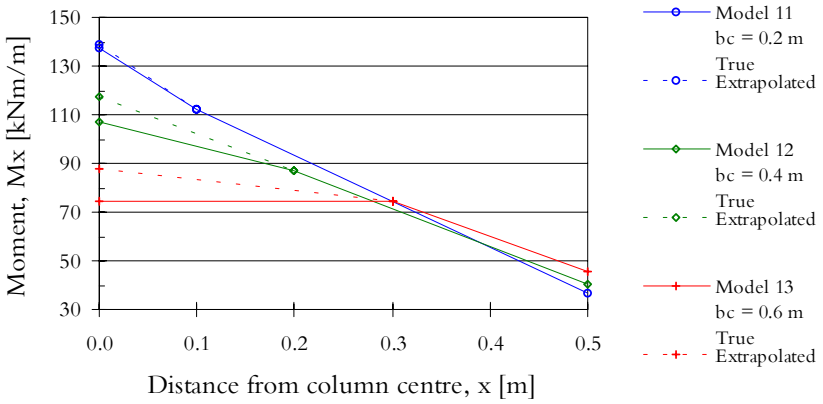

Figure 2.26 Visualisation of the real and the extrapolated moment distribution.

2.5 Comparison of the results and discussion

2.5.1 Mesh density

Figure 2.9 and *Figure* 2.10 show that the support moment, for both Abaqus and FEM-Design, increases as the mesh density increases, whereas the field moment in this case seems to be less sensitive. The support moment's dependency of the element length is more clearly illustrated in *Figure* 2.27.

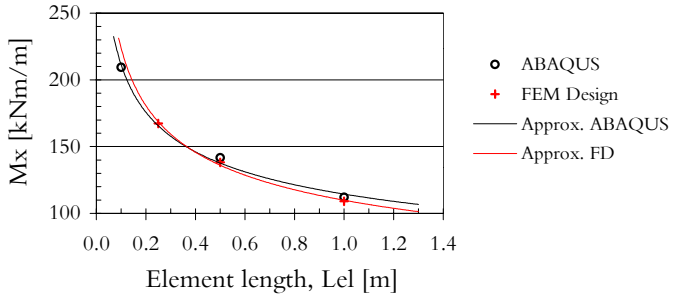

Figure 2.27 The support moment M_{xs} dependency of the mesh density, approximated as a function of the element lenght, for Abaqus and FEM-Design.

The increase of the support moment is an effect of the FE-method, which is well known around the world by the people who uses the method in research or design. Therefore, it is necessary to have some knowledge of FE-theory and realistic behaviour of structures e.g. slabs or slab systems, in order to achieve acceptable accuracy.

FEM-Design's built-in automatic mesh generator gives acceptable accuracy, at least in the case studied.

2.5.2 Element type

Figure 2.11 shows that the size of the support moment is smaller for the model with solid elements than the model with shell elements when the element length is equal to 1 m. This is due to the fact that solid elements have a more tangible material thickness than the shell element, which is only allotted a physical thickness in a three-dimensional structure. The solid elements give therefore a better response in bending than the shell elements. It is necessary to point out that the plate and the shell elements give acceptable accuracy of bending problems and in addition a much faster calculation.

Figure 2.12 shows that the support moment for the models differ less, when the element length has decreased to 0.5 meters. The support moment has also increased for both the models, but more for the model with solid elements. The shell element is less sensitive of the element length, due to the fact that the number of integration points and dofs increases less rapidly compared to the one with solid elements.

2.5.3 Column width

Figure 2.13, where the column stiffness is applied at one node, shows that the response of the moment distribution for the three different Abaqus models are almost equivalent, even if the column width varies between the models. In addition, the support moment also increases a small amount, as the column width increases, see *Table* A.5 in *Appendix* A. This is caused by the linear elastic FE-theory. An increasing column width results in an infinitely increasing reaction force at the node when the stiffness is applied at one node. This is not a realistic response, because when the span width between the column and the wall decreases, simultaneously as the column width increases, the realistic response should instead be a decreasing support moment.

The same responses can be found in the models with the same conditions analysed by FEM-Design, see *Figure* 2.18.

Figure 2.14-2.17, shows a more realistic response of the moment distribution when the column stiffness is applied at several nodes. Observe that the models in *Figure* 2.14-2.16 are modelled with shell elements, whereas the three models in *Figure* 2.17 are modelled with solid elements.

The same responses are found for the models analysed by FEM-Design, see *Figure* 2.19.

2.5.4 Modelling of the column stiffness

Figure 2.20 and *Table* A.13, where the column width b_c = 0.2 m and the column stiffness is applied at different numbers of nodes, shows that the support moment varies between 123 and 142 kNm/m, but in a comprehensive view all the support moments are quite well gathered. Both for the model with the column stiffness applied at one node and the models with the column stiffness applied at several nodes.

Figure 2.21 and *Table* A.14, where the column width b_c = 0.4 m, shows that the models with the column stiffness applied at several nodes are well gathered in consideration of the support moment, whereas the model with the column stiffness applied at one node has about 40% higher support moment than the other models.

Figure 2.22 and *Table* A.15, with the column width b_c = 0.6 m shows the same kind of response and difference as above, but the difference has increased to about 81% higher support moment.

One important detail that can be observed in all three figures is that the size of the *edge* support moment corresponds quite well between the model with the column stiffness applied at one node and the models with the column stiffness applied at several nodes. This observation is important for design and this issue will be discussed in detail in *Section* 5.4.2.

The models analysed by FEM-Design, see *Figure* 2.23-2.25, show in general the same behaviour as for the Abaqus models, but it is important to remember that the result of the three models plotted in each figure is not quite comparable when the modelling differ quite a lot, see *Figure* 2.28. On the other hand, it is observed that the size of the support moment approach each other figure by figure, for the two types of models with the column stiffness applied at 1 node (auto mesh) and 8 nodes (sparse mesh), respectively, compare in *Figure* 2.23-2.25. This depends on the fact that a wider column in the models with sparse mesh results in lower moments, when it allows a generation of bigger elements in the surrounding area of the column. In reality the difference should disappear or at least be much smaller, if the mesh generator would generate the column stiffness with only one element. In these cases, the mesh generator generates the column stiffness with five elements, which of course increases the support moment in the area of the column.

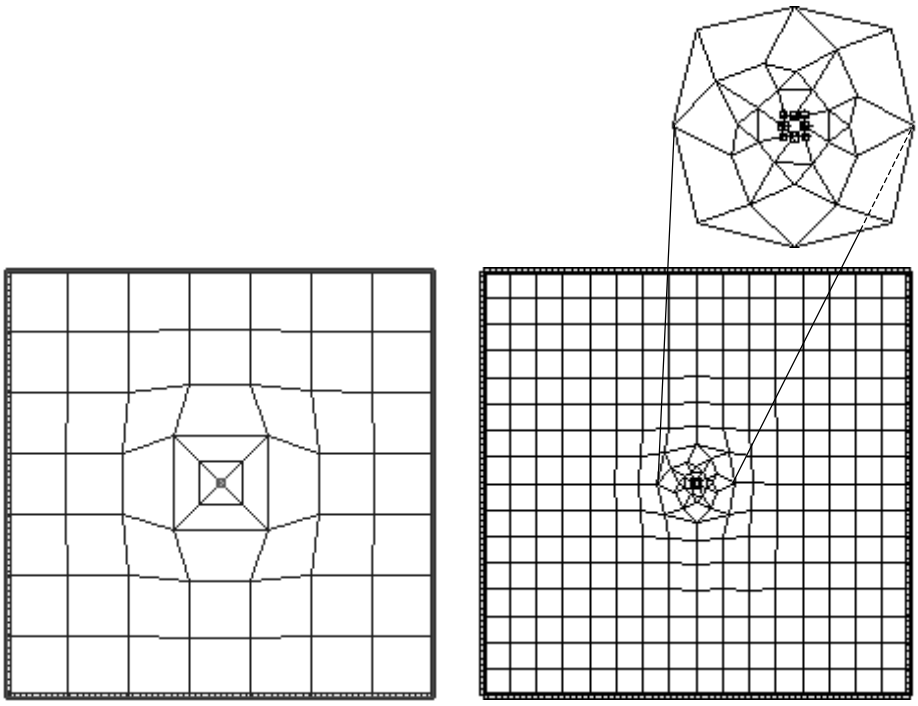

a) b)

Figure 2.28 The mesh density for: a) model 21 (1 node, auto mesh), b) model 24 (8 nodes, sparse mesh).

In comparison of the maximum support moment (in column centre) it is found that the importance of modelling the column stiffness applied at several nodes increases for more widely columns when difference between the support moments increases as the column width increases, see *Table* 2.11.

Column width, b_c [m]	**Support moment [kNm/m]**		**Ratio 8 nodes/1 node**
	8 nodes	**1 node**	
0.2	125.79	141.79	0.89
0.4	102.14	145.51	0.70
0.6	81.89	146.23	0.56

Table 2.11 Comparison of the maximum support moment between the models with the column stiffness applied at one node and eight nodes.

2.5.5 Advantage of the multi spring concept

The idea of the multi spring concept is to model the column stiffness in such a way that the maximum support moment of an interior column becomes more realistic i.e. more useful in design.

As showed in S*ection* 2.4.4 and discussed in S*ection* 2.5 the modelling of the column stiffness applied at one node, does not give a realistic response considering the maximum support moment. The most important observation can be summarised as follows:

- Different column widths give not any considerable changes of the size of the support moment. A wider column gives a little higher support moment – where it in reality should decrease.

A more realistic way to model the column stiffness is to distribute the column stiffness at several nodes, as done in the models analysed in *Section* 2.4.4. The most important observations from these analyses can be summarised in that:

- Different column widths give noticeable changes of the support moment's magnitude.
- A wider column gives lower support moment – as in reality.
- It is enough to model the column stiffness with one element i.e. applied at eight nodes even for quite large columns.

In summary, this means that models where the column stiffness is applied at several nodes give a more realistic response compared to use of only one node. Additionally, it exist a smallest column width of about 0.2 m, where the usage of the multi spring concept does not improve the calculations. The effect of the load or the thickness of the plates has not been investigated, which can affect the last conclusion. Accordingly, the multi spring concept can be recommended to model columns and walls with a width $\geq 0.2\ \mathrm{m}$.

2.5.6 Comparison between Abaqus and FEM-Design

Table 2.12-2.14, show that both the moment distribution and the displacement agrees very well between FEM-Design and Abaqus for all the comparable models. The moments calculated by Abaqus is slightly higher than the moments calculated by FEM-Design, this is probable depending on a small difference of the degree of freedoms per node between the two types of elements. Abaqus shell element has five degrees of freedom and FEM-Design's plate element has three degrees of freedoms per node.

Distance, x [m]	Moment, M_x [kNm/m]		Ratio FD/A	Displacement, u_z [m]		Ratio FD/A
	FEM-Design	Abaqus		FEM-Design	Abaqus	
0.0	138.22	141.71	0.98	-0.919	-0.923	1.00
0.5	26.16	26.60	0.98	-1.478	-1.487	0.99
1.0	7.77	7.43	1.05	-2.300	-2.314	0.99
1.5	-6.66	-7.40	0.98	-3.154	-3.174	0.99
2.0	-15.94	-16.21	0.98	-3.873	-3.899	0.99
2.5	-21.71	-21.99	0.99	-4.368	-4.399	0.99
3.0	-24.84	-25.12	0.99	-4.583	-4.617	0.99
3.5	-25.74	-26.03	0.99	-4.490	-4.525	0.99
4.0	-24.62	-24.91	0.99	-4.084	-4.117	0.99
4.5	-21.55	-21.82	0.99	-3.382	-3.411	0.99
5.0	-16.50	-16.74	0.99	-2.425	-2.447	0.99
5.5	-9.41	-9.58	0.98	-1.273	-1.285	0.99
6.0	-0.18	-0.21	0.86	-0.012	-0.012	1.00

Table 2.12 Comparison of moment M_x and displacement u_z between models analysed by Abaqus and FEM-Design. The column width b_c = 0.2 m and the column stiffness is applied at one node (model 2).

Distance, x [m]	Moment, M_x [kNm/m]		Ratio FD/A	Displacement, u_z [m]		Ratio FD/A
	FEM-Design	Abaqus		FEM-Design	Abaqus	
0.0	141.99	145.51	0.98	-0.234	-0.235	1.00
0.5	27.76	28.21	0.98	-0.810	-0.816	0.99
1.0	9.01	8.65	1.04	-1.664	-1.675	0.99
1.5	-5.73	-6.11	0.94	-2.562	-2.579	0.99
2.0	-15.23	-15.50	0.98	-3.333	-3.355	0.99
2.5	-21.16	-21.43	0.99	-3.886	-3.913	0.99
3.0	-24.41	-24.68	0.99	-4.164	-4.194	0.99
3.5	-25.42	-25.70	0.99	-4.136	-4.167	0.99
4.0	-24.38	-24.66	0.99	-3.798	-3.828	0.99
4.5	-21.37	-21.63	1.00	-3.167	-3.193	0.99
5.0	-16.39	-16.61	0.99	-2.280	-2.300	0.99
5.5	-9.36	-9.51	0.98	-1.200	-1.211	0.99
6.0	-0.18	-0.20	0.90	-0.012	-0.012	1.00

Table 2.13 Comparison of moment M_x and displacement u_z between models analysed by Abaqus and FEM-Design. The column width b_c = 0.4 m and the column stiffness is applied at one node (model 6).

Distance, x [m]	Moment, M_x [kNm/m]		Ratio FD/A	Displacement, u_z [m]		Ratio FD/A
	FEM-Design	Abaqus		FEM-Design	Abaqus	
0.0	142.70	146.23	0.98	-0.104	-0.105	0.99
0.5	28.07	28.52	0.98	-0.683	-0.688	0.99
1.0	9.24	8.89	1.04	-1.543	-1.554	0.99
1.5	-5.56	-5.93	0.94	-2.450	-2.466	0.99
2.0	-15.09	-15.36	0.98	-3.231	-3.252	0.99
2.5	-21.05	-21.32	0.99	-3.795	-3.821	0.99
3.0	-24.33	-24.60	0.99	-4.084	-4.114	0.99
3.5	-25.36	-25.63	0.99	-4.069	-4.100	0.99
4.0	-24.34	-24.61	0.99	-3.744	-3.774	0.99
4.5	-21.34	-21.60	0.99	-3.126	-3.152	0.99
5.0	-16.37	-16.58	0.99	-2.253	-2.272	0.99
5.5	-9.35	-9.49	0.99	-1.187	-1.197	0.99
6.0	-0.18	-0.19	0.95	-0.012	-0.011	1.09

Table 2.14 Comparison of moment M_x and displacement u_z between models analysed by Abaqus and FEM-Design. The column width b_c = 0.6 m and the column stiffness is applied at one node (model 7).

3 Crack analyses

3.1 Introduction

Purchasers and users have asked for some verification of the crack calculations in FEM-Design.

An experimental isotropically reinforced square concrete slab, loaded with a concentrated centred force, McNiece *(1978),* is modelled and FE-analysed in Abaqus and FEM-Design, see *Figure* 3.1. The experimental results are compared with the result to verify the crack calculation in FEM-Design. Unfortunately, no documentation of crack appearance and crack widths existed in the paper by McNiece, so such comparisons were not possible.

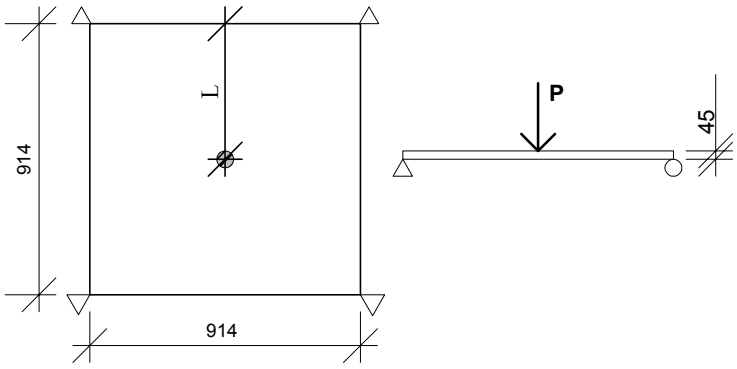

Figure 3.1 The geometry of the reinforced concrete slab

3.2 Method

The Abaqus model is analysed with a nonlinear concrete model. The obtained load intensities at different displacements are compared with a corresponding concrete model in FEM-Design. The outcome of bending moments over the centred cross section from the point load perpendicular to the slab edge *line L,* see *Figure* 3.1, and the centre node deflections are presented in tables and compared as ratios of ABAQUS/Explicit over FEM-Design. The crack pattern is compared in figures at the same load intensities. Finally, the load-displacement curves from the experiment are compared with the two FE-models.

3.3 FE-analyses

3.3.1 ABAQUS/Explicit

The cracking of the concrete is modelled with so-called smeared approach i.e. the concrete is modelled with *tension softening*. The postcracking tensile behaviour is defined in a stress-displacement relationship. The element side is chosen as the characteristic length of the elements and the fracture energy, G_f = 100 Nm/mm^2. Element type is S4R, a 4-node shell element with one Gauss-Point and 5 Degrees of Freedom (DOF). The FE-mesh is created by dividing the slab sides in to 40 elements, each.

3.3.2 FEM-Design

The modelling in FEM-Design is made with the help of the *wizard*. The same geometry and shape of the FE-mesh as for Abaqus are used. A new customised concrete is created to simulate the McNeice slab, see *Figure* 3.3. The applied reinforcement is presented in *Figure* 3.2

The FE-analysis in FEM-Design is not a real non-linear analysis i.e. that uses parameters that describe the material behaviour. Instead, FEM-design considers the decrease in the slab stiffness due to cracking (option *Consider cracking* is activated), see *Figure* 3.4. FEM-Design uses an iterative procedure where the slab from the beginning is assumed to be uncracked (State 1). Sections where the tensile stresses exceed the concrete strength are considered to be cracked (State 2). Sections loaded below the yield limit i.e. where the tensile stress is lower than the strength of the concrete, are considered to be uncracked. The stiffness calculation considers the required or the applied reinforcement depending on which option has been selected. The next load step is based on the stiffness distribution from the previous iteration step.

When the deflection from two iterations do not differ more than a predefined percentage or the maximum number of allowed calculations has been reached, the calculation stops.
If no convergence is possible the error in percent between the two last iterations will be displayed, see also *FEM-Design's Plate manual*.

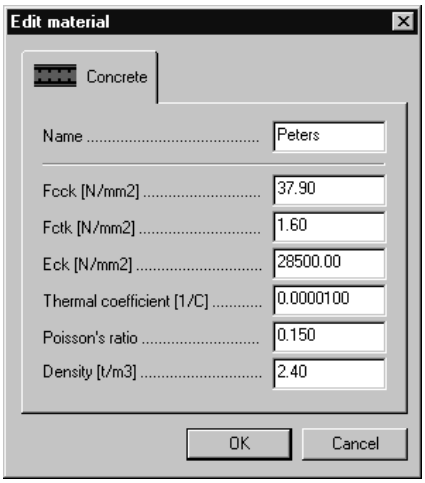

Figure 3.3 Material editing in FEM-Design according to the experimental slab, McNeice (1978).

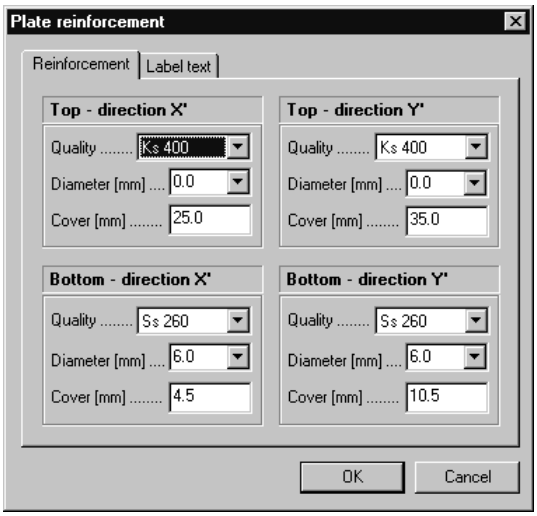

Figure 3.2 The dialog box of the reinforcement properties.

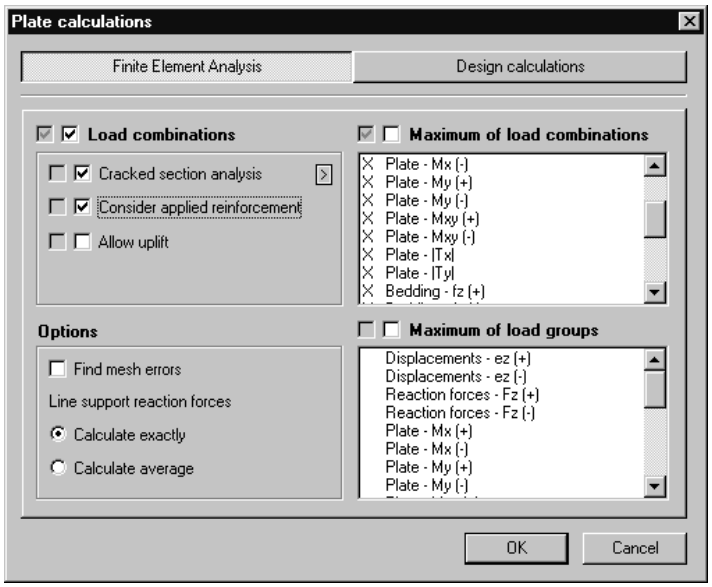

Figure 3.4 The dialog box of the FE-calculations.

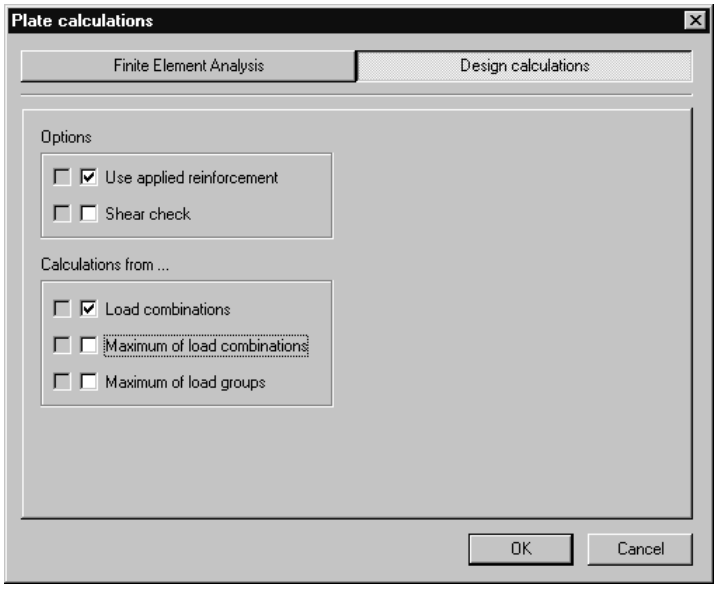

Figure 3.5 The dialog box of the design calculations.

3.4 Comparison and discussion of the results

The crack propagation and the centre node deflection are compared in figures and the corresponding bending moments in tables for each load step, and thereafter discussed. Observe that the element no 1 is the element closest to the concentrated force in the centre and so on towards to the edge of the slab.

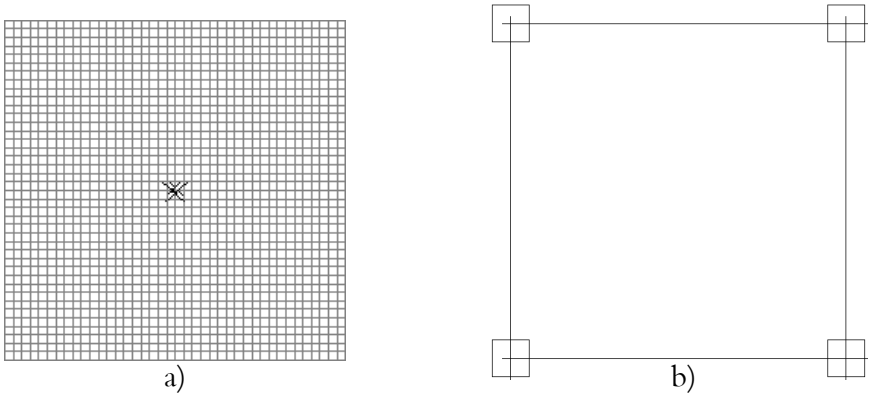

Figure 3.6 Cracks subjected to the load 1.50 kN in a) ABAQUS, deflection 0.227 mm and b) FEM-Design, deflection 0.197 mm

Element no	ABAQUS/Explicit [kNm/m]	FEM-Design [kNm/m]	Ratio AB/FD
1	0.62	0.84	0.74
2	0.53	0.60	0.88
3	0.47	0.51	0.92
4	0.43	0.46	0.93
5	0.40	0.42	0.95
6	0.38	0.39	0.97
7	0.36	0.37	0.97
8	0.34	0.35	0.97
9	0.33	0.34	0.97
10	0.32	0.33	0.97
11	0.32	0.32	1.00
12	0.31	0.32	0.97
13	0.31	0.31	1.00
14	0.31	0.31	1.00
15	0.31	0.31	1.00
16	0.31	0.31	1.00
17	0.31	0.31	1.00
18	0.32	0.32	1.00
19	0.32	0.32	1.00
20	0.32	0.32	1.00

Table 3.1 Comparison of bending moments at the load 1.50 kN

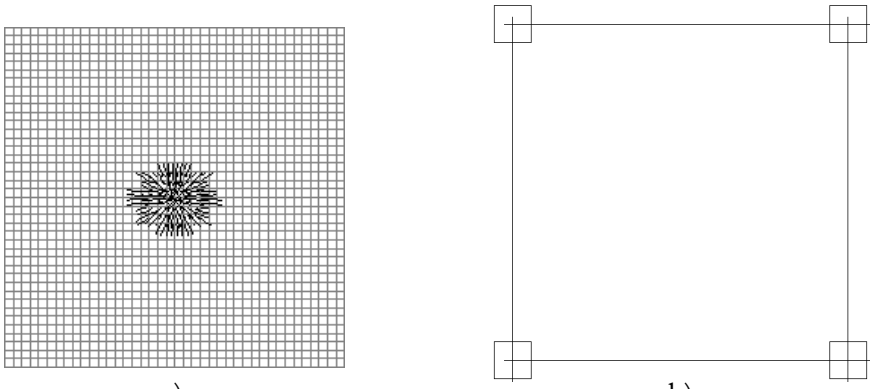

Figure 3.7 Cracks in the slab subjected to the concentrated load 2.15 kN in a) ABAQUS, deflection 0.327 mm and b) FEM-Design, deflection 0.285 mm

Element no	ABAQUS/Explicit [kNm/m]	FEM-Design [kNm/m]	Ratio AB/FD
1	0.88	1.10	0.80
2	0.74	0.82	0.90
3	0.67	0.78	0.86
4	0.62	0.64	0.93
5	0.58	0.61	0.95
6	0.54	0.57	0.95
7	0.52	0.54	0.96
8	0.49	0.51	0.96
9	0.48	0.51	0.96
10	0.47	0.51	0.96
11	0.46	0.46	1.00
12	0.45	0.46	0.98
13	0.45	0.45	1.00
14	0.44	0.45	0.98
15	0.44	0.45	0.98
16	0.45	0.45	1.00
17	0.45	0.45	1.00
18	0.45	0.45	1.00
19	0.46	0.46	1.00
20	0.46	0.46	1.00

Table 3.2 Comparison of bending moments at load 2.15 kN

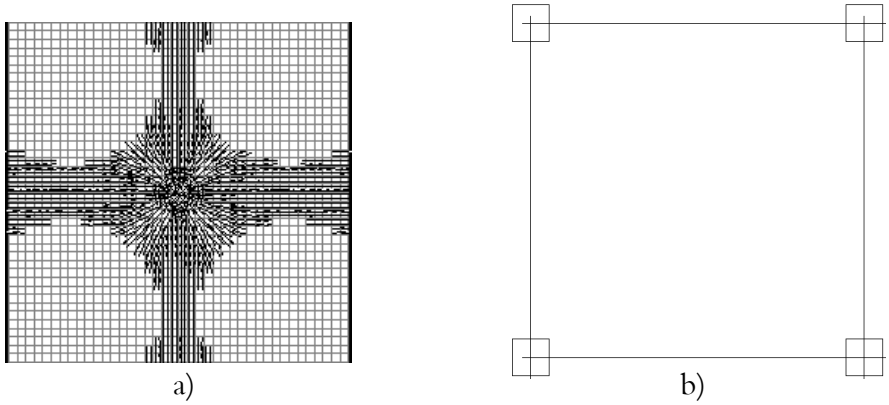

Figure 3.8 Cracks in the slab subjected to the concentrated load 2.88 kN in a) ABAQUS, deflection 0.445 mm and b) FEM-Design, deflection 0.396 mm

Element no	ABAQUS/Explicit [kNm/m]	FEM-Design [kNm/m]	Ratio AB/FD
1	1.14	1.57	0.73
2	0.99	1.18	0.84
3	0.90	0.83	1.08
4	0.81	0.83	0.98
5	0.76	0.83	0.98
6	0.72	0.81	0.89
7	0.68	0.75	0.89
8	0.66	0.71	0.93
9	0.64	0.68	0.93
10	0.64	0.68	0.94
11	0.62	0.63	0.98
12	0.61	0.62	0.98
13	0.60	0.61	0.98
14	0.60	0.61	0.98
15	0.60	0.60	1.00
16	0.60	0.60	1.00
17	0.61	0.60	1.02
18	0.61	0.61	1.00
19	0.61	0.61	1.00
20	0.61	0.62	0.98

Table 3.3 Comparison of bending moments at load 2.88 kN

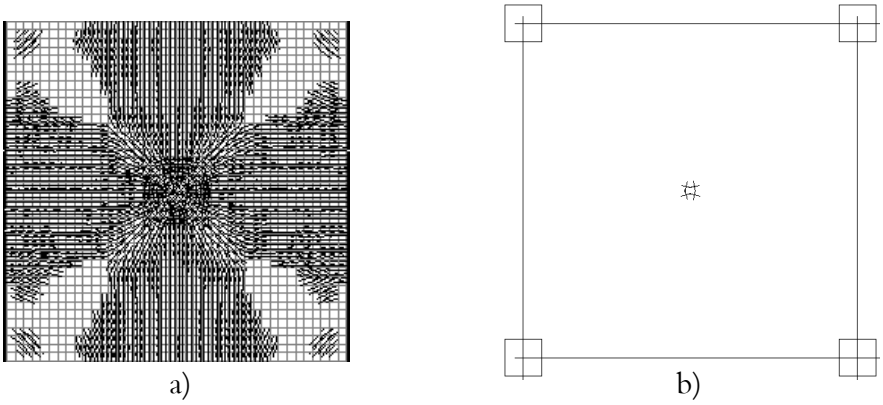

Figure 3.9 Cracks in the slab subjected to the concentrated load 3.81 kN in a) ABAQUS, deflection 0.630 mm and b) FEM-Design, deflection 0.531 mm

Element no	ABAQUS/Explicit [kNm/m]	FEM-Design [kNm/m]	Ratio AB/FD
1	1.51	2.12	0.71
2	1.28	1.76	0.73
3	1.16	1.11	1.05
4	1.07	1.12	0.96
5	1.02	0.93	1.10
6	0.97	0.93	1.04
7	0.92	0.96	0.96
8	0.89	0.90	0.99
9	0.86	0.86	1.00
10	0.84	0.84	1.00
11	0.82	0.82	1.00
12	0.81	0.82	0.99
13	0.80	0.83	0.96
14	0.80	0.83	0.96
15	0.80	0.83	0.96
16	0.80	0.82	0.98
17	0.81	0.82	0.99
18	0.81	0.82	1.00
19	0.82	0.81	1.01
20	0.82	0.81	1.01

Table 3.4 Comparison of bending moments at load 3.81 kN

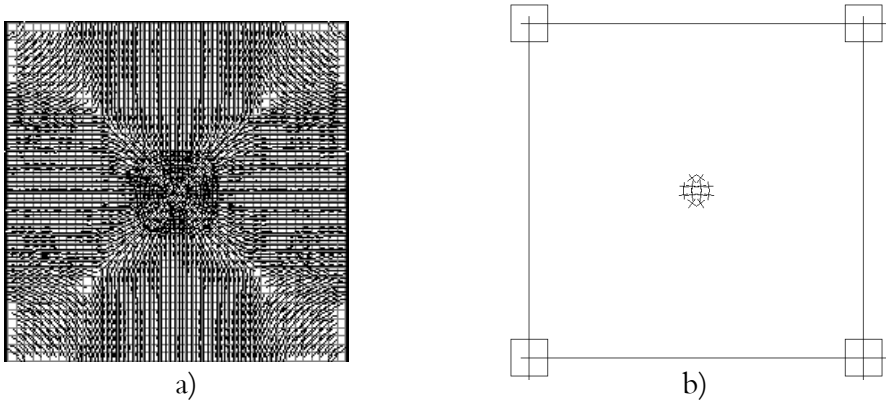

Figure 3.10 Cracks in the slab subjected to the concentrated load 4.26 kN in a) ABAQUS, deflection 0.735 mm and b) FEM-Design, deflection 0.743 mm

Element no	ABAQUS/Explicit [kNm/m]	FEM-Design [kNm/m]	Ratio AB/FD
1	1.70	2.25	0.76
2	1.44	1.83	0.79
3	1.28	1.60	0.80
4	1.18	1.13	1.04
5	1.12	1.14	0.98
6	1.07	1.00	1.07
7	1.03	0.93	1.11
8	1.00	0.97	1.03
9	0.98	1.02	0.96
10	0.95	0.98	0.97
11	0.93	0.94	0.99
12	0.92	0.92	1.00
13	0.91	0.90	1.01
14	0.90	0.89	1.01
15	0.90	0.89	1.01
16	0.90	0.89	1.01
17	0.91	0.89	1.02
18	0.91	0.90	1.01
19	0.92	0.91	1.02
20	0.92	0.91	1.02

Table 3.5 Comparison of bending moments at load 4.26 kN

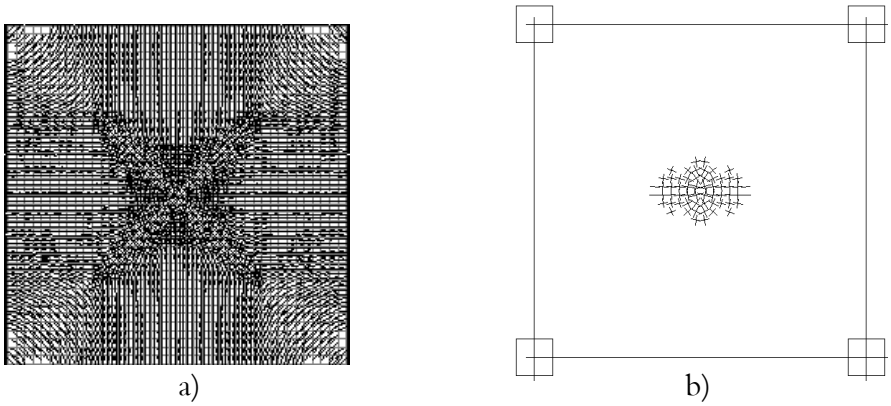

Figure 3.11 Cracks in the slab subjected to the concentrated load 4,84 kN in a) ABAQUS, deflection 0.908 mm and b) FEM-Design, deflection 0.962 mm

Element no	ABAQUS/Explicit [kNm/m]	FEM-Design [kNm/m]	Ratio AB/FD
1	1.87	2.86	0.65
2	1.58	1.89	0.84
3	1.40	1.57	0.89
4	1.28	1.35	0.95
5	1.21	1.35	0.95
6	1.51	1.19	1.27
7	1.11	1.19	1.01
8	1.08	1.04	1.04
9	1.05	1.04	1.01
10	1.04	0.97	1.07
11	1.02	0.96	1.06
12	1.01	0.95	1.06
13	1.01	1.02	0.99
14	1.01	1.08	0.94
15	1.00	1.06	0.94
16	1.01	1.05	0.96
17	1.01	1.05	0.96
18	1.01	1.08	0.94
19	1.02	1.01	1.01
20	1.02	0.91	1.12

Table 3.6 Comparison of bending moments at load 4.84 kN

Table 3.1-3.6 shows that the bending moment agrees very well between Abaqus and FEM-Design at the same loads. The largest difference appears at the concentrated load in centre of the slab, in all tables.

The first cracks in Abaqus appears at the load 1.50 kN in comparison to FEM-Design, where the first cracks appears at the load 3.37 kN, see *Figure* 3.12. The large difference depends on the crack models implemented in the two programs. The model in Abaqus describes the material behaviour according to a postfailure relationship, in this case a stress-displacement relationship. A crack becomes visible when the tensile stresses exceed the tensile strength of the concrete. The crack propagation depends on the given fracture energy G_f and the characteristic length of the elements ΔL. In FEM-Design, the formal crack width is displayed according to Swedish design rules, which are for the most part based on crack safety with respect to corrosion and bearing capacity. With other words, Abaqus displays immediately an initiated crack in the slab, whereas FEM-Design displays a crack when it affects the slabs bearing capacity or the impact of corrosion.

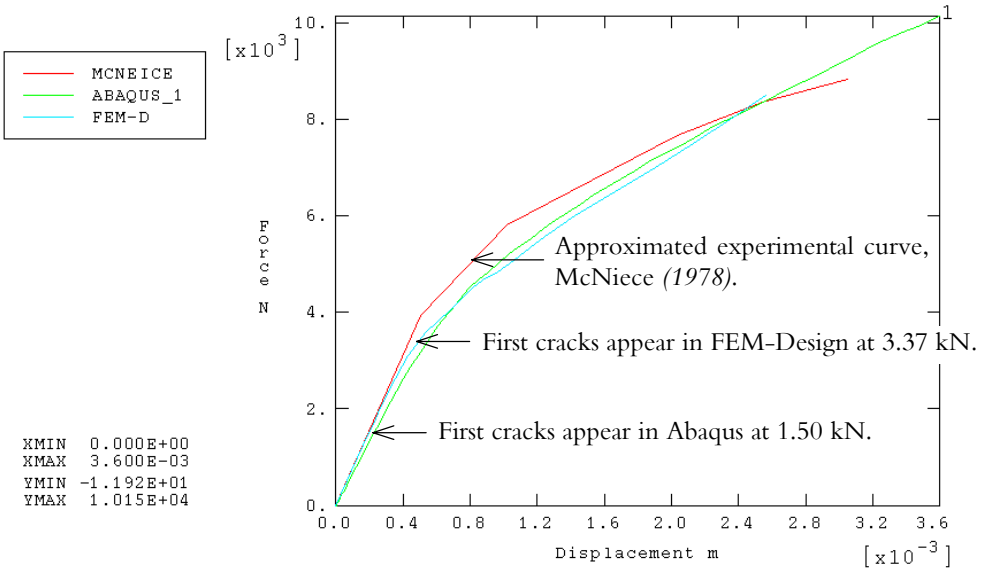

Figure 3.12 The load displacement curve from ABAQUS and FEM-Design compared with the experimental, McNiece (1978).

Figure 3.12 shows that the slope has changed noticeable before the first cracks have appeared, which just shows that the initiated cracks affect FEM-Design's stiffness calculations before they displays.

Another, but not the crucial weakness in the comparison is that the elements are not identical. FEM-Design uses eight or six node elements with three degree of freedom and ABAQUS/Explicit a four-node element with up to six degree of freedom. However, FEM-Design shows good agreement both with the experimental and the Abaqus load-displacement curve, see *Figure* 3.12. Observe that the Abaqus model does not include a compressive failure criterion in the concrete, therefore the plate cannot be loaded to failure, as seen in *Figure* 3.12.

Finally, when FEM-Design shows very good agreement with the experimental load-displacement curve using the Swedish design rules for crack initiation and estimation of crack widths, the conclusion must be that FEM-Design calculates the crack appearance and the crack widths in an adequate way for *design* purposes.

The entire sequence of crack propagation is presented in *Appendix B*.

4 Design of reinforcement

4.1 Introduction

Purchasers and users of FEM-Design have asked for verifications of the calculations in consideration of internal forces and reinforcement quantities for flat slab floors. In design handbooks it is often told that calculations of reinforcement quantities based on FE-theory gives a so unpractical distribution of the reinforcement that the result is unsuitable for practical use.

In this section, design moments, reinforcement quantities and distribution distances from traditional design methods and FEM-Design's reinforcement distributions are compared.

4.2 Method

Two in Sweden well-established design methods The Yield Line Theory and The Strip Method are used to design model 22, see defined geometry in *Chapter* 2. The redistributed moments and the distribution distances according to the traditionally design methods are compared both between each other and with the ordinary distribution by FEM-Design. The design is performed according to Swedish code, but without considering partial coefficients.

Material	Young's Modulus, E [GPa]	Poisson's ratio, ν	Tensile strength, [MPa]	Compressive strength, [MPa]	Diameter of bar ϕ, [mm]
Concrete (K30)	30	0.2	1.6	21.5	-
Steel (Ks 500)	200	0.3	500	500	12

Table 4.1 Material characteristics

The Yield Line Theory

The yield line theory is *an upper bound method* of analysing slabs subjected to flexure. Slabs are normally under-reinforced with much less than balanced amounts of steel on a strength basis. Thus with progressively increased loading, some of the steel reaches its yield point before the slab reaches its ultimate strength. When steel yields locally, there is a readjustment of stiffness and redistribution of resisting internal moments. Relatively large, local changes of curvature occur and, provided sections possess sufficient ductility, progressive yielding under increasing load intensity eventually leads to the formation of a collapse mechanism. The mechanism consists of relatively flat segments of the slab divided by relatively narrow yielding zones. The yielding zones are idealised and called yield lines. For the purpose of analysis, a collapse mechanism is assumed. A displacement is applied to a convenient point and this permits the corresponding displacements of the loading and the rotations at the yield lines to be determined from the geometry. The work done by the loading is equated to the energy dissipated by the slab. To simplify the calculations, it is assumed that the yield lines rotate without changing the intensity of the moments about their axes of rotation. This implies that the slab behaves in a perfectly plastic manner and that the segments between the yield lines are flat and rigid.

The main advantages of yield line theory are that it requires relatively simple calculations. Its greatest use is in assessing the strength of existing slabs, although it can be used as a design method. In the analytical procedure, for a particular trial mechanism and a given reinforcement pattern, the collapse load intensity can be determined from the work equation. For different trial mechanisms obtains different load intensities and the safest loading is the smallest obtained load intensity. This is because any given mechanism provides an upper bound, or upper limit on the collapse load, and it is necessary to find the lowest upper bound.

The Strip Method

In 1956, Professor Arne Hillerborg presented the strip method. This method is based on the *lower bound theorem* of the theory of plasticity. This means that the calculation leads to the safe side of designing at the Ultimate Limit State, provided that the reinforced concrete slab has a sufficiently plastic behaviour.
The solutions should give adequate safety in most cases, possibly with the exceptions of slabs of very high strength concrete and with high ratios of reinforcement.

The lower bound theorem of the theory of plasticity states that if a moment distribution can be found which fulfil the equilibrium equations, and the slab is able to carry these moments, the slab has sufficiently safety in the ultimate limit state. In the strip method this theorem has been reformulated in the following way:

Find a moment distribution, which fulfils the equilibrium equations. Design the reinforcement for these moments.

The moment distribution has only to fulfil the equilibrium equations, but no other conditions, such as the relations between moments and curvatures. This means that many different moment distributions are possible, in principle an infinite number of distributions. For practical design it is important to find a solution which is favourable in terms of economy and behaviour under service conditions.

Torsional moments complicate the design procedure and also often require more reinforcement. Solutions without torsional moments are therefore preferred where this is possible. Such solutions correspond to the *simple strip method*, which is based on the following principle:

In the simple strip method the load is assumed to be carried by strips that run in the reinforcement directions. No torsional moments act in these strips.

The simple strip method can only be applied where the strips are supported so that they can be treated like beams. This is not generally possible with slabs that are supported by columns. To solve such structures the *advanced strip method* technique has to be used. This method is very powerful and also simple to use for many cases in practical design. The limitation is that it requires certain regularity in the slab shape and loading conditions.

In the simple strip method the slab is divided into strips in the directions of the reinforcement, which carry different parts of the total load. Usually only two directions are used, corresponding to the x- and y-directions. Each strip is then considered statically as a one-way strip, which can be analysed with ordinary static for beams. The whole load within each part of the slab is assumed to be carried by strips in one reinforcement direction.

The load is preferably carried with a minimum of cost, which normally means with a minimum amount of reinforcement. As a first approximation this usually means that the load should be carried in the direction towards the nearest support. If the slab is rectangular the load should be carried in the shortest direction.

A consequence of these considerations is that a suitable dividing line between areas with different load bearing directions is a straight line, which starts at a corner of a slab with a distributed load. The dividing lines are normally assumed to be *lines of zero shear force*. For a square simply supported concrete slab the line is simply drawn in an angle of 45 degrees.

If the slab is of rectangular shape the line should be drawn closer to the shorter side. Where a fixed edge and a freely supported edge meet, the line of zero shear force should be drawn much closer to the free edge than the fixed edge.

Reinforcement design

The relative moment ratio is defined as

$$\bar{m} = \frac{M}{b \cdot d \cdot f_{cck}} \quad [-] \tag{4.1}$$

where M is the design moment [Nm/m]
b is the with and in this case always 1 meter [m]
d is the effective cross section height [m]
f_{cck} is the concrete compressive strength [Pa]

The mechanical reinforcement ratio is defined as

$$\omega = 1 - \sqrt{1 - 2\bar{m}} \quad [-] \tag{4.2}$$

The reinforcement area is calculated as

$$A_s = \frac{M}{d\left(1 - \frac{\omega}{2}\right) f_{yk}} \quad \left[m^2 / m\right] \tag{4.3}$$

where f_{yk} is the yield limit for the reinforcement [Pa]

To make sure that the cross section is under-reinforced the following conditions has to bee full filled i.e. plastic behaviour

$$\omega \le \omega_{bal}$$

$$\bar{m} \le \bar{m}_{bal}$$

where the balanced value of the mechanical reinforcement ratio is calculated according to

$$\omega_{bal} = 0,8 \cdot \frac{\varepsilon_{cu}}{\varepsilon_{cu} + \varepsilon_{sk}} = 0,8 \cdot \frac{3,5}{3,5 + 2,5} \approx 0,467$$

where $\varepsilon_{sk} = \frac{f_{yk}}{E_{sk}} = \frac{500 \cdot 10^6}{200 \cdot 10^9} = 2,5\ ‰$

and the relative moment as

$$\bar{m}_{bal} = \omega_{bal}\left(1-\frac{\omega_{bal}}{2}\right) = 0,467\cdot\left(1-\frac{0,467}{2}\right) \approx 0,358$$

4.3 Yield line theory

The corresponding geometry is illustrated in *Figure* 4.1 and the theory of the used design method can be found in e.g. *The Swedish Concrete Handbook - Design, section 6.5:34.*

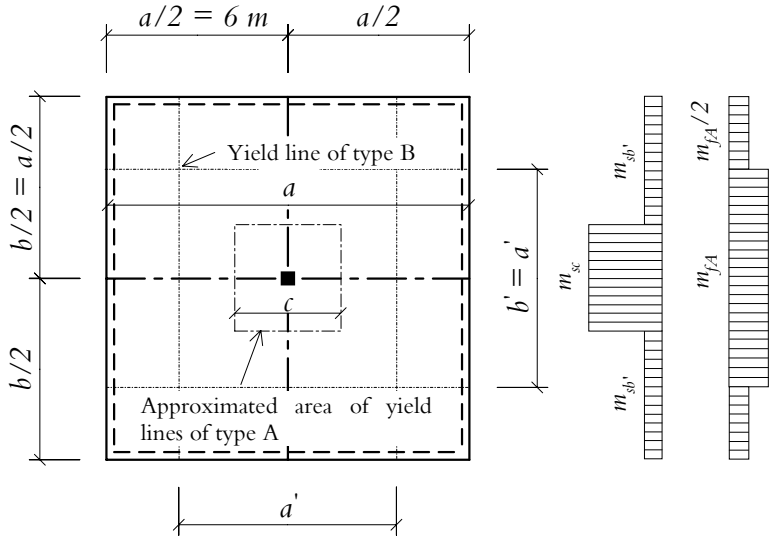

Figure 4.1 *The principle geometry of the flat slab floor (model 22) and the distribution of the moments in x-direction according to the yield line theory.*

4.3.1 Moments and distribution

The design column load is in this case calculated as

$$P_c = q\cdot a'\cdot b' = 9\cdot\left(2\cdot 0.6\cdot 6\right)^2 = 466.56\ kN$$

and the distribution distance *c* as

$$c = 0.5\sqrt{\frac{P_c}{q}} = 0.5\sqrt{\frac{466.56}{9}} = 3,6\ \ m$$

The unreduced column support moment according to yield lines of type A is calculated as

$$m_{sA\,unred} = 0.15P_c = 0.15 \cdot 466.56 \approx 69.98\ kNm/m$$

and the term of the reduction moment as

$$\Delta m_{sA} = \frac{3P_c b_c}{16c} = \frac{3 \cdot 466.56 \cdot 0.4}{16 \cdot 3.6} \approx 9.72\ kNm/m$$

The support moment according to yield lines of type B is calculated as

$$m_{sB} = \frac{ql^2}{8} = \frac{9 \cdot 5.8^2}{8} \approx 37.85\ kNm/m$$

The field moment is the largest of

$$m_{fc} = \frac{ql^2}{16} = \frac{9 \cdot 5.8^2}{16} = 18.92\ kNm/m$$

$$m_{f\,norm} = \frac{P_c}{24} = \frac{466.56}{24} = 19.44\ kNm/m$$

Design moments and distribution distances

The design support moment of type A is calculated as

$$m_{sc} = m_{sA\,unred} - \Delta m_{sA} = 69.98 - 9.72 = 60.26\ kNm/m$$

The design support moment of type B is calculated as

$$m_{sb'} = m_{sB} - \frac{m_{sc} \cdot c}{b'} = 37.85 - \frac{60.26 \cdot 3.6}{2 \cdot 0.6 \cdot 6} = 7.72\ kNm/m$$

The design field moment is equal to

$$m_{fA} = m_{f\,norm} = 19.44\ kNm/m$$

The support moment of type A is distributed over the length *c* and sideways along the distance *c* and the support moment of type B is distributed over the length *c* and sideways along the distance *b*.

The field moment is distributed over the length *a* and sideways along both the middle and the edge strip. Along the middle strip with the width *b*' is the reinforcement designed for the full intensity of the field moment and along the two edge strips for the half size of the intensity.

The distribution of the moments in the x-direction is illustrated in *Figure* 4.1. Due to the symmetry of the plate the distribution of the moments in y-direction is similar to the x-direction.

4.3.2 Reinforcement quantities

The quantities of reinforcement are calculated according to *Equation* 4.1-4.3, design moments in *Section* 4.3.1 and distances of concrete cover in *Figure* 4.2.

Maximum and minimum allowed reinforcement areas

According to Swedish code in *BBK 94* the *minimum distance* between the bars on account of *workability* is

$$s_{\min} = 2\phi = 2 \cdot 12 = 24\ mm$$

which gives the *maximum* allowed reinforcement area in the structure as

$$A_{s\max} = b \cdot \frac{A_\phi}{s_{\min}} = 1000 \cdot \frac{113}{24} \approx 4708\ mm^2/m$$

The *maximum distance* between the bars on account of *cracks* is

$$s_{\max} = 2h = 2 \cdot 200 = 400\ mm$$

which gives the *minimum* required reinforcement area in the structure as

$$A_{s\min} = b \cdot A_\phi / s_{\max} = 1000 \cdot 113/400 \approx 283\ mm^2/m$$

Finally, the quantity of the applied reinforcement has to fulfils the requirements

$$A_{s\min} \le A_s \le A_{s\max} \qquad 4.4$$

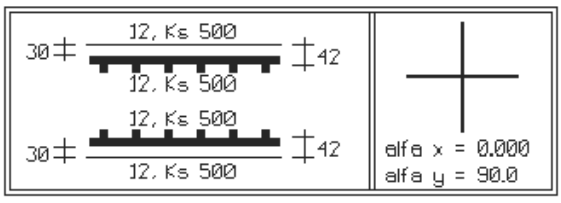

Figure 4.2 The defined reinforcements and distances of concrete cover.

Top reinforcement

The reinforcement in x-direction for the *column strip* according to both yield lines of type A and B is calculated as

$$\bar{m} = \frac{67.98 \cdot 10^3}{0.164^2 \cdot 21.5 \cdot 10^6} \approx 0.1176 < \bar{m}_{bal} \quad OK!$$

$$\omega = 1 - \sqrt{1 - 2 \cdot 0.1176} \approx 0.1254 < \omega_{bal} \quad OK!$$

$$A_s = \frac{67.98 \cdot 10^3}{0.164\left(1 - \frac{0.1254}{2}\right)500} \approx 884{,}5\ mm^2/m$$

and in y-direction to

$$\bar{m} = \frac{67.98 \cdot 10^3}{0.152^2 \cdot 21.5 \cdot 10^6} \approx 0.1369 < \bar{m}_{bal} \quad OK!$$

$$\omega = 1 - \sqrt{1 - 2 \cdot 0.1369} \approx 0.1478 < \omega_{bal} \quad OK!$$

$$A_s = \frac{67.98 \cdot 10^3}{0.152\left(1 - \frac{0.1478}{2}\right)500} \approx 965{,}8\ mm^2/m$$

The reinforcement in x-direction for the areas outside the column strip i.e. $c \cdot \frac{b-c}{2}$ according to yield lines of type B, is calculated as

$$\bar{m} = \frac{7.72 \cdot 10^3}{0.164^2 \cdot 21.5 \cdot 10^6} \approx 0.0134 < \bar{m}_{bal} \quad OK!$$

$$\omega = 1 - \sqrt{1 - 2 \cdot 0.0134} \approx 0.0134 < \omega_{bal} \quad OK!$$

$$A_s = \frac{7.72 \cdot 10^3}{0.164\left(1 - \frac{0.0134}{2}\right)500} \approx 94{,}8\ mm^2/m$$

and in y-direction to

$$\bar{m} = \frac{7.72 \cdot 10^3}{0.152^2 \cdot 21.5 \cdot 10^6} \approx 0.0155 < \bar{m}_{bal} \quad OK!$$

$$\omega = 1 - \sqrt{1 - 2 \cdot 0.0155} \approx 0.0157 < \omega_{bal} \quad OK!$$

$$A_s = \frac{7.72 \cdot 10^3}{0.152\left(1 - \frac{0.0157}{2}\right)500} \approx 102.4\ mm^2/m$$

Bottom reinforcement

The reinforcement in x-direction for the *field strip* is calculated according to

$$\bar{m} = \frac{19.96 \cdot 10^3}{0.164^2 \cdot 21.5 \cdot 10^6} \approx 0.0345 < \bar{m}_{bal} \quad OK!$$

$$\omega = 1 - \sqrt{1 - 2 \cdot 0.0345} \approx 0.0351 < \omega_{bal} \quad OK!$$

$$A_s = \frac{19.96 \cdot 10^3}{0.164\left(1 - \frac{0.0351}{2}\right)500} \approx 247.8\ mm^2/m$$

and in y-direction to

$$\bar{m} = \frac{19.96 \cdot 10^3}{0.152^2 \cdot 21.5 \cdot 10^6} \approx 0.0402 < \bar{m}_{bal} \quad OK!$$

$$\omega = 1 - \sqrt{1 - 2 \cdot 0.0402} \approx 0.0410 < \omega_{bal} \quad OK!$$

$$A_s = \frac{19.96 \cdot 10^3}{0.152\left(1 - \frac{0.0410}{2}\right)500} \approx 268.1\ mm^2/m$$

The applicable bending reinforcement areas and its distribution lengths and widths are gathered in *Table* 4.2, observe that the requirements according to *Equation* 4.4 is taken in account and that needed anchor lengths or joint lengths are not included in the distribution distances.

Considered strip	Distribution length [m]	Distribution width [m]	Reinforcement area [mm²/m]	
			A_{sx}	A_{sy}
Column, top	3.60	3.60	884.5	965.8
Outside column, top	3.60	2×4.20	(94.8) 283.0	(102.4) 283.0
Field, bottom	12.00	7.20	(247.8) 283.0	(268.1) 283.0
Edge, bottom	12.00	2×2.40	(123.9) 283.0	(134.1) 283.0

Table 4.2 *The quantities of the bending reinforcement areas and its distribution lengths and widths according to the yield line theory (areas in brackets are the calculated).*

4.4 Strip method

The corresponding geometry is illustrated in *Figure* 4.3 and the theory of the used design method can be found in e.g. *The Strip Method Design Handbook*.

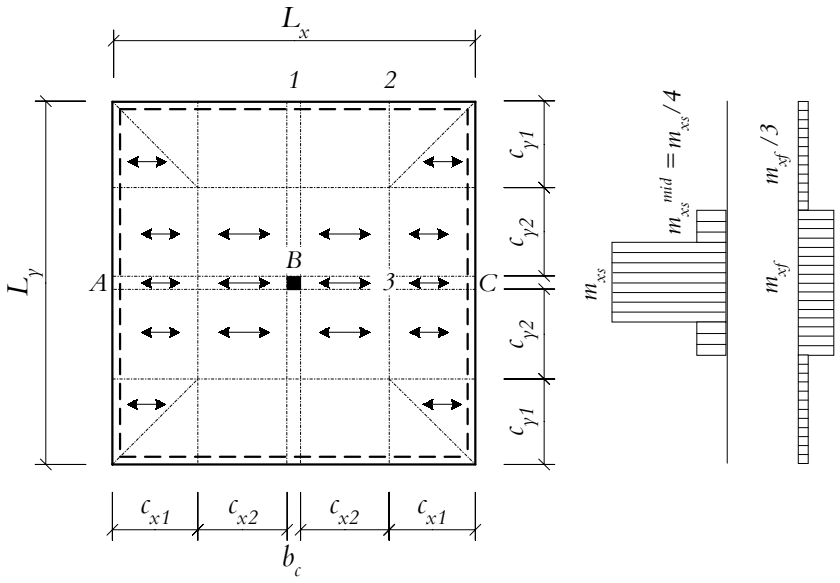

Figure 4.3 *The principle geometry of the flat plate floor (model 22) and distribution of the moments in x-direction according to the strip method.*

4.4.1 Moments and distribution

The slab is calculated, as a continuous beam over the column according to elastic theory and due to the symmetry the moments in y-direction is similar to the x-direction.

The average column support moment is calculated as

$$m_{xs}^{B} = \frac{ql^2}{8} = \frac{9 \cdot 5.8^2}{8} \approx 37.9 \; kNm/m$$

The length of the strips, see *Figure* 4.3, are determined as

$$c_{x2} = \frac{l}{2} - \frac{m_{xs}^{B} - m_{xs}^{C}}{ql} = \frac{5.8}{2} - \frac{-37,9 - 0}{9 \cdot 5.8} = 3.63 \; m$$

$$c_{x1} = l - c_{x2} = 5.8 - 3.63 = 2.17 \; m$$

and the average field moment is calculated as

$$m_{xf}^{BC} = \frac{qc_{x2}^2}{2} + m_{xs}^{B} = \frac{9 \cdot 3.63^2}{2} - 37.9 \approx 21.4 \; kNm/m$$

In corner supported elements, see *Figure* 4.4, both the support and field moments can be sideways redistributed to strips where the reinforcement is more useful in consideration of e.g. resistance against bending and cracks.

The moment is redistributed according to the formula

$$m_i^{av} c_i = m_i^{col} \beta c_i + m_i^{side} (1 - \beta) c_i \qquad 4.5$$

where $\beta \leq 0.5$

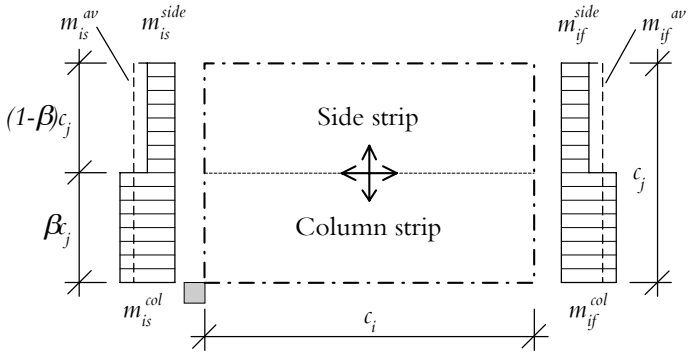

Figure 4.4 Redistribution in j-direction of the moments in i-direction for a corner supported element according to the advanced strip method.

To satisfy the equilibrium and the requirement that the edge moments for a corner supported strip element shall be appropriate as design moments a control parameter must fulfil the condition

$$\frac{1-\beta}{2} \le \alpha \le 0.7 \qquad 4.6$$

The control parameter α depends on the ratio between the moments in the side strip and the column strip according to

$$\alpha = \frac{m_f^{side} - m_s^{side}}{m_f^{av} - m_s^{av}} \qquad 4.7$$

where m_f^{side} is the redistributed field moment in the side strip [mm^2/m]

m_s^{side} is the redistributed column support moment in the side strip [mm^2/m]

m_f^{av} is the average field bending moment [mm^2/m]

m_s^{av} is the average column support moment [mm^2/m]

Design moments and distribution distances

When β here is chosen to 0.5 the condition become

$$0.25 \le \alpha \le 0.7$$

If the redistributed design support moment in the side strip in this case, is assumed to be $k = 0.25$ times smaller than the design support moment in the column strip i.e. $m_i^{side} = km_i^{col}$, and inserted in *Equation* 4.5, the redistributed moment in the column strip can be calculated as

$$m_{xs}^{col} = \frac{m_{xs}^{av}}{\beta + k(1-\beta)} = \frac{37.9}{0.5 + \frac{1}{4}(1-0.5)} \approx 60.6\ kNm/m$$

which gives

$$m_{xs}^{side} = km_{xs}^{col} = \frac{1}{4} \cdot 60.6 \approx 15.2\ kNm/m$$

The maximum design field moment is kept unredistributed i.e.

$$m_{xf} = 21.4\ kNm/m$$

In the triangular corner strip the design field moment is redistributed with respect of conditions between the elementary cases, to one third of the maximum design field moment.

When all the design moments is determined the control is performed as

$$0.25 \le \alpha = \frac{m_{xf}^{side} - m_{xs}^{side}}{m_{xf}^{av} - m_{xs}^{av}} = \frac{21.4 + 15.2}{21.4 + 37.9} \approx 0.62 \le 0.7 \quad OK!$$

The distribution distances can be determined directly from the moment curve or by hand according to Hillerborg *(1996),* see *Equation* 2.45, 2.46 and *Fig.* 2.10.1. In this case, when the moment distribution is assumed to be unknown on account of traditional design, the distances are calculated by hand.

The half of the top reinforcement is distributed over the length

$$\gamma c_{x2} + \Delta L = 0.59 \cdot 3.63 + 0 = 2.14\ m \qquad 4.8$$

and the other half over the length

$$\frac{2}{3}\gamma c_{x2} + \Delta L = \frac{2}{3} \cdot 0.59 \cdot 3.63 + 0 = 1.43\ m \qquad 4.9$$

The design support moment is distributed over the lengths according to *Equation* 4.8-4.9 and sideways along the distance $(0.5b_c+c_{y2})$.

The field moment is distributed over the length L_x and sideways along both the side strips and the edge strips. Along the side strips with the width (b_c+2c_{y2}) the reinforcement is designed for the full intensity of the field moment and along the two edge strips with the widths c_{y1} for one third of the intensity.

The redistributed moments working in the x-direction are illustrated in *Figure* 4.3. Due to the symmetry of the plate the distribution of the moments in y-direction is similar to the moments in x-direction.

4.4.2 Reinforcement quantities

The quantities of reinforcement are calculated according to *Equation* 4.1-4.3, design moments in *Section* 4.4.1 and distances of concrete cover in *Figure* 4.2.

Top reinforcement

The top reinforcement in x-direction for the *column strip*, is calculated as

$$\bar{m} = \frac{60.6 \cdot 10^3}{0.164^2 \cdot 21.5 \cdot 10^6} \approx 0.1048 < \bar{m}_{bal} \quad OK!$$

$$\omega = 1 - \sqrt{1 - 2 \cdot 0.1048} \approx 0.1110 < \omega_{bal} \quad OK!$$

$$A_{sxs}^{col} = \frac{60.6 \cdot 10^3}{0.164\left(1 - \frac{0.1110}{2}\right)500} \approx 782,4\ mm^2/m$$

and in y-direction as

$$\bar{m} = \frac{60.6 \cdot 10^3}{0.152^2 \cdot 21.5 \cdot 10^6} \approx 0.1220 < \bar{m}_{bal} \quad OK!$$

$$\omega = 1 - \sqrt{1 - 2 \cdot 0.1220} \approx 0.1305 < \omega_{bal} \quad OK!$$

$$A_{sys}^{col} = \frac{60.6 \cdot 10^3}{0.152\left(1 - \frac{0.1305}{2}\right)500} \approx 853,0\ mm^2/m$$

The reinforcement in x-direction for the *side strip*, is calculated as

$$\bar{m} = \frac{15.2 \cdot 10^3}{0.164^2 \cdot 21.5 \cdot 10^6} \approx 0.0263 < \bar{m}_{bal} \quad OK!$$

$$\omega = 1 - \sqrt{1 - 2 \cdot 0.0263} \approx 0.0266 < \omega_{bal} \quad OK!$$

$$A_{sxs}^{side} = \frac{15.2 \cdot 10^3}{0.164\left(1 - \frac{0.0266}{2}\right)500} \approx 187,9\ mm^2/m$$

and in y-direction to

$$\bar{m} = \frac{15.2 \cdot 10^3}{0.152^2 \cdot 21.5 \cdot 10^6} \approx 0.0306 < \bar{m}_{bal} \quad OK!$$

$$\omega = 1 - \sqrt{1 - 2 \cdot 0.0306} \approx 0.0311 < \omega_{bal} \quad OK!$$

$$A_{sys}^{side} = \frac{15.2 \cdot 10^3}{0.152\left(1 - \frac{0.0311}{2}\right)500} \approx 203,2\ mm^2/m$$

Bottom reinforcement

The reinforcement in x-direction for the *field strip*, is calculated according to

$$\overline{m} = \frac{21.4 \cdot 10^3}{0.164^2 \cdot 21.5 \cdot 10^6} \approx 0.0370 < \overline{m}_{bal} \quad OK!$$

$$\omega = 1 - \sqrt{1 - 2 \cdot 0.0370} \approx 0.0377 < \omega_{bal} \quad OK!$$

$$A_{sxf}^{field} = \frac{21.4 \cdot 10^3}{0.164\left(1 - \frac{0.0377}{2}\right)500} \approx 266.0\ mm^2/m$$

and in y-direction to

$$\overline{m} = \frac{21.4 \cdot 10^3}{0.152^2 \cdot 21.5 \cdot 10^6} \approx 0.0431 < \overline{m}_{bal} \quad OK!$$

$$\omega = 1 - \sqrt{1 - 2 \cdot 0.0431} \approx 0.0441 < \omega_{bal} \quad OK!$$

$$A_{syf}^{field} = \frac{21.4 \cdot 10^3}{0.152\left(1 - \frac{0.0441}{2}\right)500} \approx 287.9\ mm^2/m$$

The reinforcement in x-direction for the *edge strip*, is calculated according to

$$\overline{m} = \frac{\frac{1}{3} \cdot 21.4 \cdot 10^3}{0.164^2 \cdot 21.5 \cdot 10^6} \approx 0.0123 < \overline{m}_{bal} \quad OK!$$

$$\omega = 1 - \sqrt{1 - 2 \cdot 0.0123} \approx 0.0124 < \omega_{bal} \quad OK!$$

$$A_{sxf}^{edge} = \frac{\frac{1}{3} \cdot 21.4 \cdot 10^3}{0.164\left(1 - \frac{0.0124}{2}\right)500} \approx 87.1\ mm^2/m$$

and in y-direction to

$$\overline{m} = \frac{7.1 \cdot 10^3}{0.152^2 \cdot 21.5 \cdot 10^6} \approx 0.0143 < \overline{m}_{bal} \quad OK!$$

$$\omega = 1 - \sqrt{1 - 2 \cdot 0.0143} \approx 0.0144 < \omega_{bal} \quad OK!$$

$$A_{syf}^{edge} = \frac{7.1 \cdot 10^3}{0.152\left(1 - \frac{0.0144}{2}\right)500} \approx 94.1\, mm^2/m$$

The applicable bending reinforcement areas and its distribution lengths and widths are gathered in *Table* 4.3, observe that the requirements according to *Equation* 4.4 is taken in account and that anchor lengths ΔL or joint lengths are not included in the given lengths of the reinforcement.

Considered strip	**Distribution length, *x* [m]**	**Distribution width, *y* [m]**	**Reinforcement area [mm²/m]**	
			A_{sx}	A_{sy}
Column, top	4.68	4.03	782.4	853.0
Side, top	4.68	2×1.81	(187.9) 283.0	(203.2) 283.0
Field, bottom	12.00	7.66	(266.0) 283.0	287.9
Edge, bottom	12.00	2×2.17	(87.1) 283.0	(94.1) 283.0

Table 4.3 *The quantities of the bending reinforcement areas and its distribution lengths and widths according to the strip method (areas in brackets are the calculated).*

4.5 Comparison and discussion of results

4.5.1 Moment distribution

The moment distributions calculated according to the two methods are compared with FEM-Design's calculated distribution of moments. In FEM-Design the design moments M'_x (including twisting moments) are determined both in *x*-direction and *y*-direction from model 22, along lines according to the location figures besides the graphs in *Figure* 4.5-4.7, see also *Figure* 4.3.

The yield line theory redistributes the support moments in a smaller area (the column strip) with a higher intensity than the strip method i.e. to be more concentrated in the column surrounding area than the strip method, which is better in consideration of punching, compare in *Figure* 4.5-4.6. The yield line theory redistributes the support moments outside the column strip even in areas where none bending moments occurs in the FE-analysis, so the strip method distributes the support moments better in consideration of bending and crack safety.

The strip method redistributes the field moments to be more similar to the FE-analyses moment distribution than the yield line theory i.e. to be more safe in consideration of bending and cracks, compare in *Figure* 4.5-4.7 and especially *Figure* 4.7.

FEM-Design's moment distribution is not really comparable with the two traditional design methods when FEM-Design calculates the moment distribution according to elastic theory at each node and the two design methods distributes a moment with the same size in a certain area. This means that the usable moments must be chosen at certain points from the FE-analyses. In *Chapter* 5 the best choice of moments and a design method based on FE-theory are discussed.

Considered strip	**Design moment [kNm/m]**		
	Yield line theory	**Strip method**	**FEM-Design**
Column, top	68.0	60.6	100.3
Outside column, top	7.7	-	-
Side, top	-	15.2	-
Field, bottom	19.4	21.3	29.2
Edge, bottom	9.7	7.1	-

Table 4.4 *Comparison of the size of the redistributed moments between the yield line theory and the strip method.*

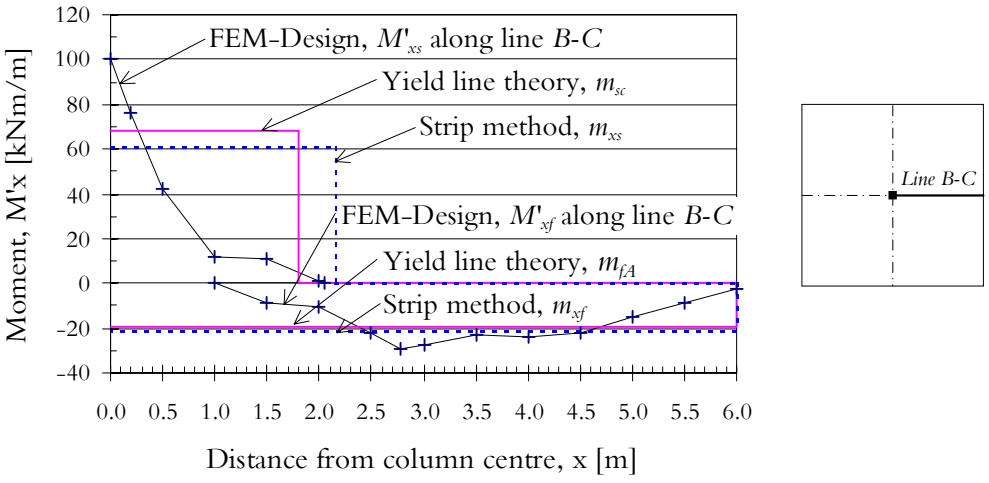

Figure 4.5 *The moment distribution M_x in the x-direction according to the yield line theory, the strip method and the FE-analysis (FEM-Design).*

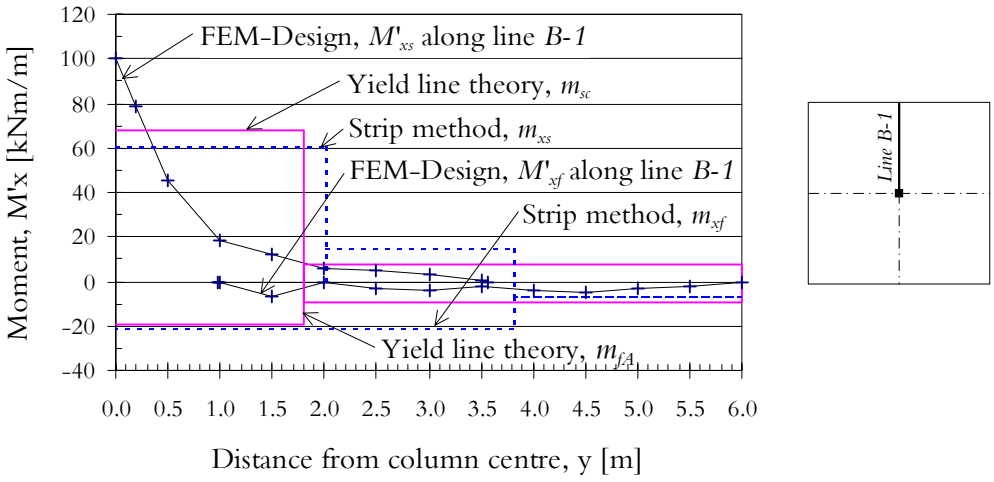

Figure 4.6 *The moment distribution M_x in the x-direction according to the yield line theory, the strip method and the FE-analysis (FEM-Design).*

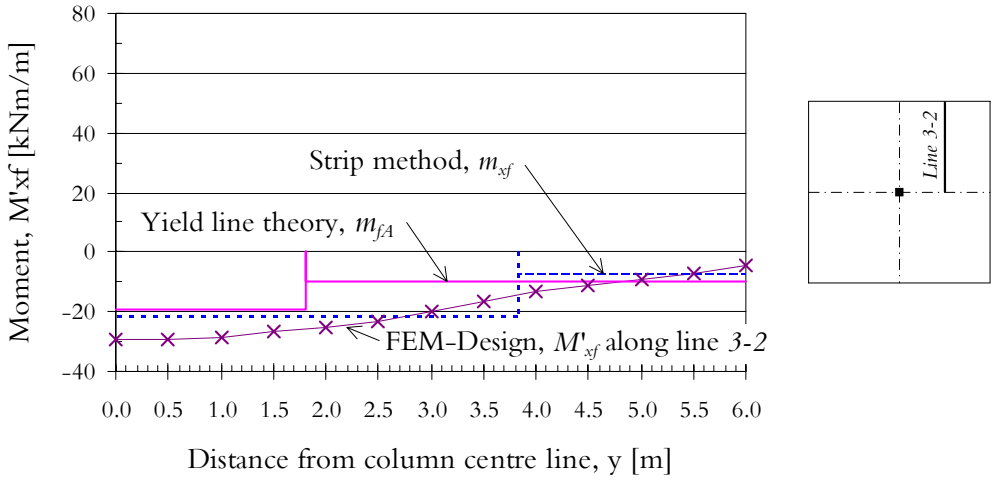

Figure 4.7 *The moment distribution M_{xf} in the y-direction according to the yield line theory, the strip method and the FE-analysis (FEM-Design).*

4.5.2 The sum of the moments

In this section the two traditional design methods are compared using the total sum of the field moments and support moments, respectively.

The total sum of the support moment or the field moments are defined as

$$\sum M = \int_A \bar{m}\, dA = \sum \bar{m}_i A_i \qquad 4.10$$

and when the sum of the areas is equal to the total distribution area the formula finally become

$$M_\Sigma = \bar{m}_i \cdot b_i \cdot l_i \qquad 4.11$$

where M_Σ is the respective total sum of the design support moments or the design field moments in direction x or y [Nm^2]

$\bar{m}_i$ is the respective average design support moment or design field moment in direction x or y [Nm/m]

b_i is the width of the sideways distributed design moment [m]

l_i is the length over which the design moment works [m]

The sum of the design moment according to the yield line theory

The total sum of the support moment according to *Equation* 4.11 and the geometry in *Figure* 4.8, gives

$$M_{\Sigma xs} = m_{sc} \cdot c^2 + m_{sb'} \cdot c \cdot b =$$
$$= 60.3 \cdot 3.6^2 + 7.7 \cdot 3.6 \cdot 12 = 1114.1\ kNm^2$$

The total sum of the field moment is

$$M_{\Sigma xf} = m_{fA} \cdot b' \cdot a + 2 \cdot \frac{m_{fA}}{2} \cdot \frac{(b - b')}{2} \cdot a =$$
$$= 19.4 \cdot 7.2 \cdot 12 + 2 \cdot \frac{19.4}{2} \cdot \frac{(12 - 7.2)}{2} \cdot 12 = 2234.9\ kNm^2$$

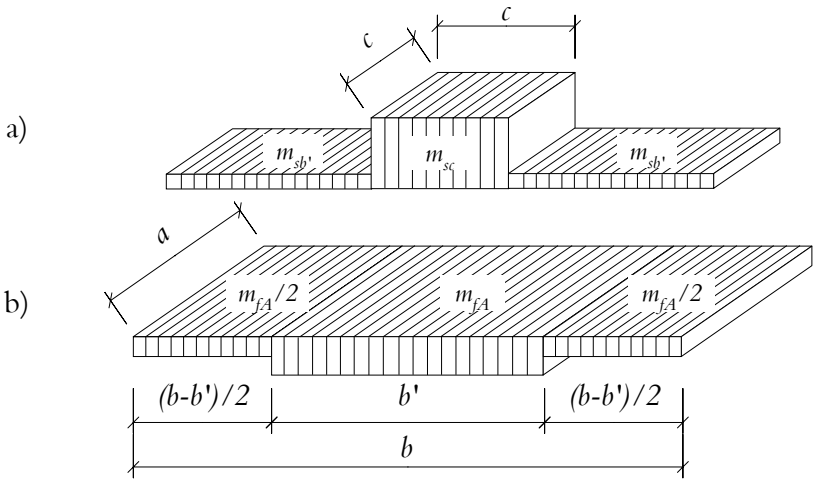

Figure 4.8 The distribution of a) the design support moment and b) the design field moment according to the yield line theory.

The sum of the design moment according to the strip method

The total sum of the support moment according to *Figure* 4.9, is

$$M_{\Sigma xs} = \frac{1}{2} m_{xs} \left[\left(b_c + 2\gamma c_{x2} \right) + \left(b_c + 2\frac{2}{3}\gamma c_{x2} \right) \right] \left(b_c + 2\beta c_{y2} \right) +$$

$$+ \frac{1}{2} \cdot 2 \frac{m_{xs}}{4} \left[\left(b_c + 2\gamma c_{x2} \right) + \left(b_c + 2\frac{2}{3}\gamma c_{x2} \right) \right] \left(1 - \beta \right) c_{y2} =$$

$$= \frac{1}{2} \cdot 60.6 \left[\left(0.4 + 2 \cdot 2.14 \right) + \left(0.4 + 2 \cdot 1.43 \right) \right] \left(0.4 + 2 \cdot 0.5 \cdot 3.63 \right) +$$

$$+ \frac{1}{2} \cdot 2 \cdot \frac{60.6}{4} \left[\left(0.4 + 2 \cdot 2.14 \right) + \left(0.4 + 2 \cdot 1.43 \right) \right] 0.5 \cdot 3.63 = 1187.3 \; kNm^2$$

The total sum of the field moment is

$$M_{\Sigma xf} = m_{xf} \cdot \left(b_c + 2c_{y2} \right) L_x + \frac{m_{xf}}{3} \left[L_y - \left(b_c + 2c_{y2} \right) \right] L_x =$$

$$= 21.4 \left(0.4 + 2 \cdot 3.63 \right) 12 + \frac{21.4}{3} \left[12 - \left(0.4 + 2 \cdot 3.63 \right) \right] 12 = 2338.6 \; kNm^2$$

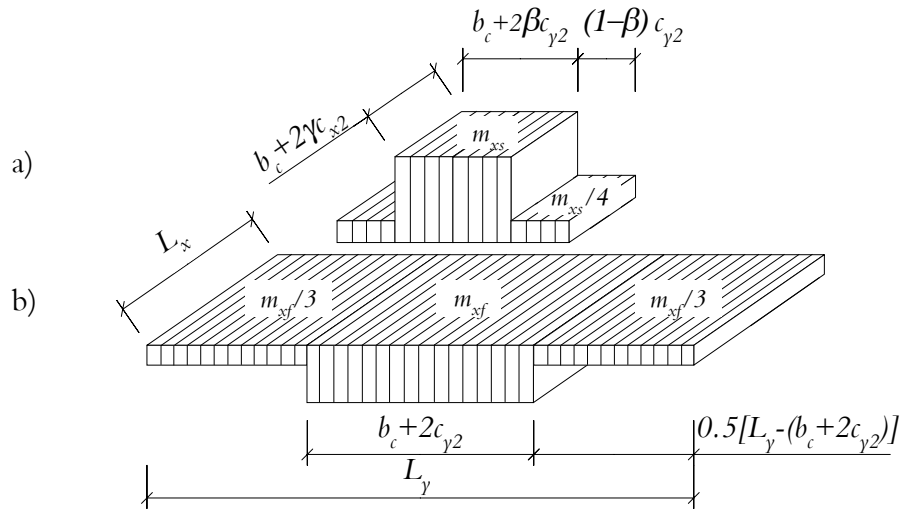

Figure 4.9 The distribution of a) the design support moment and b) the design field moment according to the strip method.

Distribution length, x [m]		**Distribution width, y [m]**		**Sum of the support moments, $M_{\Sigma xs}$ [kNm/m]**		**Sum of the field moments, $M_{\Sigma xf}$ [kNm/m]**		**Ratio YL/SM**
YL	**SM**	**YL**	**SM**	**YL**	**SM**	**YL**	**SM**	
3.6	4.68 (3.26)	3.6	4.03	781.5	969.5			0.81
3.6	4.68 (3.26)	12	2×1.81	332.6	218.3			1.52
12	12	7.2	7.66			1676.2	1967.1	0.85
12	12	2×2.4	2×2.17			558.7	371.5	1.50
			Sum:	**1114.1**	**1187.8**	**2234.9**	**2338.6**	

Table 4.5 Comparison of the sum of moment distribution between the yield line theory (YL) and the strip method (SM). The lenghts with brackets corresponds to Equation 4.9.

The strip method results in more reinforcement than the yield line theory both for the support moments (7%) and the field moments (5%), in total the strip method results in 5% more bending reinforcement than the yield line theory, see *Table* 4.5.

5 FE-based analyses and design

5.1 Introduction

Traditional design of flat slab floors starts with hand calculations of the support and field design moments, usually according to linear elastic theory. The moments are then redistributed according to the design method to give optimal reinforcement in regard of performance and financial costs. Thereafter the required reinforcement areas are calculated for each distribution area, to which additional reinforcement is added to prevent cracking and punching.

A computer-aided design method based on FE-theory calculates all internal forces at every element in the structure according to linear elastic theory. The required reinforcement areas are then given at every element in the mesh. Normally the reinforcements are not redistributed any further to obtain a reinforcement design for practical use.

It is necessary to have control on the magnitude of the internal forces e.g. moments in cases of linear elastic FE-analyses, see e.g. *Section* 2.4.6. The mesh generator must create a balanced mesh considering the element angles, the size of two adjacent element areas etc, see also *FEM-Designs Plate manual*. If the moment distribution is compared between the three models modelled with quite large difference in the mesh, see *Figure* 2.9 or *Figure* 2.10, it is clear that the size of the maximum field moment is almost independent of the FE-mesh. Therefore, it is only necessary to control the size of the maximum support moment in areas of interior columns. Observe that problems of mesh densities also occurs in plates supported by interior walls, exterior columns, and corner columns or in areas of holes.

In this section the traditionally designed reinforcement, see *Chapter* 4, is analysed by FEM-design with respect to bending, punching, cracks and deformations.

A new method is derived from the results of the analyses and the capabilities in FEM-Design. The proposed method redistributes the calculated reinforcement areas from a FE-analysis in appropriate strips with respect to bending moments, crack distribution and punching.

5.2 Method

The reinforcement quantities according to the two traditionally design methods are analysed by FEM-Design in order to check cracking, punching capacity and deformations. A FE based redistribution method is developed based on the evaluated results with respect of cracks, punching capacity and deformations. The method is used to design the same model and finally, the distributed quantities of reinforcement are compared between the methods in order to motivate the developed method's usability.

5.3 FE-analyses of the traditionally designed reinforcement

5.3.1 Yield line theory

Control of shear and punching capacity

The designed bending reinforcement areas and its distribution are applied in FEM-Design in order to control the shear capacity and its resistance against punching. The easiest way to apply the reinforcement is to use the drawing tool in FEM-Design to define the distribution lengths and widths where the reinforcement areas are defined, see *Figure* 5.1.

It is suitable to first control the applied quantity of reinforcement when cracking is not considered, in order to detect eventually areas of missing *bending* reinforcement before the control of the shear- and the punching capacity.

Figure 5.2 shows the dialog box of the missing bottom reinforcement. The bottom limit is set to zero to avoid displayed quantities of too much defined reinforcement that always appears when the reinforcements are distributed as average reinforcements.

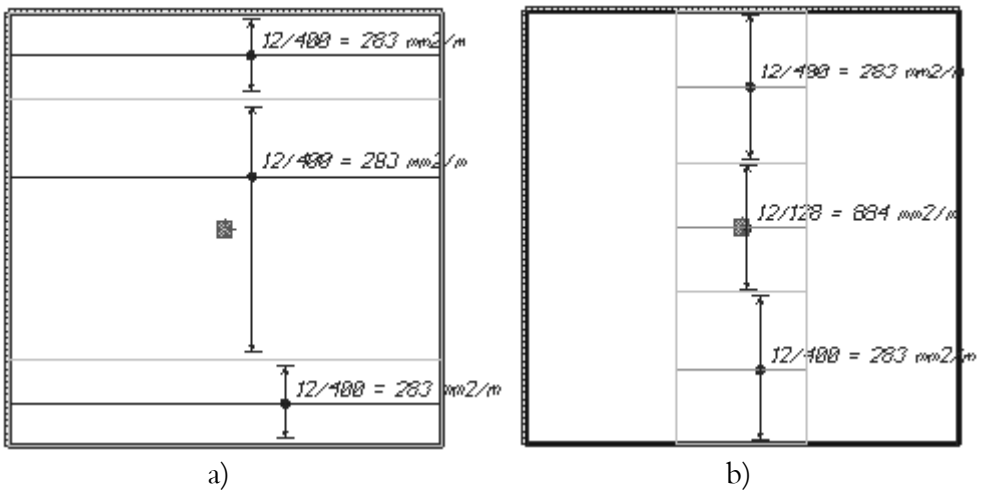

Figure 5.1 *The applied areas of bending reinforcement in a) the bottom and b) the top, in the x-direction.*

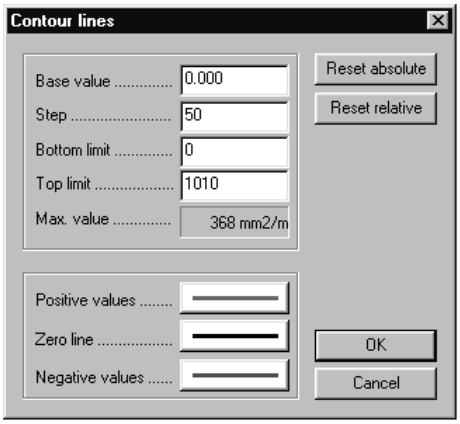

Figure 5.2 *Dialog box of missing bottom reinforcement.*

This means that only the quantities of missing reinforcement will appear in the displayed model. *Figure* 5.3a shows that 84.4 mm^2/m bottom reinforcement is missing in the field strip where the largest quantities of reinforcement are distributed. The missing reinforcement is quite little and is barely equal to one bar per each meter.

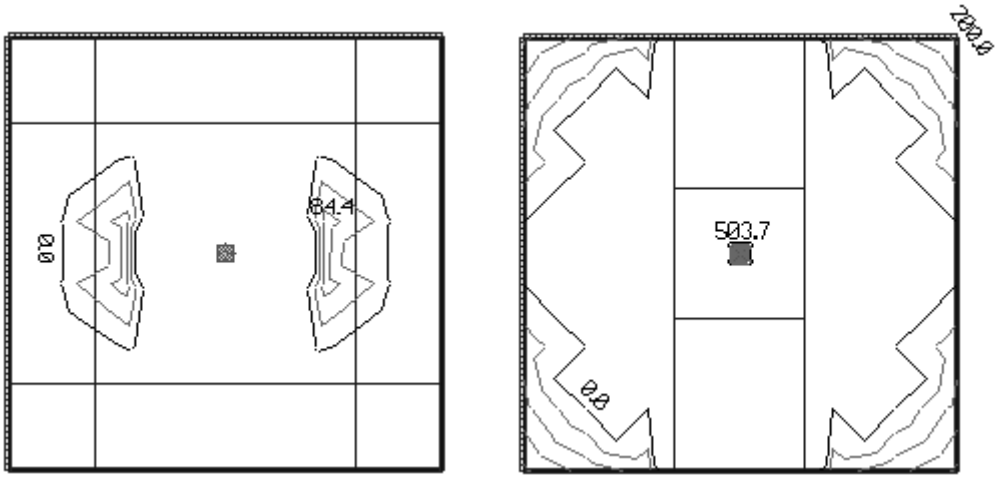

a) b)

Figure 5.3 The missing a) bottom and b) top bending reinforcement in x-direction, when cracking is not considered.

Figure 5.3b shows that a quite large quantity of top reinforcement is missing in the corners, this is due to large twisting moments and is neglected here because the problem is not concerned in this master thesis. The largest quantity of missing bending reinforcement 503.7 mm^2/m is found in centre of the column. This quantity corresponds to the difference between the applied average bending reinforcement and the calculated required bending reinforcement by FEM-Design, compare the distribution of the support moment between yield line theory and FEM-Design in *Figure* 4.5 or *Figure* 4.6.

Figure 5.4 shows that the yield line designed slab has enough shear capacity, since all shear values are zero.

The punching control performed by FEM-Design marks the column green, yellow or red. A green marked column means that the capacity of punching is enough i.e. it fulfils the criteria

$$V_u \geq V_d$$

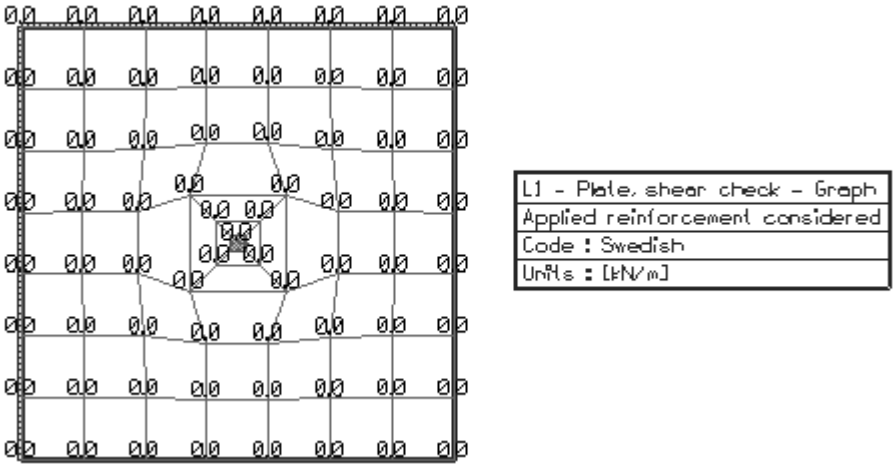

Figure 5.4 The results of the shear check, when applied bending reinforcement is considered.

An yellow column means that the punching capacity will be enough if the displayed quantity of shear reinforcement is applied in the slab i.e. it fulfils the criteria

$$V_{us} \geq V_d$$

A red column means that the punching capacity in the area of the column is not enough i.e. it does not fulfil either of the above criteria or

$$V_u < V_{us} < V_d$$

The slab does not pass the punching control in this case when only the quantity of the designed bending top reinforcement is considered (the variables are explained on the next page), see *Figure* 5.5a. One of the following actions can be used to increase the punching capacity.

1. Increasing the plate thickness or/and the quality of the concrete.
2. Applying of a beam (possible in FEM-Design) or a column head or/and a strengthening plate between the plate and the column (not yet possible in FEM-Design).
3. Increasing the amount of top reinforcement in the column strip.

Remark that 1-3 demand a consideration of the plate's location and the workability at the concreting contra the additional costs.

In this case the amount of the top reinforcement is increased in the column strip and the needed quantity to pass through the punching control can approximately be calculate as

$$A_{s\,new} = A_{s\,old}\frac{V_d}{V_{us}} \qquad 5.1$$

which not immediately gives the exact quantity, but the applied quantity does at least not exceed the required reinforcement.

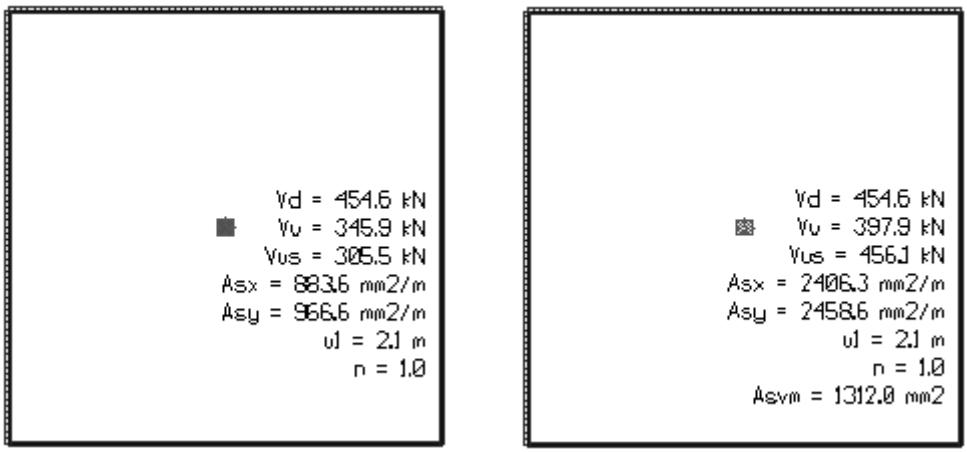

a) b)

Figure 5.5 *The results of a) the <u>not passed</u> punching control (column becomes red) when only bending reinforcement is considered and b) the <u>passed</u> punching control (column marks yellow i.e. the capacity becomes large enough with respect of applied main reinforcement and displayed amount of required shear reinforcement).*

The parameters in *Figure* 5.5a-b are defined as follows

- V_d is the design reaction force at the support.
- V_u is the punching capacity of the cross section including the concrete and the bending reinforcement.
- V_{us} is the punching capacity of the cross section including the concrete, the bending- and the shear reinforcement.

A_{sx} is the considered top bending reinforcement in x-direction.

A_{sy} is the considered top bending reinforcement in y-direction.

u_1 is the length of the critical punching perimeter.

n is a factor of eccentricity depending on eccentricity between the load carrying areas which surrounds the column.

A_{svm} is the total area of shear reinforcement in both directions that on the safe side is assumed to consist of bent bars with 60 degrees bending angle.

Location	**Distribution length, *x* [m]**	**Distribution width, *y* [m]**	**Reinforcement area [mm²/m]**	
			A_{sx}	A_{sy}
Column, top	3.60	3.60	**2406.3**	**2458.6**
Outside column, top	3.60	2×4.20	283.0	283.0
Field, bottom	12.00	7.20	283.0	283.0
Edge, bottom	12.00	2.40	283.0	283.0

Table 5.1 The necessary quantities of top reinforcement and its distribution lengths and widths on account of punching (the increased quantity is bold). Observe that the shear reinforcements are not specified.

Figure 5.5b and *Table* 5.1 show that the necessary quantity of the punching reinforcement is quite large, and it will in this case decrease the workability dramatically when the distance between the bars only becomes 47 mm in x-direction and 46 mm in y-direction. One possibility is to arrange the bars in groups with minimum allowed distance between the bars. Another is to increase the thickness of the slab.

Notice that the punching control is performed for the total amount of the applied reinforcement without considering the directions. This means that the necessary quantities of punching reinforcement in x- and y-direction can be tried out simultaneously in each direction in the column strip or applied likewise at the control. The given quantity of shear reinforcement in *Figure* 5.5b is applied likewise in both directions at practical reinforcing.

Control of cracks and deformations

The presence of cracks and their widths in flat slab floors are regulated according to Swedish code in *BBK 94*. For indoors flat slab floors there exists no maximum crack width considering the resistance against corrosion, but if the slab is not provided with a lining there almost always exists criteria of functionality such as esthetical criteria e.g. non visible cracks.

The corresponding quantity of bending reinforcement according to *Table 4.2*, are applied in FEM-Design Design and the resistance against cracks and deformations are controlled.

If the yield limit is reached somewhere in the plate two warning messages will be displayed, see *Figure* 5.6a-b. Two options is possible, to break or to continue the calculations. If *break* is chosen the analyses stops completely.

a)

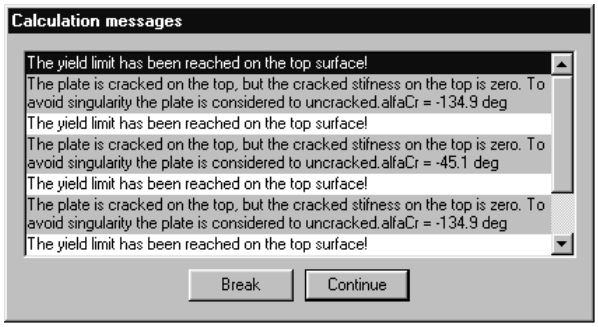

b)

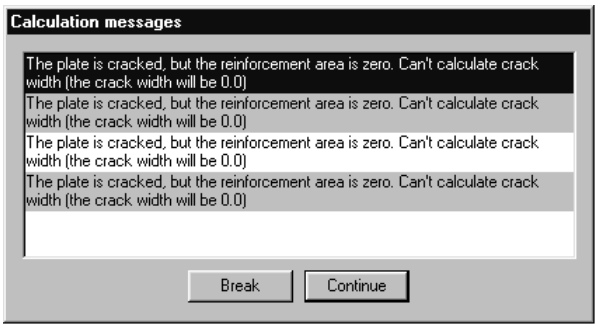

Figure 5.6 The messages during the crack calculation for a) the reached yield limit and b) the failed crack calculation in the corners on the top surface.

Is instead *continue* chosen, like in this case, the lacks of top reinforcement in the specific area leads to that neither the crack width nor the change of the stiffness can be calculated in the area, according to *Figure* 5.6a-b. At the same time the location will be pointed out, see *Figure* 5.7. Notices that corner reinforcing are not concerned in this thesis.

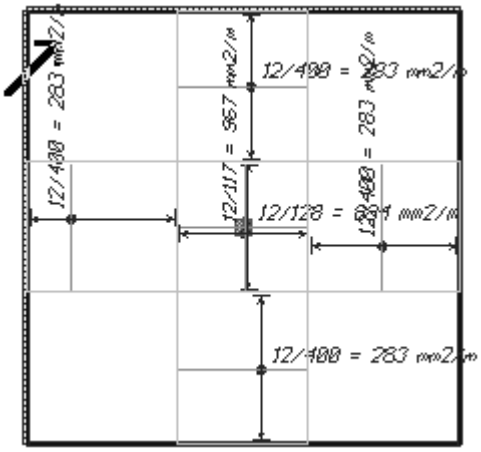

Figure 5.7 The point where the yield limit is reached on the top surface.

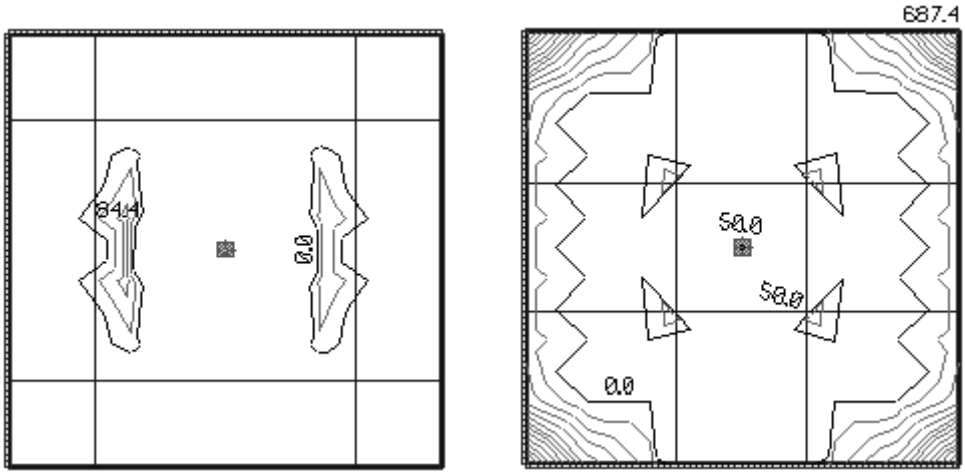

Figure 5.8 The missing a) bottom and b) top bending reinforcement in x-direction, when cracking is considered.

Figure 5.8a show that the missing quantities of bottom reinforcement have not changed in comparison with *Figure* 5.3a, despite that cracking is considered.

Figure 5.8b show that the missing quantities of top reinforcement in the corners have increased dramatically in comparison with *Figure* 5.3b, when cracking is considered. On the other hand, the missing quantities of top reinforcement above the column centre have decreased quite substantial, but the applied quantity in this area will be needed later on for the punching capacity. It is also observed that the yield line distributes too much reinforcement outside the column strip considering bending and cracks, compare *Figure* 5.8b with *Figure* 5.9b.

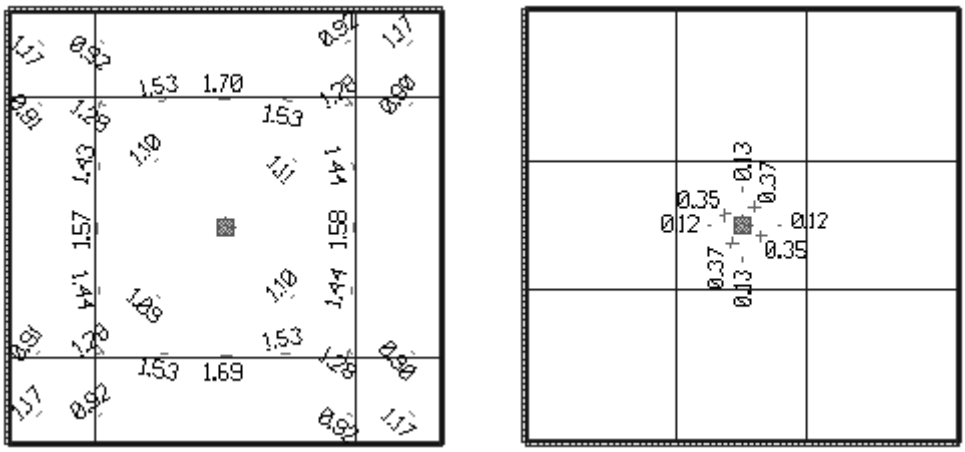

a) b)

Figure 5.9 *The crack widths and the distribution in a) the bottom and b) the top when bending reinforcement is considered.*

Figure 5.9a-b show that the slab is cracked in the bottom and the top, and the largest width of cracks appears in centre of each span in the field strips where the largest field moments acts.

To illustrate the capability of FEM-Design and its possibilities to deal with cracks the plate is assumed to be visible on both the bottom and top surface and the applied quantities of reinforcement are optimised with respect of a assumed allowed crack width of 0.20 mm. In the dialog box of the reinforcement data the quantity of the reinforcement is increased by decreasing the space between the bars, see *Figure* 5.10.

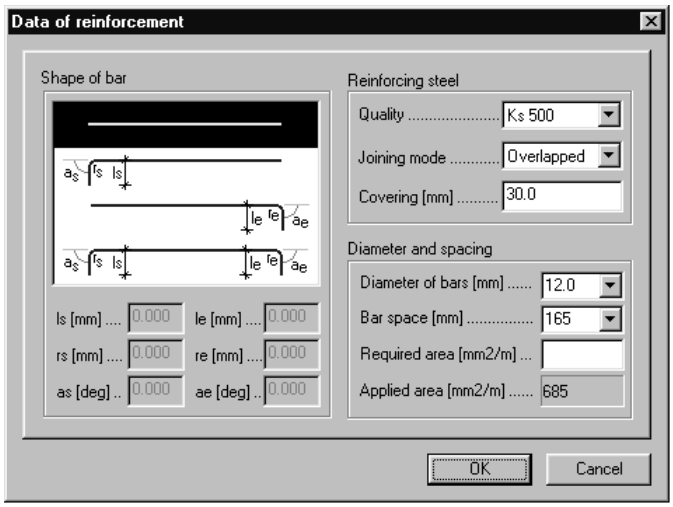

Figure 5.10 The dialog box of reinforcement data applied in a particular area.

Figure 5.11 show the distribution and the widths of the cracks at *final design* i.e. when punching reinforcement is added in the column strip, see *Figure* 5.5b, and the bottom reinforcement are increased in both the field and the edge strips until the assumed allowed maximum crack width is achieved.

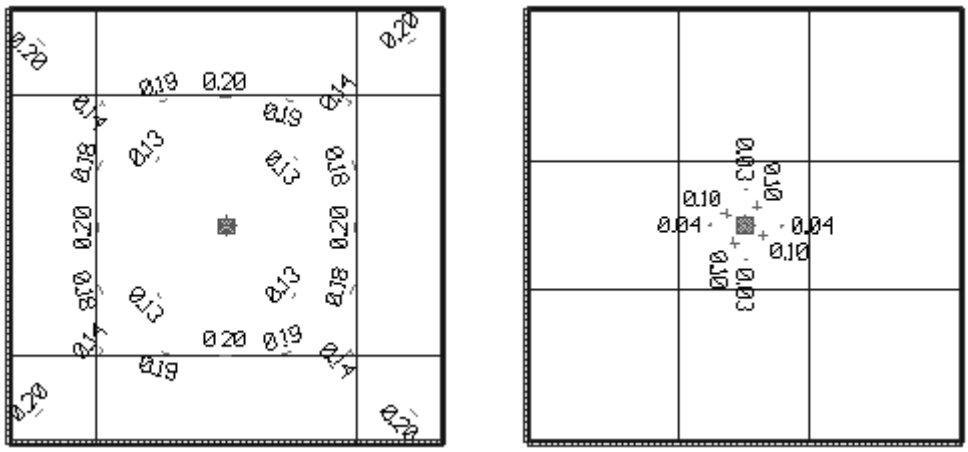

a) b)

Figure 5.11 The crack widths and the distribution in a) the bottom and b) the top at final design i.e. when punching reinforcement is applied and the bottom reinforcement are increased in both the field and the edge strips until a crack width of maximum 0.20 mm is achieved.

The maximum allowed deformation i.e. deflection is not given in the Swedish code, on the other hand the customer usually gives some criteria. Here is a more generally criteria used according to

$$w \le \frac{l}{400} = \frac{6}{400} = 0.015\,m \qquad 5.2$$

Figure 5.12 shows that the largest deflection is 9.4 mm, which is about 60% of the design criterion.

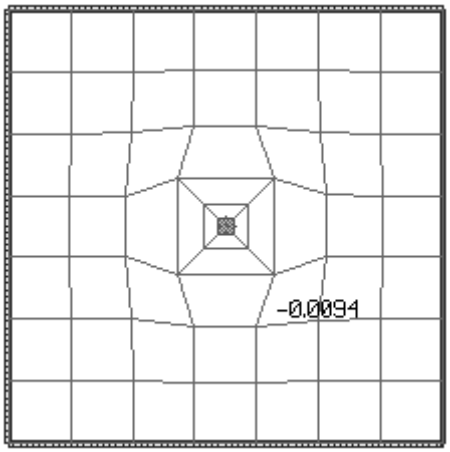

Figure 5.12 The largest deflection in the slab at the final design when cracking is considered.

The necessary quantities of reinforcement for the final design are specified in *Table* 5.2.

Location	**Distribution length, x [m]**	**Distribution width, y [m]**	**Reinforcement area [mm²/m]**	
			A_{sx}	A_{sy}
Column, top	3.60	3.60	(884.5) 2406	(884.5) 2459
Outside column, top	3.60	2×4.20	(283) 283	(283) 283
Field, bottom	12.00	7.20	(283) 891	(283) 919
Edge, bottom	12.00	2×2.40	(283) 685	(283) 685

Table 5.2 The quantities of applied reinforcement areas and its distribution lengths and widths at final design i.e. with respect of punching and a maximum allowed crack width of 0.20 mm (areas in brackets are the bending reinforcement at start).

5.3.2 Strip method

Control of shear and punching capacity

Figure 5.13 show the applied quantities of bending reinforcement according to *Table* 4.3. Notice that the reinforcement in the column and the side strip are applied only with the longer lengths i.e. according to *Equation* 4.8 in order to simplify the optimisation of the reinforcement at the control of the punching capacity.

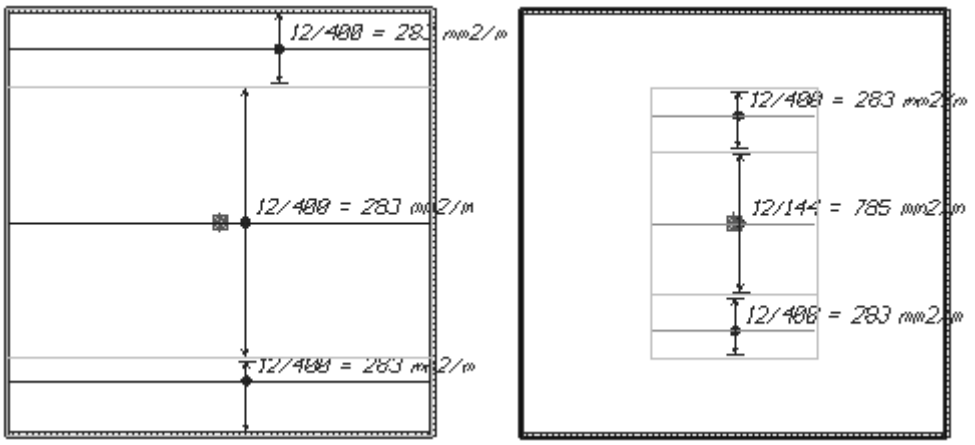

Figure 5.13 The applied areas of a) bottom bending reinforcement A_{sxf} and b) top bending reinforcement A_{sxs} in the x-direction.

Figure 5.14a shows that the same quantity of bottom reinforcement is missing as for the yield line design. *Figure* 5.14b shows that the strip method distributes the top reinforcement worse than the yield line design in the area of the column in comparison with required reinforcement according to FEM-Design, see *Section* 5.3.1. On the other hand, the strip method distributes the top reinforcement in the side strip better than the yield line theory in consideration of the locations of bending moments in the slab.

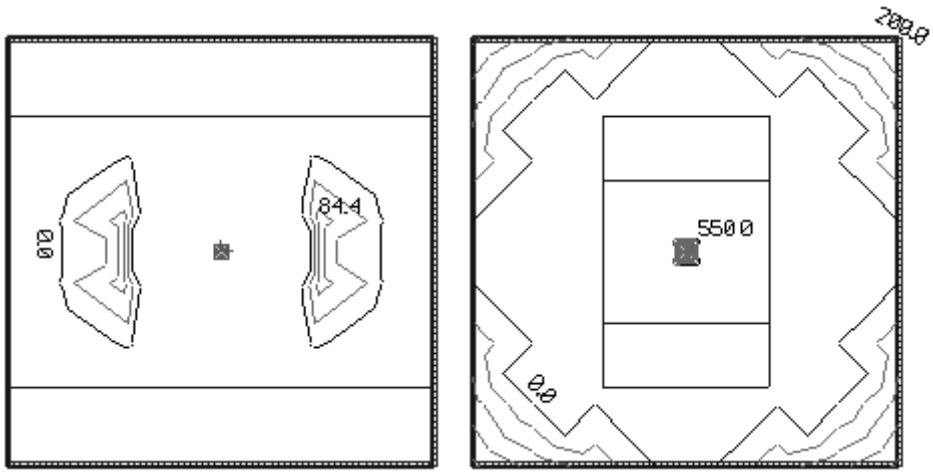

Figure 5.14 The missing areas of a) bottom reinforcement and b) top reinforcement, when cracking not is considered.

Figure 5.15 shows that the strip method designed slab has enough shear capacity, since all shear values are zero.

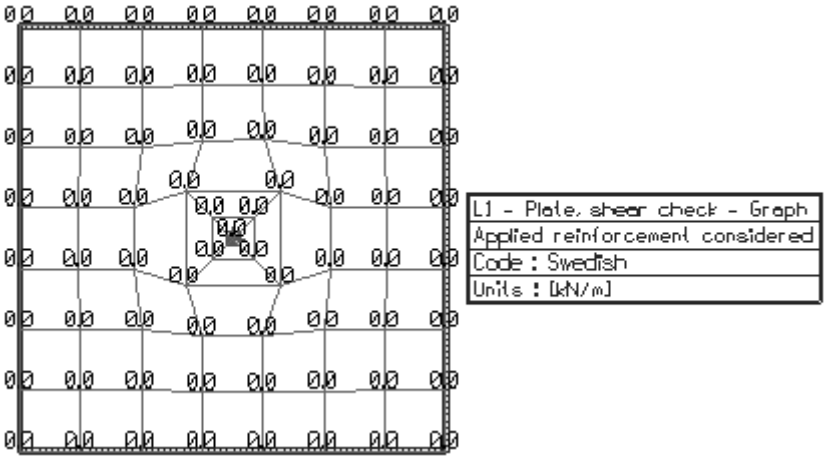

Figure 5.15 The results of the shear check, when applied bending reinforcement is considered.

Figure 5.16 shows the not passed punching control when only the applied quantity of bending reinforcement is considered. *Figure* 5.17 shows the passed punching control. Observe that the results are the same as for the yield line designed slab in *Section* 5.3.1, compare with *Figure* 5.5b. The design criteria and the variables are explained in *Section* 5.3.1, like the possible ways to increase the punching capacity.

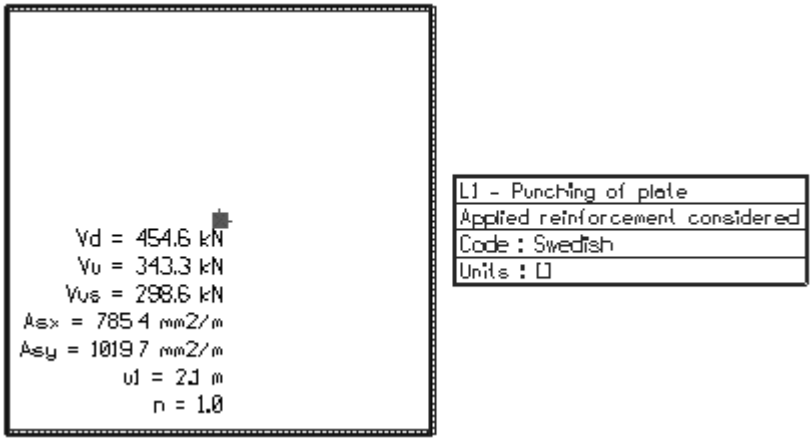

Figure 5.16 *The results of the <u>not passed</u> punching control (the column becomes red) when applied bending reinforcement is considered.*

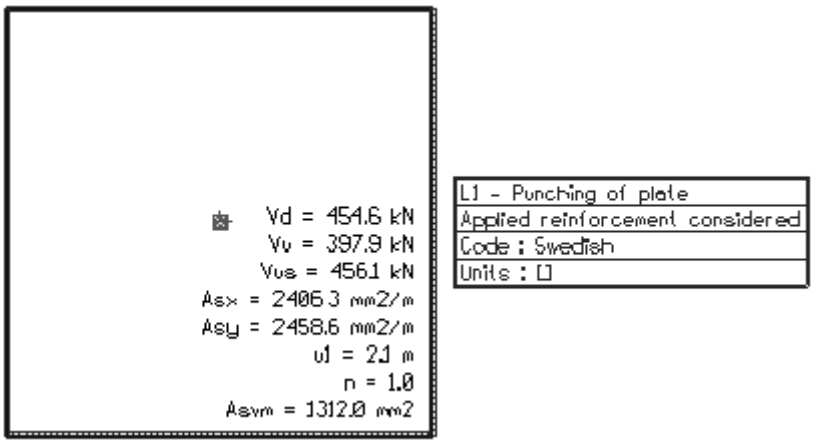

Figure 5.17 *The results of the <u>passed</u> punching control (the column becomes yellow) when the punching capacity becomes large enough with respect to both applied main reinforcement and added shear reinforcement.*

Control of cracks and deformations

Like in *Section* 5.3.1 the corresponding quantities of designed *bending* reinforcement according to *Table* 4.3, are applied in FEM-Design and the resistance against cracks and deformations are controlled.

Figure 5.18a shows that the missing bottom reinforcement has increased a little in the field strip when cracking is considered. This confirms that the calculated moment distribution according to linear elastic theory is quite suitable for plate's behaviour in Serviceability State. In comparison between *Figure* 5.18a and *Figure* 5.14a, it is seen that the crack analysis by FEM-Design redistributes the internal moments with respect of the changed stiffness i.e. the appearance of cracks, and therefore even the missing reinforcement. Compare *Figure* 5.18a and the appearance of cracks in *Figure* 5.19.

Figure 5.18b shows that the missing top reinforcement has increased quite much in the corners when cracking is considered. On the other hand, the missing top reinforcement has decreased in centre of the column, compare with *Figure* 5.14b.

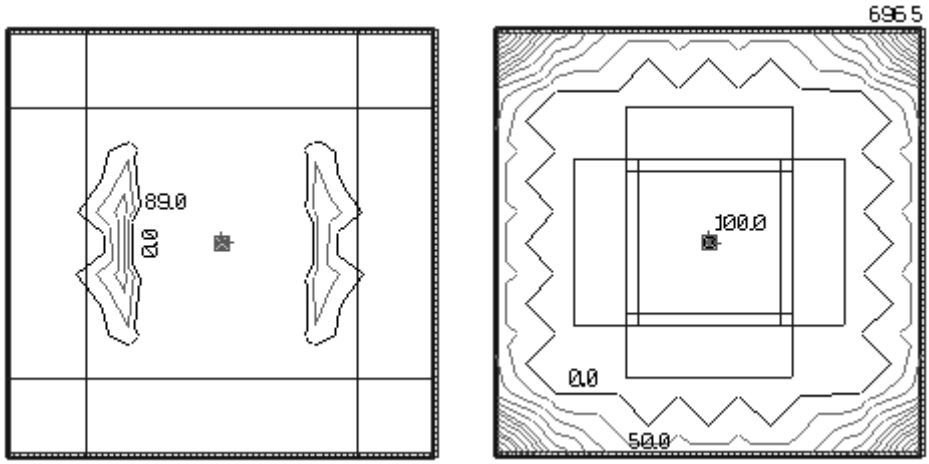

a) b)

Figure 5.18 The missing a) bottom and b) top reinforcement in x-direction, when reinforcement according to and cracking is considered.

Figure 5.19a-b show that the slab is cracked in the bottom and the top, and the largest width of cracks appears in centre of each span in the field strips where of course the largest field moments acts.

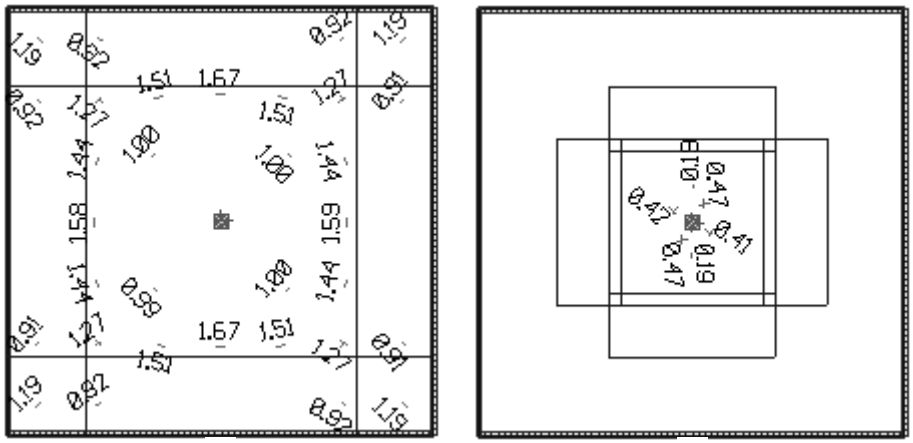

a) b)

Figure 5.19 The crack widths and the distribution in a) the bottom and b) the top when only bending reinforcement according to Table 4.3 *is considered.*

Like before FEM-Design's possibilities are used to optimise the reinforcement with respect to the allowed crack width of 0.20 mm. Note that the yield limit is also here reached at the corners and the crack width is therefore not calculated in this area (not considered in the thesis).

The quantity of the reinforcement is increased in the dialog box of the reinforcement data like before, by decreasing the space between the bars.

Figure 5.20 shows the distribution and the widths of the cracks for the *final design* i.e. punching reinforcement is considered, see *Figure* 5.17, and the bottom reinforcements are increased in both the field and the edge strips until the assumed maximum crack width is achieved. The necessary quantities of applied reinforcements are specified in *Table* 5.3.

Location	**Distribution length, *x* [m]**	**Distribution width, y [m]**	**Reinforcement area [mm²/m]**	
			A_{sx}	A_{sy}
Column, top	4.68	4.03	(785) 2406	(857) 2459
Side, top	4.68	2×1.81	(283)	(283)
Field, bottom	12.00	7.66	(283) 891	(287) 942
Edge, bottom	12.00	2×2.17	(283) 702	(283) 702

Table 5.3 The quantities of the applied reinforcement areas for the final design i.e. with respect of punching and a maximum crack width of 0.20 mm (areas in brackets are the bending reinforcement from start).

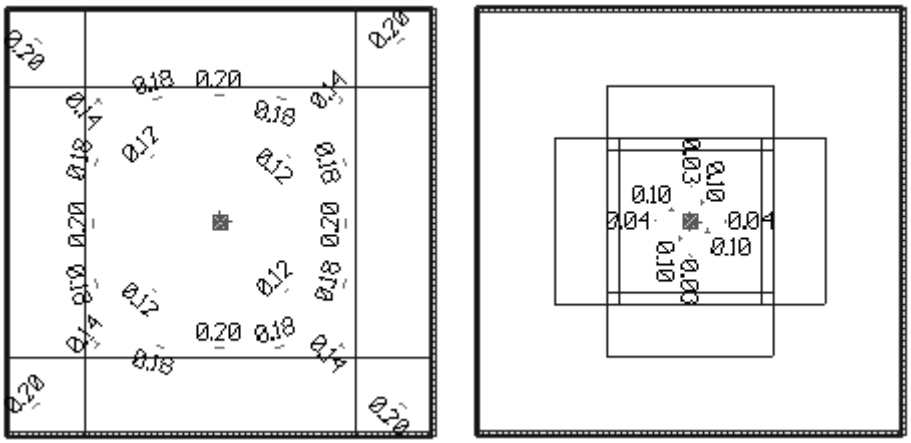

a) b)

Figure 5.20 The crack widths and the distribution in a) the bottom and b) the top at final design i.e. when punching reinforcement is applied and the bottom reinforcement are increased in both the field and the edge strips until a crack width of maximum 0.20 mm is achieved.

Figure 5.21 shows that the largest deflection is 9.3 mm, which means that the maximum deflection in the slab is less than the deflection criteria given in *Equation* 5.2.

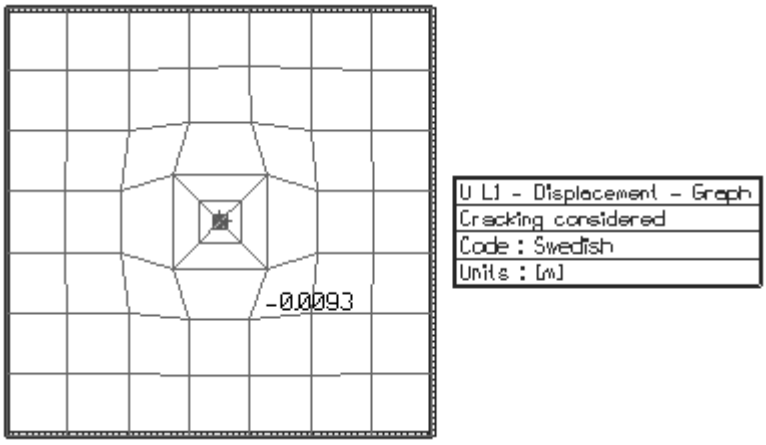

Figure 5.21 The largest deflection in the slab for the final design when cracking is considered.

5.4 Proposed new FE-based design method

In *Section* 4 the design moments, the reinforcement quantities and the distribution distances are determined approximately using hand calculations. A possibility to get more correct distribution distances are to determine the required quantities of bending reinforcement and both the laterally and the longitudinally distribution directly from FEM-design. It would also be convenient and spare a lot of time to take advantage of all possibilities in FEM-Design. The purposes of the new proposed method are to:

- Simplify the estimation of necessary bending reinforcement quantities and laterally and longitudinally redistribution distances directly from FE-results.
- Give a distribution that at the final design decreases the bending cracks and is suitable for the punching capacity.

5.4.1 Selection of the distribution distances

According to the Swedish code:

1. Distribution of reinforcement is recommended to be based on linear elastic theory to ensure correct behaviour in Serviceability State i.e. in both uncracked and cracked conditions, see e.g. Hillerborg *(1996)*.
2. Both bending and torsional moments shall be considered as design moments, see *BBK 94, 6.5.2.1.*
3. Condition of moments in the whole plate shall be considered i.e. the dependencies between the moments in the plate shall be considered, see *BBK 94, 6.5.2.1.*
4. If the design moments vary along a section perpendicular to the length of the reinforcement, the reinforcement design can be performed with average moments within areas of certain widths, provided that the plate's total resistance not changes appreciably. This means that laterally distribution distances can be chosen arbitrary, provided that the resistances are large enough, see *BBK 94, 6.5.3.1.*
5. At calculations according to elastic theory or equilibrium theory, like the strip method, it is possible to specify different moment curves in different directions and finish the reinforcements according to a so-called displaced tension forced curve. At calculations according to the yield line theory this method is not really applicable. All reinforcement that is allotted to a certain yield line shall instead be anchored outside this yield line, because a shortening of the reinforcement changes the position of the yield lines, see *BBK 94, 6.5.8.2.*

The calculation of design moments performed by FEM-Design considers both the bending moments and the torsional moments in the whole plate, simultaneously. The required bending reinforcement is calculated proportional to the design moments with respect of defined reinforcements and concrete cover in each direction. User defined quantities of reinforcement can be applied in eligible areas considering the required reinforcement, resistance against shear, punching, cracks and deformations, as demonstrated in *Section* 5.3.1-2 and in the following sections. Finally, the conclusion is that FEM-Design fulfils all the requirements according to Swedish code and in addition, saves time and a lot of calculations, but the problem is to distribute the user defined reinforcement in suitable areas, which ensures enough resistance against bending, shear, punching, cracks and deformation.

The derived methods *longitudinal* distribution distances for both the top and the bottom reinforcement is determined with respect of the curve of required reinforcement A'_s in each direction, because the reinforcement areas are proportional to the moments. This will allow a determination of both the distribution distances and the quantities of the reinforcement in the same figure.

The *lateral* distribution of the top reinforcement in the *column strip* is established with respect of FEM-Design's calculation of the punching capacity, which is based on the theory that the internal moments and the shear forces are polar symmetrically distributed around the column centre i.e. the lateral distance is equal to the longitudinal distance. But, if this distance is used as the lateral distribution then no respect is taken to unsymmetrical plates i.e. the lateral distribution of moments can be wider in the plate's longer direction, and the resistance against cracks in the top of the plate runs the risk to be deteriorated. Therefore, it is better to determine the lateral redistribution from the longitudinal distribution of required reinforcement i.e. from the curve of required reinforcement in perpendicular direction to reinforcing direction, when this distances changes with the plate's length.

Accordingly, the *lateral* distribution of the top reinforcement in the *side strip* becomes equal to the remaining part of the lateral distribution of required reinforcement, see *Figure* 5.27.

The *lateral* distribution of the bottom reinforcement in the *field* and the *edge strip* is established with respect of the crack pattern in bottom of the plate, see *Figure* 5.19a. This when the cracks in the bottom are gathered in a circle around the column and the largest cracks appear in an almost straight line parallel with the slab edge in each span. So, the most appropriate lateral distribution distance seems to be equal to the total width of the column and the side strip.

5.4.2 Selection of the design moments

Dick Lundell, a skilled designer at Skanska Teknik, Malmö, discovered a connection between FEM-Design and the yield line theory that is based on the part of N Nylander's and S Kinnunen's method to distribute the calculated support moment, see e.g. Elfgren, L *et al (1969)*. Therefore Dick recommends that the column edge moment should be used as the design support moment.

To verify Lundell's recommendation the calculated design moment of the two traditional methods are compared with the available results of moment distribution in FEM-Design. Both the support moments at the centre and the edge of the column are compared for different mesh densities i.e. lengths of the elements.

The design support moment according to the yield line theory, see *Section* 4.3.1 or *Table* 4.4, was calculated to

$$m_s = 68.0\ kNm/m$$

The design support moment according to the strip method, see *Section* 4.4.1 or *Table* 4.4, was calculated to

$$m_s = 60.6\ kNm/m$$

The edge support moment according to FEM-Design, see *Figure* 5.22, is determined to

$$m_{xs}^{edge} = 75.9\ kNm/m$$

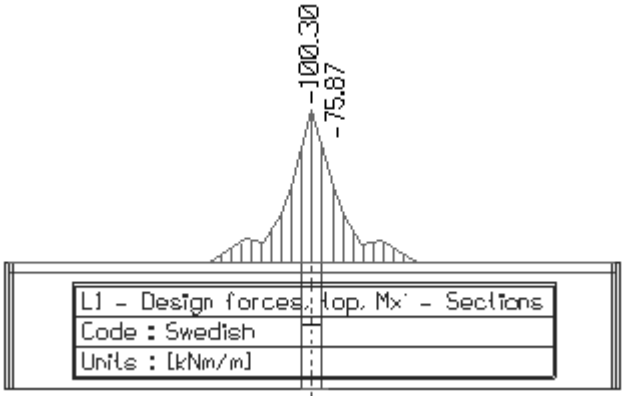

Figure 5.22 The design support moment M'_{xs} in centre and at the edge of the column in model 22 [kNm/m].

In comparison between the design support moment determined by FEM-Design and the two calculated it is seen that FEM-Design calculates the edge support moment about 12-25% larger than the traditional methods. However, this affects only a small area at the column and the design moment is also on the safe side.

Figure 5.23 shows that the *edge* support moment is less sensitive in consideration of the mesh density than the *centre* support moment i.e. confirms Lundell's recommendation.

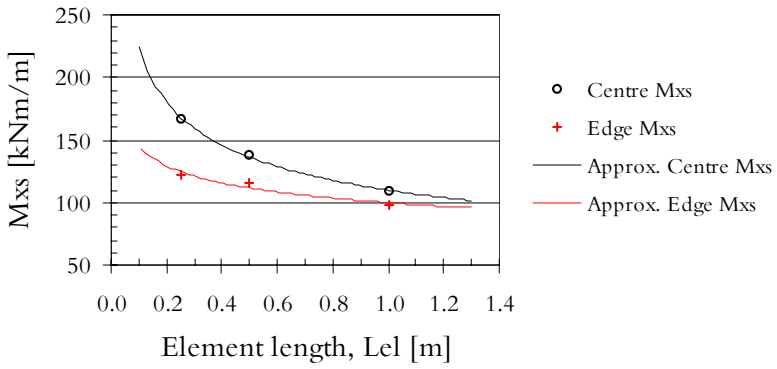

Figure 5.23 Support moment at the centre and the edge of the column in dependency of the mesh density for FEM-Design.

Finally, it can be established that it is suitable to choose the *edge* support moment for interior columns as a representative design support moment, when the automatic mesh generator is used in FEM-Design. In cases of a *user defined mesh* it is recommended to verify the calculated design support moment with one of the traditional design methods. On the other hand, when the maximum field moment seems to be less sensitive of the mesh, it is not necessary to control the size of the maximum field moment, see *Section* 2.4.

5.4.3 Reinforcement quantities and distribution distances

The shape of the moment distribution and the defined longitudinal and lateral distribution distances are illustrated in *Figure* 5.24-26.

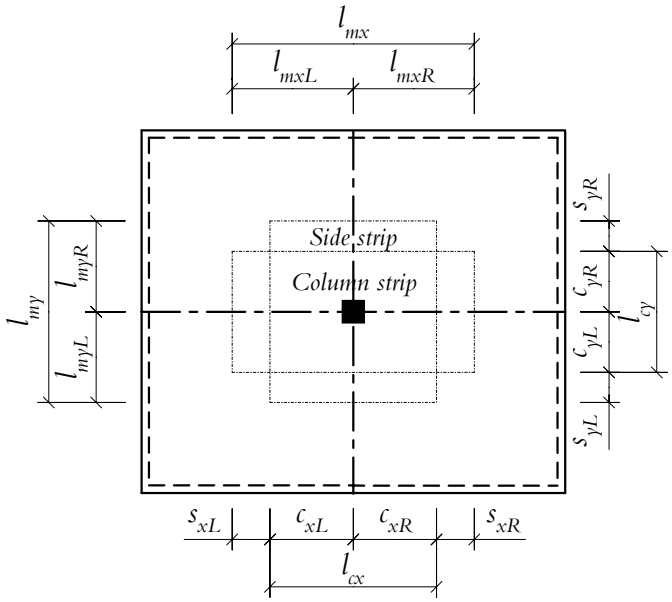

Figure 5.24 Defined strips and distribution distances for the top reinforcement.

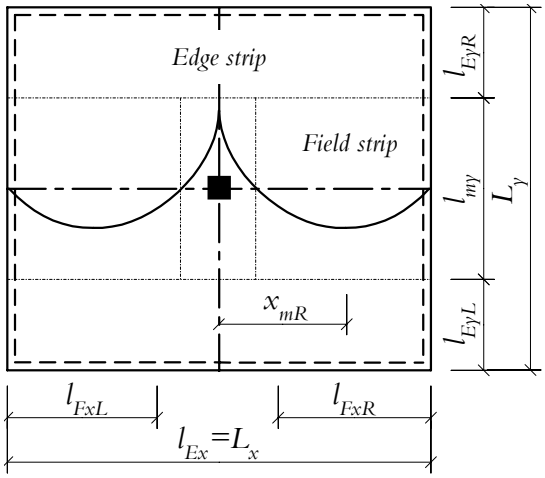

Figure 5.25 Defined strips and distribution distances for the bottom reinforcement, and the shape of the moment distribution.

Top reinforcement

The *longitudinally* distribution i.e. the length of the top reinforcement A_{sxs} in the column and the side strips is measured in *Figure* 5.26a, which is viewed with the option required top reinforcement A_{sxs} in the x-direction, is determined to

$$c_{xR} = c_{xL} = 2.05\ m \quad \Rightarrow \quad l_{cx} = 2 \cdot 2.05 = 4.10\ m$$

The *laterally* distribution i.e. the width of the top reinforcement A_{sxs} in the column strip is measured in *Figure* 5.26b, which is viewed with the option required top reinforcement A_{sys} in the y-direction, is determined to

$$c_{yR} = c_{yL} = 2.05\ m \quad \Rightarrow \quad l_{cy} = 2 \cdot 2.05 = 4.10\ m$$

The distribution distances of the top reinforcement A_{sys} in y-direction determines always analogies to they above i.e. the *longitudinally* distance is equal to

$$c_{yR} = c_{yL} = 2.05\ m$$

and the *laterally* distance is equal to

$$c_{xR} = c_{xL} = 2.05\ m$$

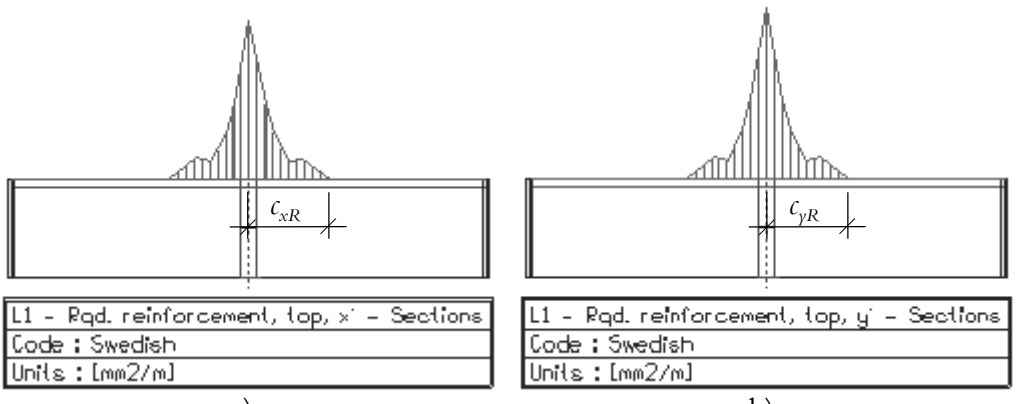

a) b)

Figure 5.26 The measured distance that corresponds to a) the longitudinally and b) the laterally distribution of the top reinforcement A_{sxs} in the column strip.

The total width of both the column and the side strip is measured in *Figure* 5.27, which is viewed with the option required top reinforcement A_{sxs} perpendicular to the reinforcing direction, is determined to

$$l_{myR} = l_{myL} = 3.57\ m \quad \Rightarrow \quad l_{my} = 2 \cdot 3.57 = 7.14\ m$$

with which the *lateral* distribution distance of the top reinforcement A_{sxs} in the *left* and the *right side strips*, due to the symmetry is calculated as

$$s_{yL} = s_{yR} = l_{myR} - c_{yR} = 3.57 - 2.05 = 1.52\ m$$

Due to the symmetry the area of the top reinforcement distributed both *longitudinal* and *lateral* in both the *right* and the *left* column strip is determined to

$$A_{sxs}^{cL} = A_{sxs}^{cR} = A_{sxs}^{A} = 1017.76\ mm^2/m$$

and the average area of the top reinforcement distributed *longitudinal* and *lateral* in the *right* and the *left side strips* is calculated as

$$\overline{A}_{sxs}^{sL} = \overline{A}_{sxs}^{sR} = \frac{A_{sxs}^{B} + A_{sxs}^{C}}{2} = \frac{79.37 + 0}{2} = 39.69\ mm^2/m$$

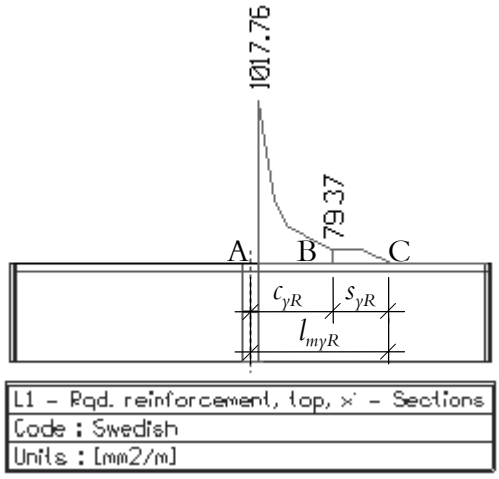

Figure 5.27 The distances and the quantities of the reinforcements that corresponds to the laterally distribution of the top reinforcement A_{sxs} in both the column and the side strips viewed in y-direction.

The total width of both the column and the side strip is measured in *Figure* 5.28, viewed with the option required top reinforcement A_{sys} perpendicular to reinforcing direction, and is determined to

$$l_{mxR} = l_{mxL} = 3.57\ m \quad \Rightarrow \quad l_{mx} = 2 \cdot 3.57 = 7.14\ m$$

with which the *laterally* distribution distances of the top reinforcement A_{sys} in the *left* and the *right side strips*, due to the symmetry are calculated as

$$s_{xL} = s_{xR} = l_{mxR} - c_{xR} = 3.57 - 2.05 = 1.52\ m$$

Due to the symmetry the average area of the top reinforcement distributed *longitudinal* and *lateral* in both the *right* and the *left column strip* is determined to

$$A_{sys}^{cL} = A_{sys}^{cR} = A_{sys}^{D} = 1101.12\ mm^2/m$$

and the average area of the top reinforcement distributed *longitudinal* and *lateral* in the *right* and the *left side strip* is calculated as

$$\overline{A}_{sys}^{sL} = \overline{A}_{sys}^{sR} = \frac{A_{sys}^{E} + A_{sys}^{F}}{2} = \frac{80.67 + 0}{2} = 40.34\ mm^2/m$$

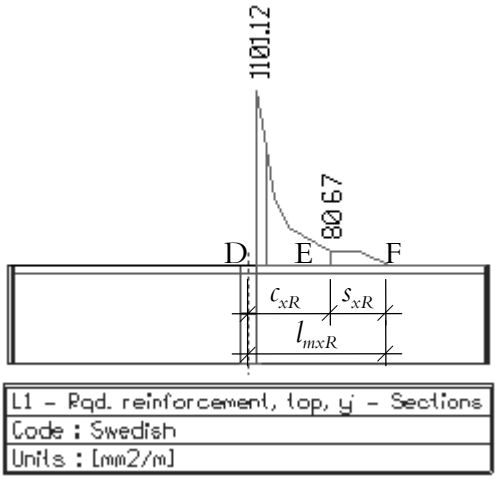

Figure 5.28 *The distances and the quantities of the reinforcements that corresponds to the laterally distribution of the top reinforcement A_{sys} in both the column and the side strips viewed in x-direction.*

Bottom reinforcement

The *longitudinally* distribution distance of the bottom reinforcement in the *field strip* is measured in *Figure* 5.29a viewed with the option required bottom reinforcement in x-direction, and is due to the symmetry determined to

$$l_{FxR} = l_{FxL} = 5.00\ m$$

in the same figure also the distance from the column centre to the *maximum required bottom reinforcement* in x-direction is measured to

$$x_{mR} = x_{mL} = 2.78\ m$$

The corresponding distances in y-direction, see *Figure* 5.29b, are determined to

$$l_{FyR} = l_{FyL} = 5.00\ m$$

$$y_{mR} = y_{mL} = 2.78\ m$$

The *lateral* distribution distances of the *edge strips* reinforced in x-direction are determined from the width of the flat slab floor and the total distribution width of the column and the side strip i.e. the middle strip, as

$$l_{EyR} = l_{EyL} = \left(L_y - l_{my}\right)/2 = \left(12 - 7.14\right)/2 = 2.43\ m$$

and due to the symmetry, for the *edge strips* reinforced in y-direction, as

$$l_{ExR} = l_{ExL} = 2.43\ m$$

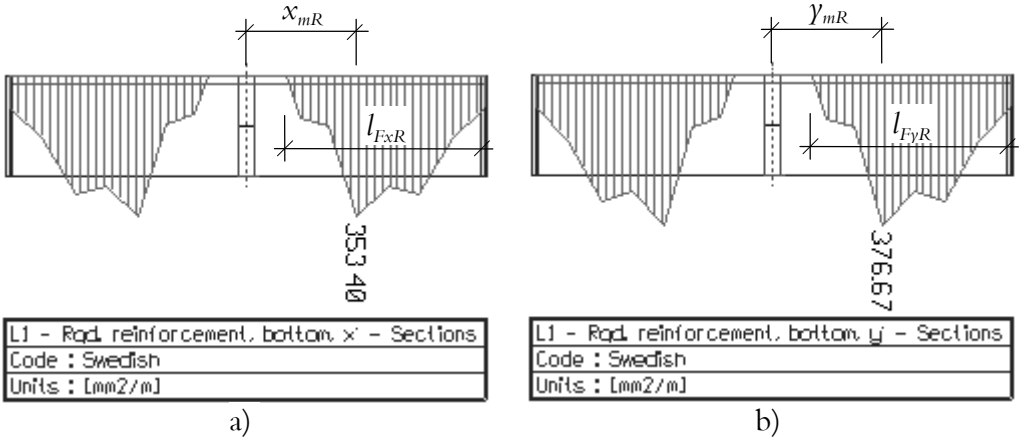

Figure 5.29 The longitudinally distribution distances and the maximum quantities of the bottom reinforcement a) A_{sxf} and b) A_{syf} in the field strips viewed in each reinforcing direction.

A help line is drawn parallel with each edge in order to simplify the displaying of the required bottom reinforcement, see *Figure* 5.30.

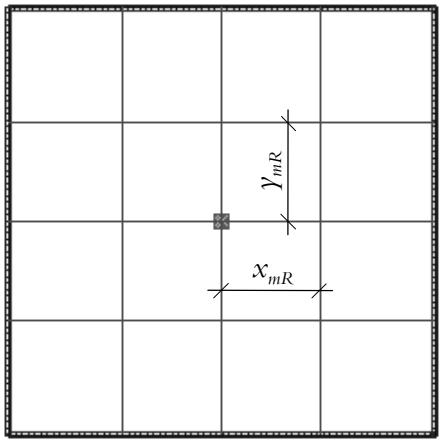

Figure 5.30 A help line drawn in the model by FEM-Design's drawing tools in order to simplify the displaying of the required bottom reinforcement along a section line perpendicular to the reinforcing direction.

The area of the *bottom* reinforcement in *x-direction* distributed longitudinally and laterally in the *right* and the *left field strip*, see *Figure* 5.31a, is due to the symmetry determined as

$$A_{sxf}^{FR} = A_{sxf}^{FL} = A_{sxf}^{G} = 353.40\ mm^2/m$$

and the average area of the *bottom* reinforcement in *x-direction* distributed longitudinally and laterally in the *right* and the *left edge strip* is due to the symmetry calculated as

$$\overline{A}_{sxf}^{ER} = \overline{A}_{sxf}^{EL} = \frac{A_{sxf}^{H} + A_{sxf}^{I}}{2} = \frac{193.59 + 85.76}{2} \approx 139.68\ mm^2/m$$

The area of the *bottom* reinforcement in *y-direction* distributed longitudinally and laterally in the *right* and the *left field strip*, see *Figure* 5.31b, is due to the symmetry determined as

$$A_{syf}^{FR} = A_{syf}^{FL} = A_{syf}^{J} = 374.31\ mm^2/m$$

and the average area of the *bottom* reinforcement in *y-direction* distributed longitudinally and laterally in the *right* and the *left edge strip* is due to the symmetry calculated as

$$\overline{A}_{syf}^{ER} = \overline{A}_{syf}^{EL} = \frac{A_{sxf}^{K} + A_{sxf}^{L}}{2} = \frac{205.22 + 86.86}{2} \approx 146.04\ mm^2/m$$

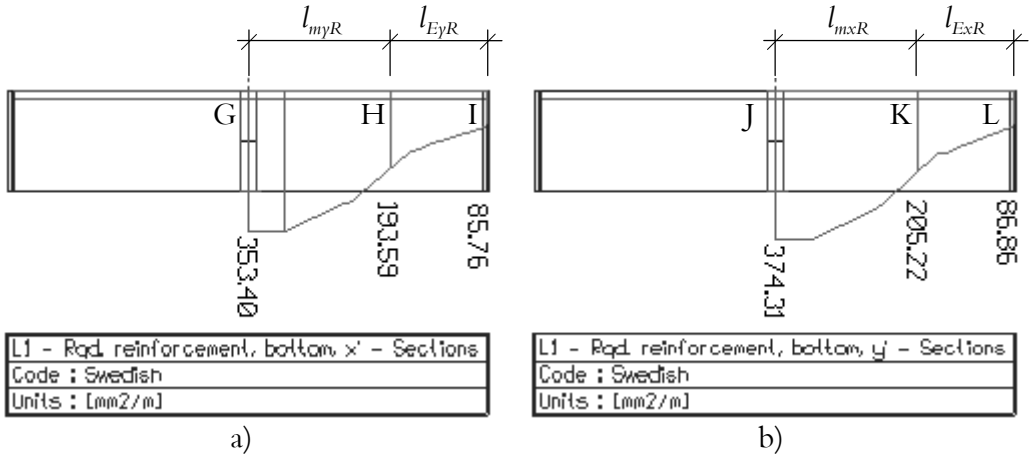

Figure 5.31 *The laterally distribution distances and the quantities that corresponds to the bottom reinforcement a) A_{sxf} and b) A_{syf} in both the field and the edge strips, viewed perpendicular to the reinforcing direction.*

The applicable average bending reinforcement areas and its longitudinally and laterally distribution distances are gathered in *Table* 5.4. Observe that the requirements according to *Equation* 4.4 are considered.

Location	**Distribution length, x [m]**	**Distribution width, y [m]**	**Reinforcement area [mm²/m]**	
			A_{sx}	A_{sy}
Column, top	4.10	4.10	1017.76	1101.12
Side, top	4.10	2×1.52	(36.69) 283.00	(40.43) 283.00
Field, bottom	2×5.00	7.14	353.40	374.31
Edge, bottom	12	2×2.43	(139.68) 283.00	(146.04) 283.00

Table 5.4 *The quantities of the redistributed bending reinforcement areas and its lengths and widths according to the FE based method (areas in brackets are the calculated).*

5.4.4 FE-analysis of the FE-designed reinforcement

Control of shear and punching capacity

Figure 5.32a-b show the distributed quantities of bending reinforcement according to *Table* 5.4.

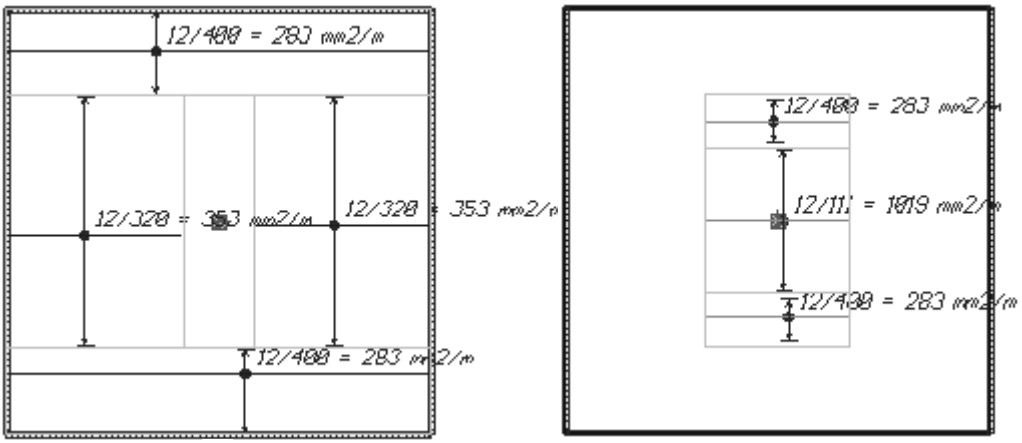

Figure 5.32 The applied areas of bending reinforcement in a) the bottom and b) the top, in x-direction.

Figure 5.33 shows the dialog box of the missing bottom reinforcement. The bottom limit is set to zero to avoid displayed quantities of to much reinforcement.

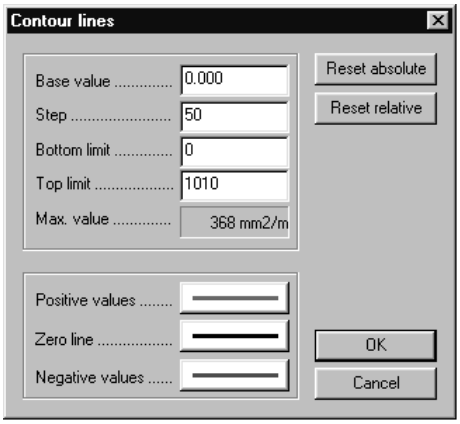

Figure 5.33 The dialog box of the missing reinforcement.

Figure 5.34a shows no missing bottom reinforcement in the field strips in contrast to the two traditional methods, besides an unimportant quantity of bottom reinforcement between the two field strips.

Figure 5.34b shows that the top reinforcement is very well distributed and it is only missing a quantity of top reinforcement in the corners like for the two previous analyses, which not is considered in the thesis. On the other hand, a quantity of top reinforcement in centre of the column is missing, which corresponds to the difference between the required reinforcement in the column centre calculated by FEM-Design and the reinforcement applied with respect of the required reinforcement at the column edge. The missing quantity is less than the missing quantities for the traditional methods, which depends on that the required quantity of the edge reinforcement is chosen in this method to be distributed to minimize cracks. Likewise is also the maximum required bottom reinforcement in the field strip.

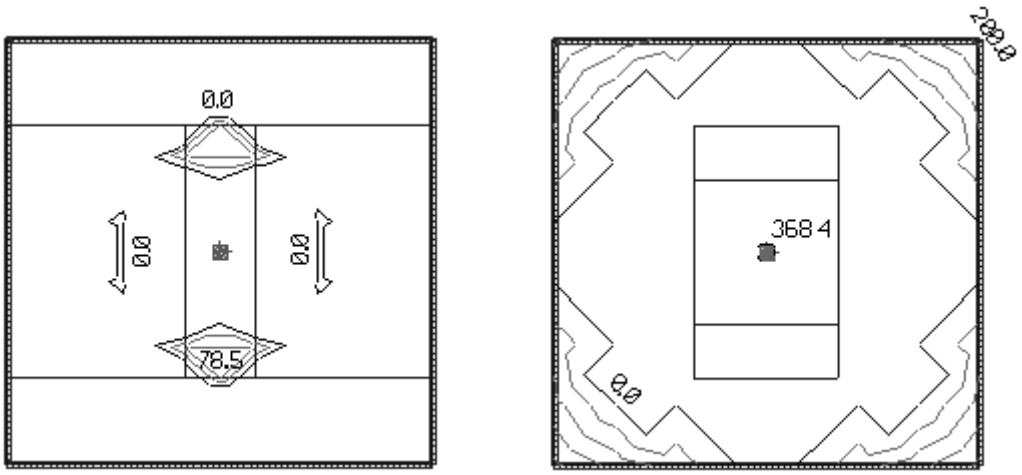

Figure 5.34 The missing reinforcement in a) the bottom and b) the top when bending reinforcement according to Table 5.4 *is considered.*

The control of the shear capacity is passed as easily as before, see *Figure* 5.35.

Figure 5.36a shows the not passed punching control when only the applied quantity of bending reinforcement is considered. *Figure* 5.36b shows the passed punching control with the corresponding quantities of applied main reinforcements and the required shear reinforcement. The result coincides with the two previous analyses.

The design criteria and the variables are explained in *Section* 5.3, like the possible ways to deal with a not passed punching control, see also *Appendix* C.

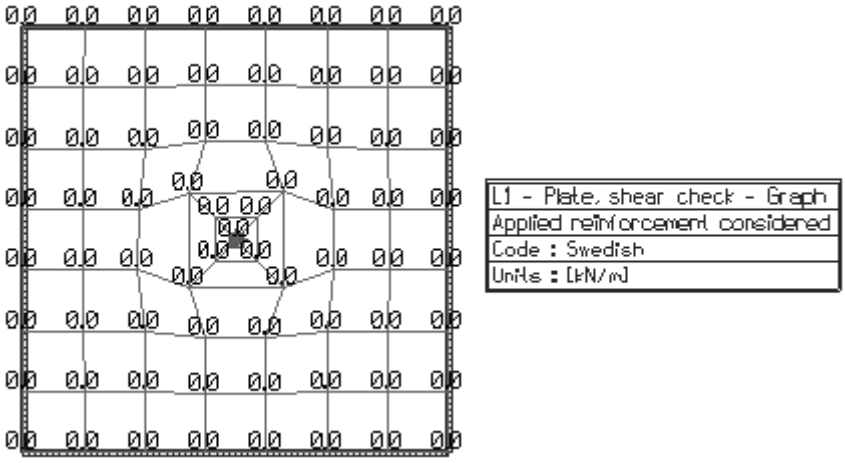

Figure 5.35 *The results of the shear check, when the bending reinforcements are applied according to the FE based redistribution method.*

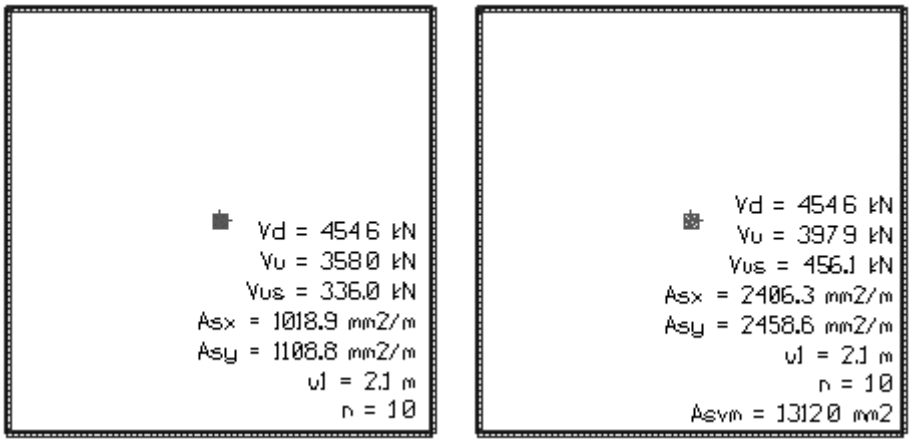

a) b)

Figure 5.36 *The results of a) the <u>not passed</u> punching control (column marks red) when only applied bending reinforcement is considered and b) the <u>passed</u> punching control (column marks yellow) i.e. the capacity becomes large enough with respect of applied main reinforcements and displayed amount of required shear reinforcement.*

Control of cracks and deformations

Like in the sections before the quantities of designed *bending* reinforcement according to *Table* 5.4 are applied again in FEM-Design to control crack widths and deformations.

Figure 5.37a shows that it is missing a small quantity of bottom reinforcement in centre of the plate, but it does not affect the crack pattern, see *Figure* 5.38a. The missing reinforcement in the middle has decreased a little when the cracking is considered.

Figure 5.37b shows that the top reinforcement is very well distributed in consideration of cracks and in comparison with the strip method, see *Figure* 5.18b, when the amount of missing top reinforcement is much smaller in the centre and even in the corners. This depends on that both the top and the bottom reinforcement are chosen to be more concentrated in the column and the field strips where the curvature is larger i.e. the plate becomes stiffer.

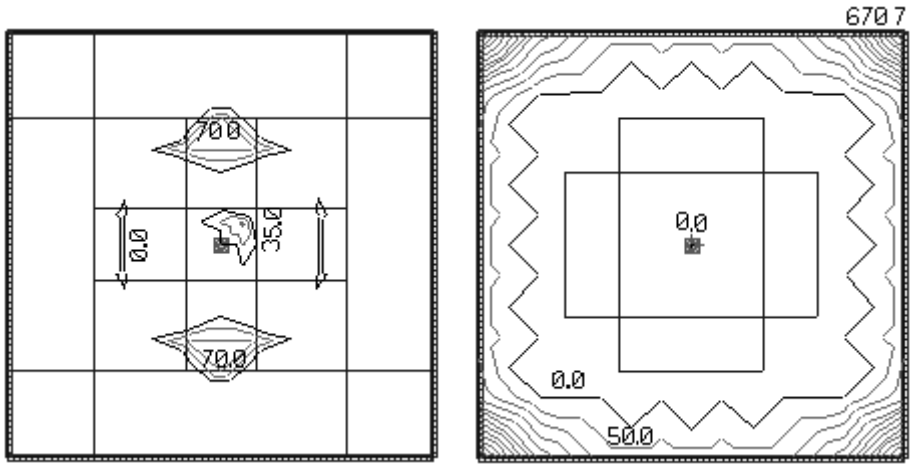

a) b)

Figure 5.37 The missing a) bottom and b) top reinforcement in x-direction, when bending reinforcement according to Table 5.4 *and cracking is considered.*

Figure 5.38b confirms the above made conclusions when it shows a more distributed crack pattern and even narrower crack widths than the strip method, compare with *Figure* 5.19b.

Figure 5.38a shows that the concentrated bottom reinforcement in the field strips give better results than the strip method in consideration of both crack distribution and widths, compare with *Figure* 5.19a.

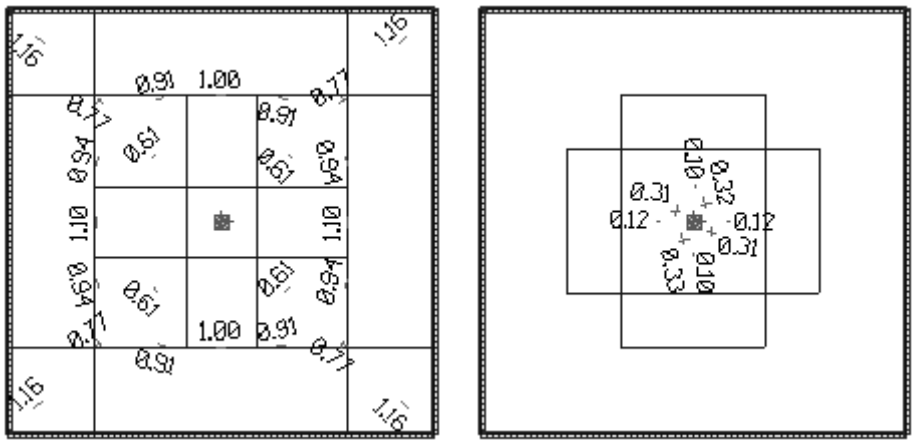

Figure 5.38 The distribution and the widths of the cracks when bending reinforcement according to Table 5.4 *is considered.*

Like before, the bottom reinforcement are increased in both the field and the edge strip until a maximum crack width of 0.20 mm is achieved in the bottom of the slab, when designed punching reinforcement is applied.

Figure 5.39 shows a similar result at *final design* as the strip method in consideration of the crack distribution and the widths. The necessary quantities of applied reinforcement are specified in *Table* 5.5.

Considered strip	**Distribution length, *x* [m]**	**Distribution width, y [m]**	**Reinforcement area [mm²/m]**	
			A_{sx}	A_{sy}
Column, top	4.10	4.10	(1017.8) 2406	(1101.1) 2459
Side, top	4.10	2×1.52	(283) 283	(283) 283
Field, bottom	2×5.00	7.14	(353.4) 898	(374.3) 935
Edge, bottom	12.00	2×2.43	(283) 690	(283) 690

Table 5.5 The quantities of applied reinforcement areas and its distribution lengths and widths at final design i.e. with respect of punching and a maximum crack width of 0.20 mm (areas in brackets are the bending reinforcement from start).

Figure 5.40 shows that the largest deflection is 9.2 mm in the slab, which means that the maximum deflection is less than the assumed deflection criteria, see *Equation* 5.2.

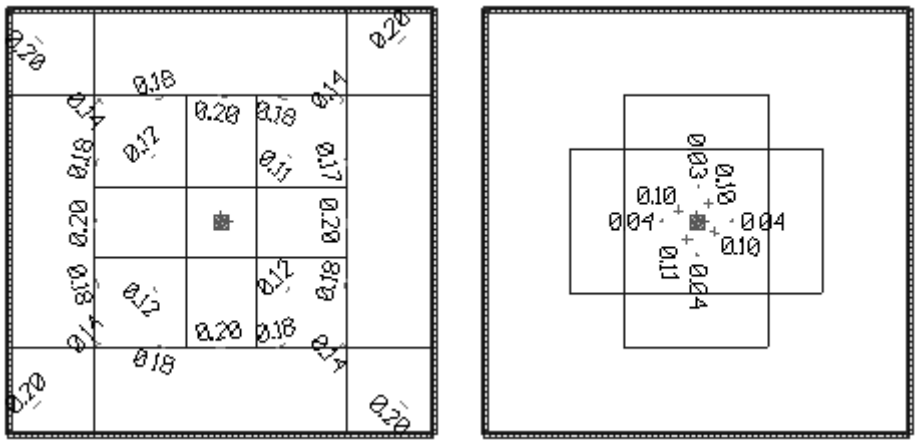

Figure 5.39 The crack widths and the distribution in a) the bottom and b) the top at final design i.e. with respect of punching and a maximum crack width of maxiumum 0.20 mm, see amount of reinforcement in Table 5.5.

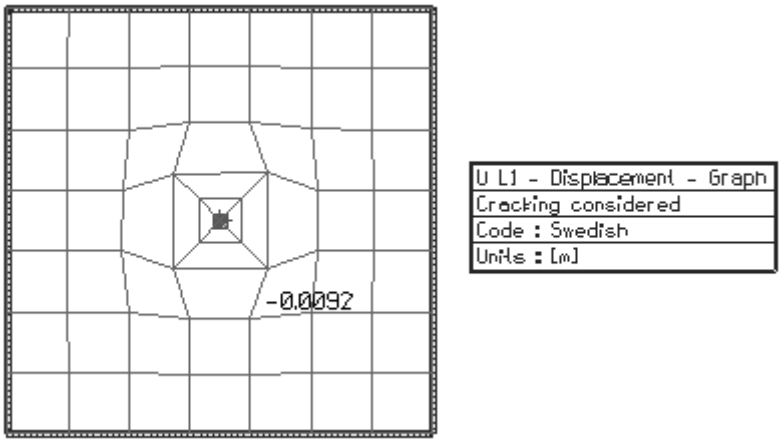

Figure 5.40 The largest deflection in the slab at final design when reinforcement according to Table 5.5 *and cracking is considered.*

5.5 Comparison and discussion of the methods

In this section, the three methods quantities of designed reinforcement are compared and discussed at different design levels. Observe that the quantity of reinforcement distributed outside the column strip by the yield line theory is placed in the table row *side, top*.

Location	Yield line theory [mm²/m]		Strip method [mm²/m]		FE-based method [mm²/m]	
	x	y	x	y	x	y
Column, top	885	966	782	853	1018	1101
Side, top	283	283	283	283	283	283
Field, bottom	283	283	283	288	353	374
Edge, bottom	283	283	283	283	283	283

Table 5.6 Comparison between the yield line theory, the strip method and the FE-based method in consideration of bending reinforcement.

Table 5.6 shows that the FE based method distributes higher quantities of reinforcement in the column and the field strip than both the yield line theory and the strip method, which distributes similar quantities of reinforcement. This depends on that the FE-based method is chosen to distribute higher quantities in the column and the field strips with respect of cracking.

Location	Yield line theory [mm²/m]		Strip method [mm²/m]		FE-based method [mm²/m]	
	x	y	x	y	x	y
Column, top	2406	2459	2406	2459	2406	2459
Column, shear	656	656	656	656	656	656
Side, top	283	283	283	283	283	283
Field, bottom	891	919	891	942	898	935
Edge, bottom	685	685	702	702	690	690

Table 5.7 Comparison between the yield line theory, the strip method and the FE-based method at final design of reinforcement i.e. with respect of punching and a crack width of maximum 0.20 mm.

Table 5.7 shows that the FE based method at final design needs less bottom reinforcement in consideration of cracks than the strip method, but more than the yield line theory. All methods require the same quantity of punching reinforcement.

The comparison of reinforcement quantities in *Table* 5.6 and *Table* 5.7 are not really representative. The best way to compare the methods is to calculate the total sum of the distributed reinforcement i.e. the total volume of the distributed reinforcement, for each method at a certain level of design.

The respective total sum of the required reinforcement areas are calculated as

$$\sum A_s = \int_A \overline{A}_s \, dA = \sum \overline{A}_{si} A_i \qquad 5.3$$

and when the area A is equal to the strips distribution area the formula becomes

$$A_{s\Sigma} = \sum \overline{A}_{si} \cdot b_i \cdot l_i \qquad 5.4$$

where $A_{s\Sigma}$ is the respective total sum of the design reinforcement area in respective strip i.e. the total volume [mm^{2}m]

$\overline{A}_{si}$ is the respective average design bottom, top or shear reinforcement area in respective area [mm^2/m]

b_i is the lateral distribution distance of the reinforcement i.e. the width of the strip [m]

l_i is the longitudinal distribution distance of the reinforcement i.e. the length of the strip [m]

Location	**Yield line theory [mm^{2}m]**	**Strip method [mm^{2}m]**	**FE-based method [mm^{2}m]**
Column, top	23 989	30 837	35 620
Side, top	17 116	9 589	7 055
Sum top:	***41 105***	***40 426***	***42 675***
Field, bottom	48 902	52 426	52 126
Edge, bottom	32 602	29 477	33 009
Sum bottom:	***81 504***	***81 964***	***85 135***
Total sum:	**122 609**	**122 389**	**127 810**

Table 5.8 Comparison between the yield line theory, the strip method and the FE-based method in consideration of total quantity of applied bending reinforcement.

Observe that the totally applied length of reinforcement i.e. the bar meters can be calculated by dividing the respective total sum with the area 113 mm^2, which corresponds to a bar with a diameter of 12 mm.

Table 5.8 shows that the yield line theory distributes about 2% more *top bending reinforcement* in totally than the strip method. The FE-based method distributes about 6% more *top bending reinforcement* than the strip method, and 4% than the yield line theory.

For the *bottom bending reinforcement* the strip method distributes about the same quantity as the yield line theory, but distributes more of the reinforcement to be concentrated in the field strips. The FE based method distributes about 4% more *bottom bending reinforcement* than both the strip method and the yield line theory.

In total, the strip method distributes about 0.2% less *bending reinforcement* than the yield line theory, which corresponds to 2 bar meters. The FE-based method distributes about 4% or about 48 bar meters more *bending reinforcement* than the strip method, and 4% or about 46 bar meters more than the yield line theory.

Location	**Yield line theory [mm^2m]**	**Strip method [mm^2m]**	**FE-based method [mm^2m]**
Column, top	63 050	91 756	81 781
Side, top	17 116	9 589	7 055
Sum top:	***80 166***	***101 345***	***88 835***
Field, bottom	156 384	168 489	131 426
Edge, bottom	78 912	73 120	80 481
Sum bottom:	***235 296***	***241 610***	***211 908***
Total sum:	**315 462**	**342 954**	**300 743**

Table 5.9 Comparison between the yield line theory, the strip method and the FE-based method at final design i.e. with respect of in totally applied punching and crack reinforcement at a maximum crack width of 0.20 mm.

Table 5.9 shows at *final design* that the FE-based method distributes about 12% less *top reinforcement* i.e. punching reinforcement, than the strip method and 11% more than the yield line theory.

For the *bottom reinforcement* the FE-based method distributes about 12% less reinforcement than the strip method i.e. less reinforcement in the field strips and more in the edge strips, and 10% less than the yield line theory.

In total, the FE-based method distributes about 12% or about 374 bar meters less reinforcement than the strip method and 5% or 130 bar meters less reinforcement than the yield line theory at *final design*.

Finally, the FE based method is recommended as a design method of flat slab floors on account of easier determination of distances and quantities, and a more powerful handling in consideration of cracks and punching. The established design method is stepwise and generally illustrated in *Appendix* C.

6 Conclusions

6.1 Summary and conclusions

Chapter 1 - Gives the background and a short historical review of plate theory to place the thesis in its general context.

Chapter 2 - The effect of varied mesh densities, element types, column widths and modelling of the column stiffness are analysed and investigated with Abaqus and FEM-Design FE-models, to find the optimal modelling parameters for flat slab floors.

It is shown that the mesh density and the modelling of the column stiffness are the most important parameters to consider in FE-analyses of flat slab floors. A denser mesh increases the size of the maximum support moments, whereas the maximum field moments are almost independent of the mesh density. However, FEM-Design's automatically generated mesh gives good result with respect to the size of the maximum support moment at interior columns. For columns wider than 0.2 m the response of the moment distribution can be improved by distributing the column stiffness over one plate element. In practice, the method can be applied to every interior column, because columns are usually wider than 0.2 m. A distributed stiffness or the multi spring concept can also be used for interior walls wider than 0.2 m.

Chapter 3 - FEM-Design's calculation of crack propagation is compared with Abaqus/Explicit at different load intensities. Finally, the load-displacement curve of FEM-Design is compared with Abaqus/Explicit and an experimental reinforced concrete slab, McNiece *(1978)*.

The crack propagation differs quite much between FEM-Design and Abaqus. The difference depends on different crack theories i.e. when a crack is considered to be a crack. The cracking in Abaqus describes the material behaviour according to a given postfailure relationship, in this case a stress-displacement relationship. The first initiated or displayed crack depends on when the tensile stress exceeds the tensile strength of the concrete. A further opening of the initiated crack depends on the fracture energy and the characteristic length of the elements. FEM-Design on the other hand, compares the tensile stress with the tensile strength of the concrete and displays in this case the formal crack width according to Swedish design rules, which are for the most part based on crack safety with respect of corrosion and bearing capacity. With other words, Abaqus displays immediately an initiated crack in the slab, whereas FEM-Design displays a crack first when it affects the slabs bearing capacity or the corrosion safety.

FEM-Design's load-displacement curve shows very good agreement with the experiment and the conclusion is that FEM-Design's crack analysis is an adequate design tool.

Chapter 4 - The principles behind traditional design methods, the yield line theory and the strip method, are shortly presented. A flat slab floor is designed according to the traditional methods and the moment distributions are compared both between each other and with FEM-Design's calculated distribution of bending moments. Furthermore, the total amount of the distributed reinforcement is compared between the two traditional methods.

It is found that FEM-Design's calculated distribution of moments is not comparable with the traditional methods. FEM-Design calculates the moments according to elastic theory at each node and the two design methods distribute moments with the same size in a certain area. This means that design moments must be chosen at certain points from the FE-analysis and be redistributed by a design method. The strip method distributes totally 5% more bending reinforcement than the yield line theory. This result coincides with Hillerborg *(1996)* - the strip method is on the safe side because it is based on the *lower bound theorem* of *the theory of the plasticity*. The yield line theory on the other hand, can be on the unsafe side if the yield lines not are chosen appropriately, because it is based on *the upper bound theorem* of *the theory of the plasticity*.

Chapters 5 - The traditionally distributed reinforcement from chapter 4 are analysed further in FEM-Design considering bending, punching, crack widths and deformations. A FE-based design method is derived with respect to the FE-analyses and the capabilities of FEM-Design. The new method is used to redistribute the reinforcement for the same slab.

Finally, the three methods total amount of reinforcement are compared at two design levels, *bending*- and *final design*.

At *final design* i.e. with respect of punching and cracking, the FE-based method distributes less reinforcement than both the yield line theory (5%) and the strip method (12%), due to a better determination of distribution distances.

In the *bending design* the FE-method distributes (4%) more reinforcement than both the strip method and the yield line theory. This depends on that maximum design quantities in the column and the field strips are chosen for the FE-based method, whereas the traditional methods use average design moments resulting in smaller reinforcement quantities.

Finally, the FE-based method is recommended as a design method of flat slab floors, because it gives a faster and more adequate determination of distribution distances and quantities both at bending- and final design.

In addition, the calculated moment distribution and displacement field in FEM-Design generally shows very good agreement with the Abaqus analyses.

6.2 General conclusions

FE-analyses can be used to design reinforcement in concrete slabs in contradiction to Hillerborg's statement *et al (1990), (1996)*. This when FE-theory calculates all effects of action with better assumptions and accuracy than any other conventional hand calculation method. In addition, a FE-analysis gives the moment distribution or like FEM-Design the distribution of required reinforcement in all direction for both the bending- and twisting moments in the whole plate, simultaneously. Of course, the reinforcement quantities like for other methods have to be redistributed into appropriate areas with respect to bending, punching, cracking etc.

FEM-Design can, within the limits of the thesis be considered to calculate the internal forces and the crack propagation correct with respect to design of flat slab floors. This apply when the automatic mesh generator is used and the *edge* support moment or reinforcement quantity is used as design value for interior columns and consequently also for interior walls.

Very few arguments arise against the use of FE-based design, especially since FEM-Design's plate module is found to be a user-friendly analytical and design tool. On the other hand, a program can always be improved from a user perspective. The most important improvement of the program is to implement the multi spring concept, which gives a more realistic response and consequently better results at design.

Another, necessary improvement is to implement some kind of possibility or possibilities to redistribute the reinforcement quantities, which enables easier and faster determination and application of user defined reinforcement. The proposed design method (FED) is one suitable method to implement, because it combines powerful FE-theory with well established traditionally design theories.

This means that the users neither have to calculate design quantities of reinforcement or distribution distances, or to apply it by hand in a FE-model.

Finally, it is quite easy to make mistakes at the modelling, because the input data is given in many different dialog boxes and to get an overview the input data either have to be saved to a file, send to the clipboard or printed out. A quicker way to check the input data can be obtained, if an *input check* option is placed on the menu, where the material and the geometry properties, the applied loads, the load combinations, the statistics etc., can be checked before the calculation and if wanted, corrected directly.

6.3 Suggestions for further research

A very limited model was used to evaluate the proposed reinforcement design method and determination of the corner reinforcement was not included. Therefore, there is a need to complement the FED-method with a way to determine the corner reinforcement and its distribution. There is also important to further investigate the FED-method in practical design of all types of flat slab floors e.g. symmetrically and asymmetrically slabs with one or several interior columns/walls without and together with exterior columns, corner columns and areas of holes and so on.

Column heads or strengthening plates is today not possible to define directly in FEM-Design, but a column modelled with the same width as the head can simulate a column head and an additional plate region defined with increased concrete cover (the effective heights have to correspond between the regions), can simulate a strengthening plate. Unfortunately, those will results in increased moments in both cases, because a wider column will result in an increased stiffness, and an additional plate region in a denser mesh due to a relatively small size of strengthening plates. Hence, the effects of the increased support moment have to be investigated with respect to final design and different design codes. Are the effects considerably, new methods to model column heads and strengthening plates has to be implemented if the possibility to model strengthening plate or column heads is wanted in the future.

References

BBK 94 (1994). *Boverkets handbok om betongkonstruktioner.* (The Swedish Building Administrations Handbook of Concrete Structures). Part 2 - Material, Performance and control. Stockholm, Sweden: The Swedish Building Administration, Divison of Buildings. ISBN 91-7332-687-9. (In Swedish).

BBK 94 (1995). *Boverkets handbok om betongkonstruktioner.* (The Swedish Building Administrations Handbook of Concrete Structures). Part 1 - Design. Stockholm, Sweden: The Swedish Building Administration, Divison of Buildings. ISBN 91-7147-253-5. (In Swedish).

Bengtsson, B Åke; Elfgren, Lennart; Hillerborg, Arne and Losberg, Anders (1969). Chapter 336 - Self-supporting Concrete Slabs In: *BYGG, Konstruktionsteknik* (Building, Design Techniques). Main part 3; Third edition. Stockholm, Sweden: AB Byggmästarens förlag. (In Swedish).

Cope, R.j. and Clark, L.A. (1984). *Concrete Slabs.* Essex, UK: Elsevier Applied Science Publishers Ltd. ISBN 0-85334-254-7.

FEM-Design (2000). *FEM-Design Plate.* Revision 3:1. Malmö, Sweden: Skanska IT Solutions AB.

Hillerborg, Arne. (1956). *Jämviktsteori för armerade betongplattor* (Equilibrium Theory of Concrete Slabs). Stockholm, Sweden: Betong 1956:4.

Hillerborg, Arne (1959). *Strimlemetoden för plattor på pelare, vinkelplattor m.m.* (The Strip Method in consideration of flat slab floors, triangular slabs and so on). Stockholm, Sweden. 54 pp. (In Swedish).

Hillerborg, Arne; Fritzell, Göte; Koritz, Harry; Kroon, Tage; Lindqvist, Herbert; Wahlström, Bengt and Wästlund, Georg. (1963). In: *Massiva betongplattor - Metodanvisningar, kommentarer och beräkningsexempel i anslutning till 1957 års konstruktionsbestämmelser för massiva betongplattor* (Solid Concrete Slabs - Instruction of methods, comments and examples of design calculations in connection to 1957-years design rules of solid concrete slabs). Stockholm, Sweden: The Swedish States Concrete Association, SVR:s Förlags AB. 97 pp. (In Swedish).

Hillerborg, Arne; Nylander, Henrik and Kinnunen, Sven. (1990). Chapter 6.5 - Slabs In: *Betonghandboken - Konstruktion* (Concrete Handbook - Design). Stockholm, Sweden: AB Svensk Byggtjänst. ISBN 91-7332-533-3. (In Swedish).

Hillerborg, Arne. (1996). *Strip Method Design Handbook.* First edition. London, UK: Chapman & Hall. ISBN 0-419-18740-5.

Johansson, K.W. (1943). *Brudlinieteorier* (Yield Line Theories). Copenhagen, Denmark: Akademisk Förlag (1963). (In Danish).

Jones, L.L. and Wood, R.H. (1967). *Yield-line Analyses of Slabs.* First edition 1967. London, UK: Thames & Hudson Ltd and Chatto & Windus Ltd.

Kinnunen, Sven. (1963). *Punching of concrete slabs with two-way reinforcement.* Stockholm, Sweden: The Royal Institute of Technology, KTH - Documents 198.

Kinnunen, Sven and Nylander, Henrik. (1960). *Punching of concrete slabs without shear reinforcement.* Stockholm, Sweden: The Royal Institute of Technology, KTH - Dokuments 158.

Langesten, Bengt. (1995). *Betongkonstruktion* (Design of Concrete Structures). Fifth edition. Stockholm, Sweden: Liber utbildning AB. ISBN 0-85334-254-7. (In Swedish).

Losberg, Anders (1960). *Design methods for structurally reinforced concrete pavements.* Gothenburg, Sweden: Chalmers University of Technology. CTH - Documents vol 250 (1961).

Lundell, Dick. (2000). *Personal communication.* Malmö, Sweden: Skanska Teknik AB.

Nylander, Henrik (1959). *Rektangulär betongplatta understödd av pelare i fältet* (Rectangular concrete slabs supported by columns in the field). Stockholm, Sweden: Nordisk Betong 1959:2. (In Swedish).

Nylander, Henrik (1959). *Cirkular platta, understödd i centrum och upplagd längs periferin. Jämnt fördelad last* (Cirkular plate, supported in centre and along the periphery. Uniformly distributed load). Stockholm, Sweden: The Royal Institute of Technology, KTH – Messages no 32. (In Swedish).

Olofsson, Thomas. (1996). *Betongplattor* (Concrete Slabs). Luleå, Sweden: Division of Structural Engineering, Luleå University of Technology. Paper 96:08. (In Swedish).

Timoshenko, Stephen P. (1953). *History of Strength of Materials. With a brief account of the history of theory of elasticity and the theory of structures.* New York, USA: McGraw-Hill (1953). 452 pp.

Timoshenko, Stephen P. and Woinowsky – Krieger, S. (1959). *Theory of Plates and Shells.* Second edition. New York, USA: McGraw-Hill (1959). 580 pp. ISBN 99-6900777-7.

Appendix A

A Tables of moment distribution considering the modelling dependencies

The tables correspond to the figures in *Section* 2.4.

A.1 Mesh density

Distance, x [m]	Model 1 L_{el} = 1.0 m	Model 2 L_{el} = 0.5 m	Model 3 L_{el} = 0.1 m
0.0	112.15	141.71	209.53
0.5	48.48	26.60	36.78
1.0	-1.86	7.43	8.75
1.5	-3.32	-7.04	-6.46
2.0	-17.57	-16.21	-15.90
2.5	-21.53	-21.99	-21.75
3.0	-25.93	-25.12	-24.92
3.5	-25.68	-26.03	-25.85
4.0	-25.50	-24.91	-24.74
4.5	-21.38	-21.82	-21.65
5.0	-17.31	-16.74	-16.56
5.5	-9.05	-9.58	-9.40
6.0	-0.75	-0.21	-0.01

Table A.1 The distribution of moments M_x in the x-direction, for different mesh densities in Abaqus. Corresponds to Figure 2.9.

Distance, x [m]	FD, Model 1 L_{el} = 1.0 m	FD, Model 2 L_{el} = 0.5 m	FD, Model 20 L_{el} = 0.25 m
0.0	108.99	138.22	167.30
0.5	53.49	26.16	35.79
1.0	-2.01	7.77	8.64
1.5	-9.48	-6.66	-6.46
2.0	-16.96	-15.94	-15.84
2.5	-21.12	-21.71	-21.63
3.0	-25.28	-24.84	-24.76
3.5	-25.16	-25.74	-25.66
4.0	-25.03	-24.62	-24.53
4.5	-21.00	-21.55	-21.45
5.0	-16.97	-16.50	-16.38
5.5	-8.81	-9.41	-9.28
6.0	-0.66	-0.18	-0.05

*Table A.2 The distribution of moments M_x in the x-direction, for different mesh densities in FEM-Design. Corresponds to Figure 2.*10.

A.2 Element type

Distance, x [m]	Model 1 Shell L_{el} = 1.0 m	Model 4 Solid L_{el} = 1.0 m
0.0	112.15	68.37
0.5	48.48	44.96
1.0	-1.86	9.49
1.5	-3.32	-4.87
2.0	-17.57	-14.29
2.5	-21.53	-21.06
3.0	-25.93	-24.15
3.5	-25.68	-25.50
4.0	-25.50	-24.01
4.5	-21.38	-21.18
5.0	-17.31	-15.81
5.5	-9.05	-9.00
6.0	-0.75	-6.21

Table A.3 The distribution of moments M_x in the x-direction, for different element types in Abaqus, L_{el} = 1.0 m. Corresponds to Figure 2.11.

Distance, x [m]	Model 2 Shell L_{el} = 0.5 m	Model 5 Solid L_{el} = 0.5 m
0.0	141.71	114.74
0.5	26.60	31.10
1.0	7.43	8.96
1.5	-7.04	-6.22
2.0	-16.21	-15.80
2.5	-21.99	-21.64
3.0	-25.12	-24.83
3.5	-26.03	-25.76
4.0	-24.91	-24.66
4.5	-21.82	-21.58
5.0	-16.74	-16.50
5.5	-9.58	-9.41
6.0	-0.21	-1.74

Table A.4 The distribution of moments M_x in the x-direction, for different element types in Abaqus, L_{el} = 0.5 m. Corresponds to Figure 2.12.

A.3 Column width

Distance, x [m]	Model 2 b_c = 0.2 m	Model 6 b_c = 0.4 m	Model 7 b_c = 0.6 m
0.0	141.71	145.51	146.23
0.5	26.60	28.21	28.52
1.0	7.43	8.65	8.89
1.5	-7.04	-6.11	-5.93
2.0	-16.21	-15.50	-15.36
2.5	-21.99	-21.43	-21.32
3.0	-25.12	-24.68	-24.60
3.5	-26.03	-25.70	-25.63
4.0	-24.91	-24.66	-24.61
4.5	-21.82	-21.63	-21.60
5.0	-16.74	-16.61	-16.58
5.5	-9.58	-9.51	-9.49
6.0	-0.21	-0.20	-0.19

Table A.5 The distribution of moments M_x in the x-direction, for different column widths in Abaqus. The column stiffness is applied at 1 node, see Figure 2.13.

Distance, x [m]	Model 8 b_c = 0.2 m	Model 9 b_c = 0.4 m	Model 10 b_c = 0.6 m
0.0	125.79	102.14	81.89
0.1	110.75	-	-
0.2	-	85.74	-
0.3	-	-	69.11
0.5	36.81	42.03	48.07
1.0	7.93	10.24	12.30
1.5	-6.76	-5.19	-3.98
2.0	-16.08	-14.93	-14.11
2.5	-21.87	-21.01	-20.42
3.0	-25.04	-24.38	-23.94
3.5	-25.97	-25.46	-25.14
4.0	-24.86	-24.48	-24.24
4.5	-21.79	-21.51	-21.34
5.0	-16.71	-16.53	-16.41
5.5	-9.57	-9.46	-9.40
6.0	-0.21	-0.19	-0.19

Table A.6 *M_x in the x-direction, for different column widths in Abaqus. Column stiffness applied at 8 nodes, see Figure* 2.14.

Distance, x [m]	Model 11 b_c = 0.2 m	Model 12 b_c = 0.4 m	Model 13 b_c = 0.6 m
0.0	137.15	106.86	74.69
0.1	112.30	-	-
0.2	-	86.69	-
0.3	-	-	74.34
0.5	36.51	40.11	45.66
1.0	7.91	9.84	11.47
1.5	-6.79	-5.43	-4.39
2.0	-16.11	-15.10	-14.35
2.5	-21.90	-21.13	-20.59
3.0	-25.06	-24.46	-24.06
3.5	-25.98	-25.53	-25.23
4.0	-24.88	-24.53	-24.31
4.5	-21.79	-21.54	-21.38
5.0	-16.72	-16.55	-16.44
5.5	-9.57	-9.47	-9.41
6.0	-0.21	-0.19	-0.19

Table A.7 *M_x in the x-direction, for different column widths in Abaqus. Column stiffness applied at 21 nodes, see Figure* 2.15.

Distance, x [m]	Model 14 b_c = 0.2 m	Model 15 b_c = 0.4 m	Model 16 b_c = 0.6 m
0.0	134.43	109.72	90.58
0.1	111.99	-	-
0.2	-	87.39	-
0.3	-	-	72.64
0.5	36.73	40.39	45.23
1.0	7.87	9.64	11.18
1.5	-6.82	-5.54	-4.56
2.0	-16.13	-15.17	-14.47
2.5	-21.92	-21.19	-20.67
3.0	-25.07	-24.50	-24.12
3.5	-25.99	-25.56	-25.27
4.0	-24.88	-24.56	-24.34
4.5	-21.80	-21.56	-21.41
5.0	-16.72	-16.56	-16.46
5.5	-9.57	-9.48	-9.42
6.0	-0.21	-0.19	-0.19

Table A.8 *M_x in the x-direction, for different column widths in Abaqus. Column stiffness applied at 40 nodes, see Figure* 2.16.

Distance, x [m]	Model 17 b_c = 0.2 m	Model 18 b_c = 0.4 m	Model 19 b_c = 0.6 m
0.0	122.78	97.74	76.10
0.1	109.45	-	-
0.2	-	85.10	-
0.3	-	-	69.49
0.5	34.68	40.17	46.56
1.0	8.75	11.23	13.36
1.5	-6.10	-4.54	-3.37
2.0	-15.66	-14.52	-13.70
2.5	-21.53	-20.68	-20.09
3.0	-24.74	-24.09	-23.65
3.5	-25.70	-25.20	-24.87
4.0	-24.61	-24.24	-24.00
4.5	-21.54	-21.27	-21.10
5.0	-16.47	-16.30	-16.18
5.5	-9.40	-9.29	-9.23
6.0	-1.74	-1.72	-1.71

Table A.9 *M_x in x-direction, for different column widths in Abaqus. Column stiffness applied at 8 nodes. Solid elements, see Figure* 2.17.

Distance, x [m]	FD, Model 2 b_c = 0.2 m	FD, Model 6 b_c = 0.4 m	FD, Model 7 b_c = 0.6 m
0.0	138.22	141.99	142.70
0.5	26.16	27.76	28.07
1.0	7.77	9.01	9.24
1.5	-6.66	-5.73	-5.56
2.0	-15.94	-15.23	-15.09
2.5	-21.71	-21.16	-21.05
3.0	-24.84	-24.41	-24.33
3.5	-25.74	-25.42	-25.36
4.0	-24.62	-24.38	-24.34
4.5	-21.55	-21.37	-21.34
5.0	-16.50	-16.39	-16.37
5.5	-9.41	-9.36	-9.35
6.0	-0.18	-0.18	-0.18

Table A.10 The distribution of moments M_x in the x-direction, for different column widths in FEM-Design. The column stiffness is applied at 1 node. The element lenght is set to 0.5 m, see Figure 2.18.

Distance, x [m]	FD, Model 21 b_c = 0.2 m	FD, Model 22 b_c = 0.4 m	FD, Model 23 b_c = 0.6 m
0.0	97.18	99.91	100.43
0.5	37.15	38.94	39.28
1.0	9.94	11.19	11.42
1.5	-1.07	-0.09	0.10
2.0	-10.16	-9.36	-9.25
2.5	-17.95	-17.32	-17.20
3.0	-22.46	-21.98	-21.89
3.5	-23.08	-22.70	-22.63
4.0	-23.34	-23.07	-23.02
4.5	-21.58	-21.41	-21.38
5.0	-15.17	-15.06	-15.04
5.5	-8.56	-8.52	-8.51
6.0	-1.85	-1.87	-1.87

Table A.11 The distribution of moments M_x in the x-direction, for different column widths in FEM-Design. The column stiffness is applied at 1 node. The element lenghts are chosen automatically by the mesh generator, see Figure 2.18.

Distance, x [m]	FD, Model 24 b_c = 0.2 m	FD, Model 25 b_c = 0.4 m	FD, Model 26 b_c = 0.6 m
0.0	114.23	86.99	68.28
0.1	111.45	-	-
0.2	-	85.40	-
0.3	-	-	64.88
0.5	32.31	42.65	46.69
1.0	10.12	9.54	14.35
1.5	-5.88	-2.43	-2.18
2.0	-15.19	-12.92	-11.18
2.5	-21.17	-20.76	-18.67
3.0	-24.90	-23.64	-22.03
3.5	-25.34	-25.09	-24.10
4.0	-24.26	-23.64	-22.49
4.5	-21.69	-20.88	-20.57
5.0	-16.17	-16.26	-15.12
5.5	-9.06	-8.60	-8.22
6.0	-0.38	-0.93	-1.14

Table A.12 The distribution of moments M_x in the x-direction, for different column widths in FEM-Design. The column stiffness is applied as 8 fictious columns. The mesh is automatically generated as sparse as possible outwards from the column elements, see Figure 2.19.

A.4 Modelling of the column stiffness

Distance, x [m]	Model 2 1 node	Model 8 8 nodes	Model 11 21 nodes	Model 14 40 nodes	Model 17 Solid, 8 nodes
0.0	141.71	*125.79*	137.15	*134.43*	*122.78*
0.1	-	110.75	112.30	111.99	109.45
0.5	26.60	36.81	36.51	36.73	34.68
1.0	7.43	7.93	7.91	7.87	8.75
1.5	-7.04	-6.76	-6.79	-6.82	-6.10
2.0	-16.21	-16.08	-16.11	-16.13	-15.66
2.5	-21.99	-21.87	-21.90	-21.92	-21.53
3.0	-25.12	-25.04	-25.06	-25.07	-24.74
3.5	-26.03	-25.97	-25.98	-25.99	-25.70
4.0	-24.91	-24.86	-24.88	-24.88	-24.61
4.5	-21.82	-21.79	-21.79	-21.80	-21.54
5.0	-16.74	-16.71	-16.72	-16.72	-16.47
5.5	-9.58	-9.57	-9.57	-9.57	-9.40
6.0	-0.21	-0.21	-0.21	-0.21	-1.74

Table A.13 The distribution of moments M_x in the x-direction, for different number of nodes with applied column stiffness in Abaqus. b_c = 0.2 m. Moments in italics and marked red are extrapolated, see Figur 2.20.

Distance, x [m]	Model 6 1 node	Model 9 8 nodes	Model 12 21 nodes	Model 15 40 nodes	Model 18 Solid, 8 nodes
0.0	145.51	*102.14*	106.86	*109.72*	*97.74*
0.2	-	85.74	86.69	87.39	85.10
0.5	28.21	42.03	40.11	40.39	40.17
1.0	8.65	10.24	9.84	9.64	11.23
1.5	-6.11	-5.19	-5.43	-5.54	-4.54
2.0	-15.50	-14.93	-15.10	-15.17	-14.52
2.5	-21.43	-21.01	-21.13	-21.19	-20.68
3.0	-24.68	-24.38	-24.46	-24.50	-24.09
3.5	-25.70	-25.46	-25.53	-25.56	-25.20
4.0	-24.66	-24.48	-24.53	-24.56	-24.24
4.5	-21.63	-21.51	-21.54	-21.56	-21.27
5.0	-16.61	-16.53	-16.55	-16.56	-16.30
5.5	-9.51	-9.46	-9.47	-9.48	-9.29
6.0	-0.20	-0.19	-0.19	-0.19	-1.72

Table A.14 The distribution of moments M_x in the x-direction, for different number of nodes with applied column stiffness in Abaqus. b_c = 0.4 m. Moments in italics and marked red are extrapolated, see Figur 2.21.

Distance, x [m]	Model 7 1 node	Model 10 8 nodes	Model 13 21 nodes	Model 16 40 nodes	Model 19 Solid, 8 nodes
0.0	146.23	*81.89*	74.69	*90.58*	*76.10*
0.3	-	69.11	74.34	72.64	69.49
0.5	28.52	48.07	45.66	45.23	46.56
1.0	8.89	12.30	11.47	11.18	13.36
1.5	-5.93	-3.98	-4.39	-4.56	-3.37
2.0	-15.36	-14.11	-14.35	-14.47	-13.70
2.5	-21.32	-20.42	-20.59	-20.67	-20.09
3.0	-24.60	-23.94	-24.06	-24.12	-23.65
3.5	-25.63	-25.14	-25.23	-25.27	-24.87
4.0	-24.61	-24.24	-24.31	-24.34	-24.00
4.5	-21.60	-21.34	-21.38	-21.41	-21.10
5.0	-16.58	-16.41	-16.44	-16.46	-16.18
5.5	-9.49	-9.40	-9.41	-9.42	-9.23
6.0	-0.19	-0.19	-0.19	-0.19	-1.71

Table A.15 The distribution of moments M_x in the x-direction, for different number of nodes with applied column stiffness in Abaqus. b_c = 0.6 m. Moments in italics and marked red are extrapolated, see Figur 2.22.

Distance, x [m]	FD, Model 2 1 node, L_{el} = 0.5 m	FD, Model 21 1 node, Auto mesh	FD, Model 24 8 nodes, Sparse mesh
0.0	138.22	97.18	114.23
0.1	115.81	85.20	111.45
0.5	26.16	37.15	32.31
1.0	7.77	9.94	10.12
1.5	-6.66	-1.07	-5.88
2.0	-15.94	-10.16	-15.19
2.5	-21.71	-17.95	-21.17
3.0	-24.84	-22.46	-24.90
3.5	-25.74	-23.08	-25.34
4.0	-24.62	-23.34	-24.26
4.5	-21.55	-21.18	-21.69
5.0	-16.50	-15.17	-16.17
5.5	-9.41	-8.56	-9.06
6.0	-0.18	-1.85	-0.38

Table A.16 The distribution of moments M_x in the x-direction, for different number of nodes with applied column stiffness in FEM-Design. The column width b_c = 0.2 m is applied at 1 node and as 8 fictious columns, see Figur 2.23.

Distance, x [m]	FD, Model 6 1 node, L_{el} = 0.5 m	FD, Model 22 1 node, Auto mesh	FD, Model 25 8 nodes, Sparse mesh
0.0	141.99	99.91	86.99
0.2	96.30	75.58	85.40
0.5	27.76	38.94	42.65
1.0	9.01	11.19	9.54
1.5	-5.73	-0.09	-2.43
2.0	-15.23	-9.36	-12.92
2.5	-21.16	-17.32	-20.76
3.0	-24.41	-21.98	-23.64
3.5	-25.42	-22.70	-25.09
4.0	-24.38	-23.07	-23.64
4.5	-21.37	-21.41	-20.88
5.0	-16.39	-15.06	-16.26
5.5	-9.36	-8.52	-8.60
6.0	-0.18	-1.87	-0.93

Table A.17 The distribution of moments M_x in the x-direction, for different number of nodes with applied column stiffness in FEM-Design. The column width b_c = 0.4 m, see Figur 2.24.

Distance, x [m]	FD, Model 7 1 node, L_{el} = 0.5 m	FD, Model 23 1 node, Auto mesh	FD, Model 26 8 nodes, Sparse mesh
0.0	142.70	100.43	68.28
0.3	73.02	63.82	64.88
0.5	28.07	39.28	46.69
1.0	9.24	11.42	14.35
1.5	-5.56	0.10	-2.18
2.0	-15.09	-9.21	-11.18
2.5	-21.05	-17.20	-18.67
3.0	-24.33	-21.89	-22.03
3.5	-25.36	-22.63	-24.10
4.0	-24.34	-23.02	-22.49
4.5	-21.34	-21.38	-20.57
5.0	-16.37	-15.04	-15.12
5.5	-9.35	-8.51	-8.22
6.0	-0.18	-1.87	-1.14

Table A.18 The distribution of moments M_x in the x-direction, for different number of nodes with applied column stiffness in FEM-Design. The column width b_c = 0.6 m, see Figur 2.25.

Appendix B

B Comparison of yield line pattern and crack propagation

This appendix shows the crack propagation in the model from ABAQUS/Explicit and FEM-Design. From the intervals 15-30 in ABAQUS/Explicit the loads are applied to the model in FEM-Design, see *Chapter* 3.

B.1 Results from FE-analysis

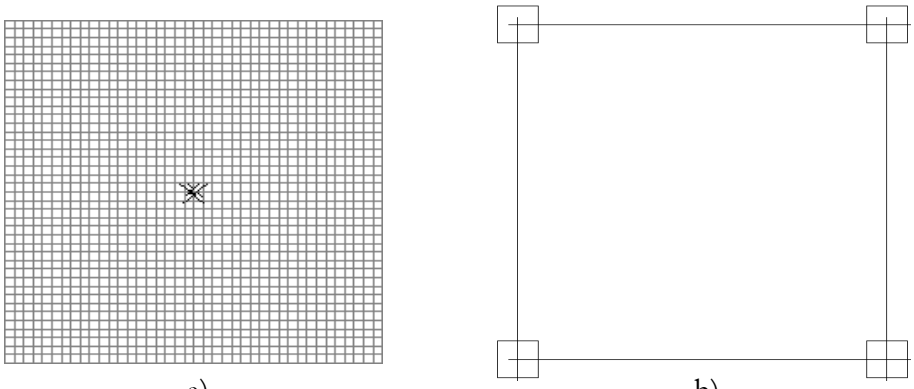

Figure B.1 Cracks in the slab subjected to the concentrated load 1.50 kN in a) ABAQUS at deflection 0.227 mm and b) FEM-Design at deflection 0.197 mm.

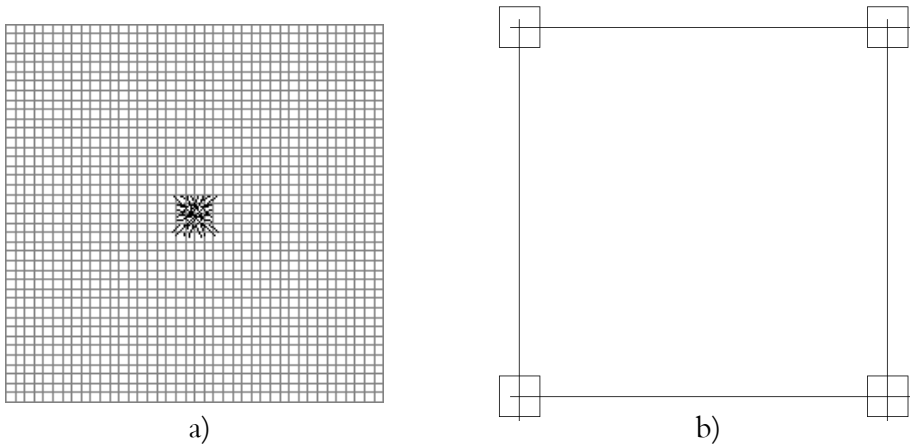

Figure B.2 *Cracks in the slab subjected to the concentrated load 1.68 kN in a) ABAQUS at deflection 0.258 mm and b) FEM-Design at deflection 0.221 mm.*

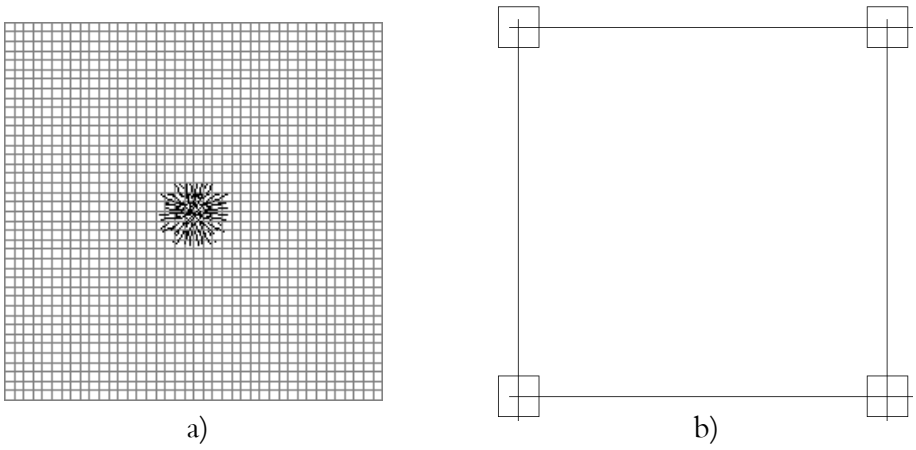

Figure B.3 *Cracks in the slab subjected to the concentrated load 1.91 kN in a) ABAQUS at deflection 0.291 mm and b) FEM-Design at deflection 0.251 mm.*

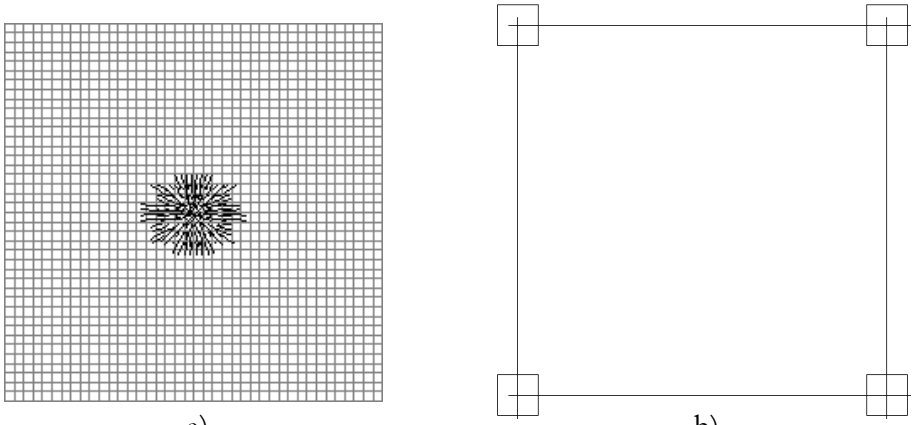

Figure B.4 Cracks in the slab subjected to the concentrated load 2.15 kN in a) ABAQUS at deflection 0.327 mm and b) FEM-Design at deflection 0.285 mm.

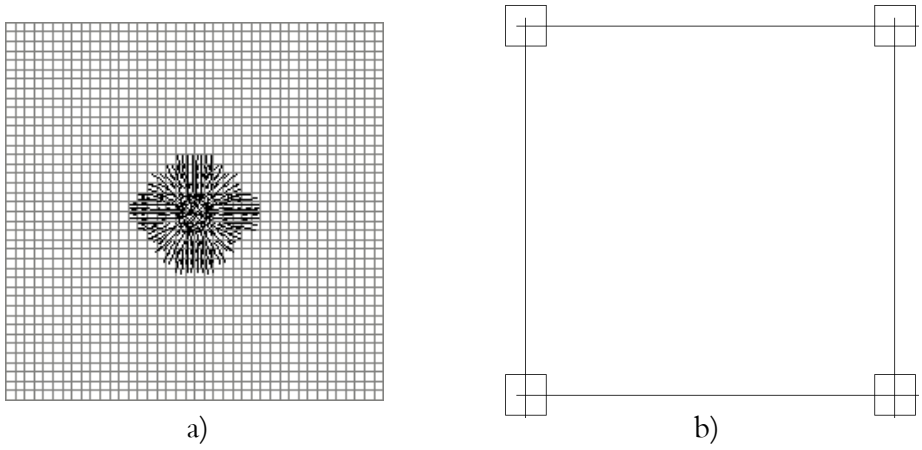

Figure B.5 Cracks in the slab subjected to the concentrated load 2.37 kN in a) ABAQUS at deflection 0.364 mm and b) FEM-Design at deflection 0.315 mm.

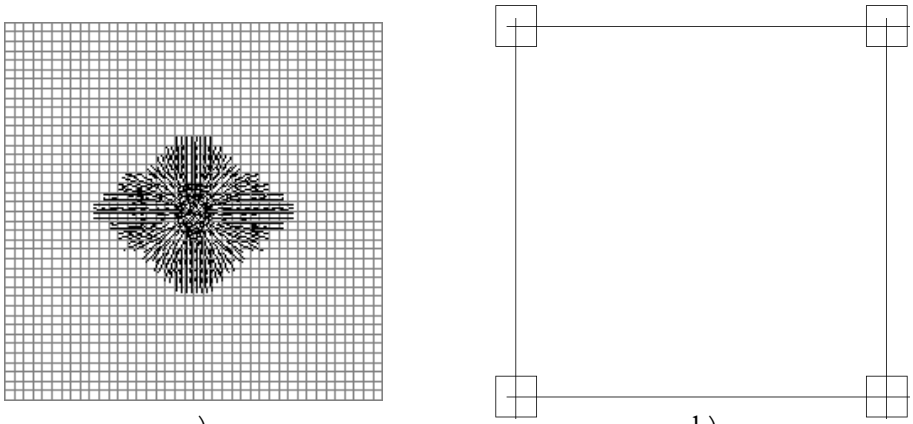

Figure B.6 *Cracks in the slab subjected to the concentrated load 2.62 kN in a) ABAQUS at deflection 0.403 mm and b) FEM-Design at deflection 0.355 mm.*

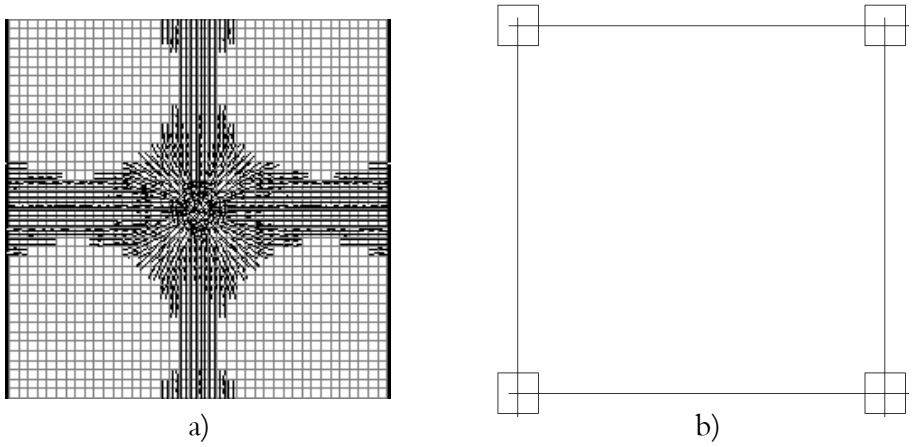

Figure B.7 *Cracks in the slab subjected to the concentrated load 2.88 kN in a) ABAQUS at deflection 0.445 mm and b) FEM-Design at deflection 0.396 mm.*

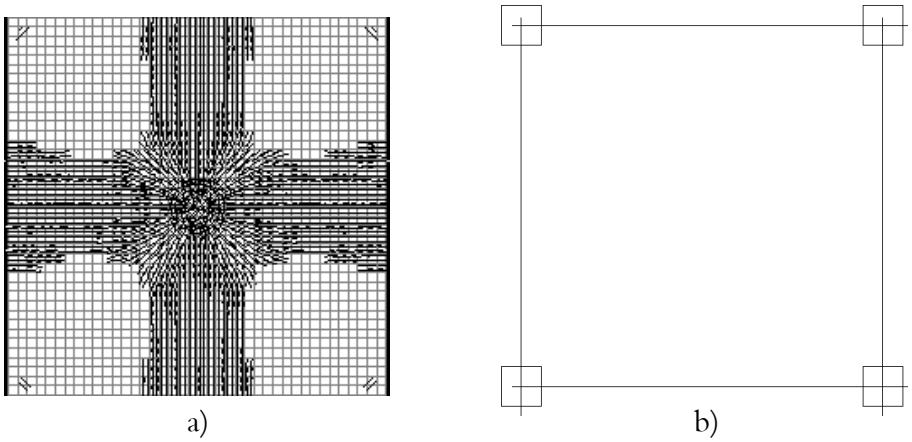

Figure B.8 *Cracks in the slab subjected to the concentrated load 3.10 kN in a) ABAQUS at deflection 0.488 mm and b) FEM-Design at deflection 0.432 mm.*

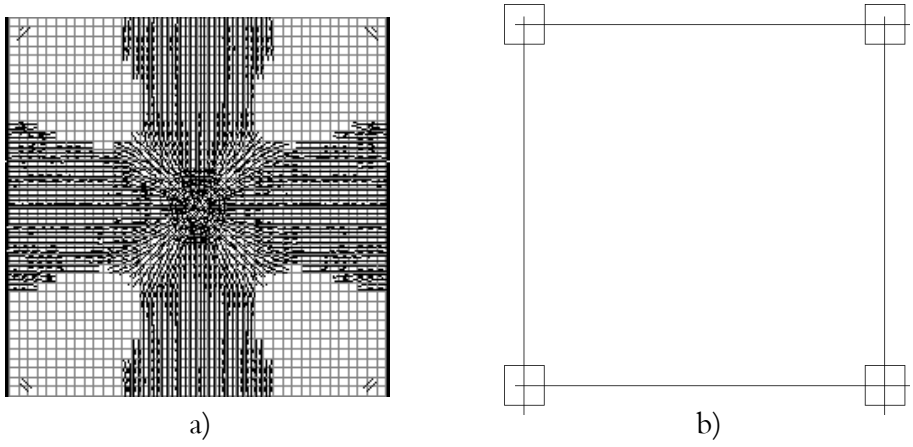

Figure B.9 *Cracks in the slab subjected to the concentrated load 3.32 kN in a) ABAQUS at deflection 0.533 mm and b) FEM-Design at deflection 0.478 mm.*

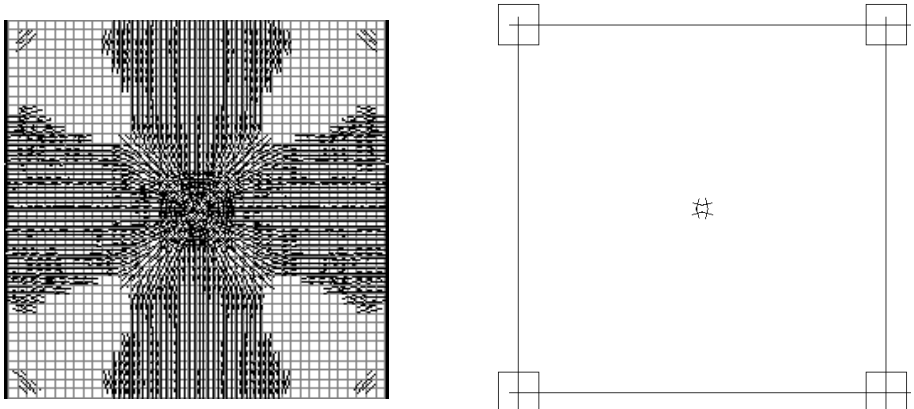

Figure B.10 Cracks in the slab subjected to the concentrated load 3.58 kN in a) ABAQUS at deflection 0.581 mm and b) FEM-Design at deflection 0.531 mm.

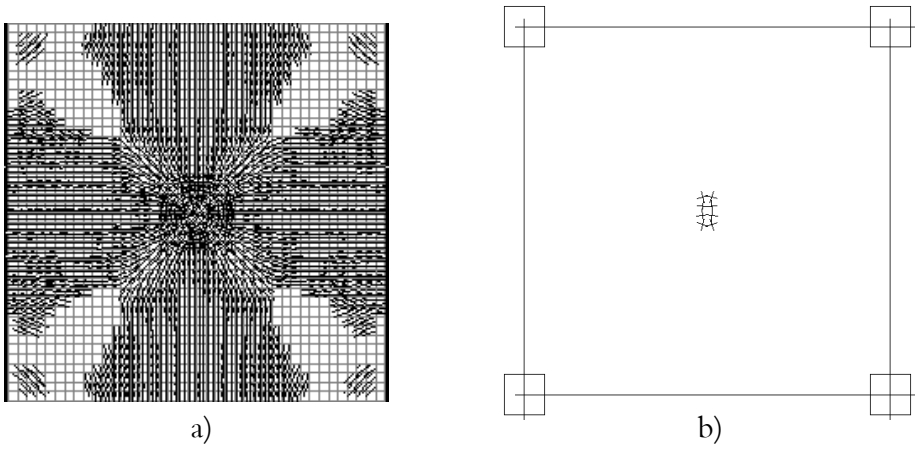

Figure B.11 Cracks in the slab subjected to the concentrated load 3.81 kN in a) ABAQUS at deflection 0.630 mm and b) FEM-Design at deflection 0.609 mm.

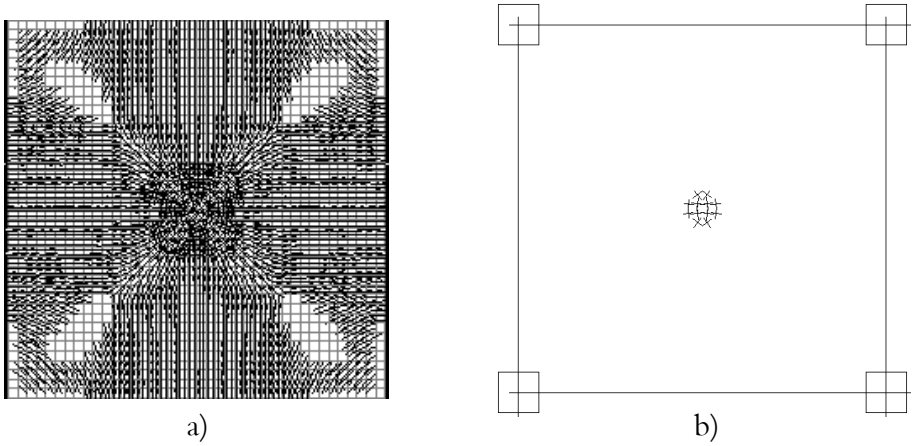

a) b)

Figure B.12 Cracks in the slab subjected to the concentrated load 4.03 kN in a) ABAQUS at deflection 0.682 mm and b) FEM-Design at deflection 0.678 mm.

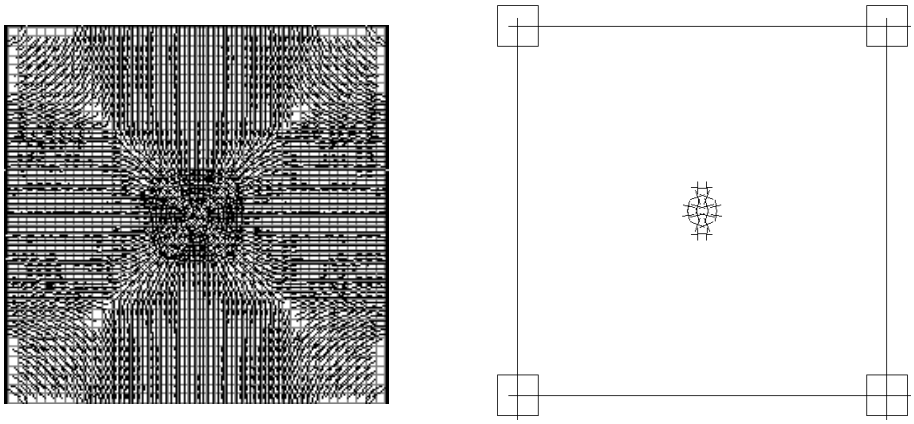

a) b)

Figure B.13 Cracks in the slab subjected to the concentrated load 4.26 kN in a) ABAQUS at deflection 0.735 mm and b) FEM-Design at deflection 0.743 mm.

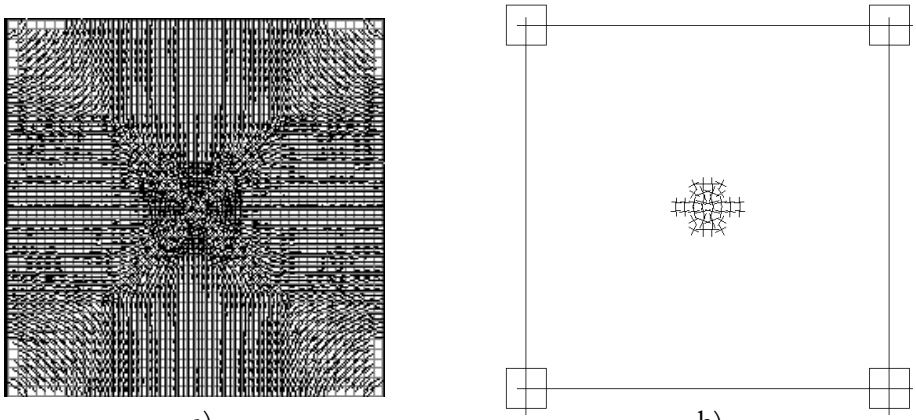

Figure B.14 Cracks in the slab subjected to the concentrated load 4.50 kN in a) ABAQUS at deflection 0.791 mm and b) FEM-Design at deflection 0.811 mm.

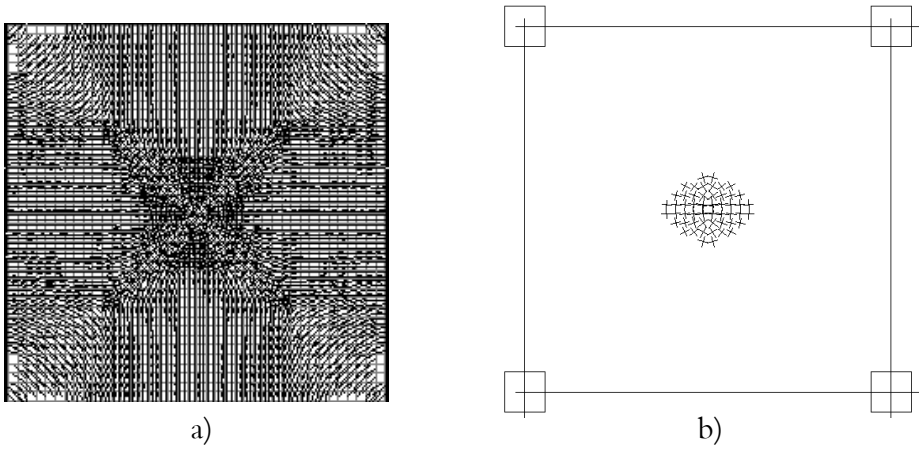

Figure B.15 Cracks in the slab subjected to the concentrated load 4.68 kN in a) ABAQUS at deflection 0.848 mm and b) FEM-Design at deflection 0.878 mm.

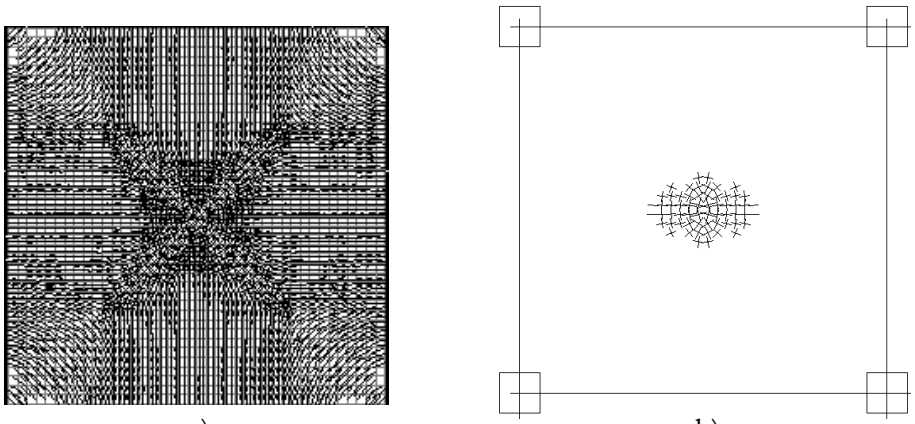

Figure B.16 Cracks in the slab subjected to the concentrated load 4.68 kN in a) ABAQUS at deflection 0.848 mm and b) FEM-Design at deflection 0.878 mm.

Appendix C

C Design method for reinforcement

The method is based on conclusions made mainly in *Chapter* 5. The method is established and optimised with respect to the capabilities of FEM-Design, but the part of the redistribution of the reinforcement can be used at designs by any design program that is based on FE-theory and have the same capabilities in consideration of required reinforcement areas, cracks and punching.

The method consists of the steps

1. Definition of the slab's geometry and material characteristics both for the concrete and the reinforcement, see *FEM-Design's plate manual.*
2. Definition of the column as an interior, an edge or a corner column with respect to punching, see *FEM-Design's plate manual.*
3. Calculations of the slab *without* considering applied reinforcement and cracking, see *FEM-Design's plate manual.*
   a) *Determination of the required top and bottom reinforcement areas and its distribution distances, see the following sections and example in Section* 5.6.3:
      - Top reinforcement in the column and the middle strips determines *without* considering cracking.
      - Bottom reinforcement in the field and the edge strips determines *without* considering cracking.
4. Applying of the determined reinforcement in intended strips, see example in *Section* 5.6.3.

5. Calculations of the slab *with* consideration of applied reinforcement, but *without* consideration of cracking, see *FEM-Design's plate manual*.

   a) Check for missing reinforcement, see example in Section 5.6.4*:*

   - Indicates if any of the required reinforcement areas are forgotten in the structure.

   b) Control of the shear capacity, see example in Section 5.6.4*:*

   - *Zero* values of the shear means that the capacity is large enough.

   c) Control of the punching capacity, see example in Section 5.6.4*:*

   - A *green* marked column means that the punching capacity is large enough.
   - A *red* marked column means that the punching capacity is not large enough. One of the following actions have to take place:
     1. Increasing of the plate thickness or/and the quality of the concrete.
     2. Applying of a beam (possible in FEM-Design) or a column head or/and a strengthening plate (not possible yet) between the bottom surface of the plate and the column top.
     3. Increasing of the top reinforcement in the column strip.

     Observe that 1-3 demand consideration of the plate's application and the workability at the concreting contra the additionally financial costs.
   - A *yellow* marked column means that the punching capacity is large enough if the displayed quantity of shear reinforcement is applied at the reinforcing.

6. Calculations of the slab with consideration of applied reinforcement and cracking, see *FEM-Design's plate manual*.

   a) Control of the crack widths, see example in Section 5.6.5*:*

   - If needed, increase areas of reinforcement in necessary strips or the plate thickness or/and the quality of the concrete.

   b) Control of deformations, see example in Section 5.6.5*:*

   - If needed, increase areas of reinforcement or the plate thickness or/and the quality of the concrete.

Remark that eventually anchor and joint lengths have to be added to the calculated lengths.

C.1 Geometry

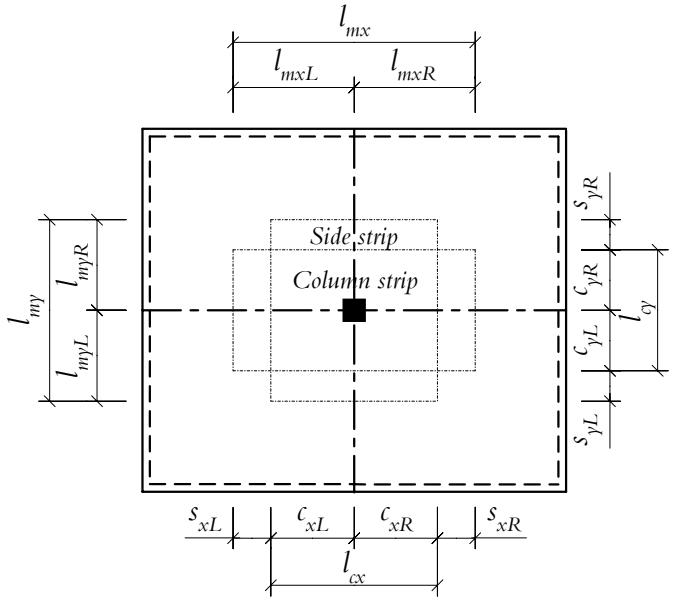

Figure C.1 Strips and distribution distances for the top reinforcement.

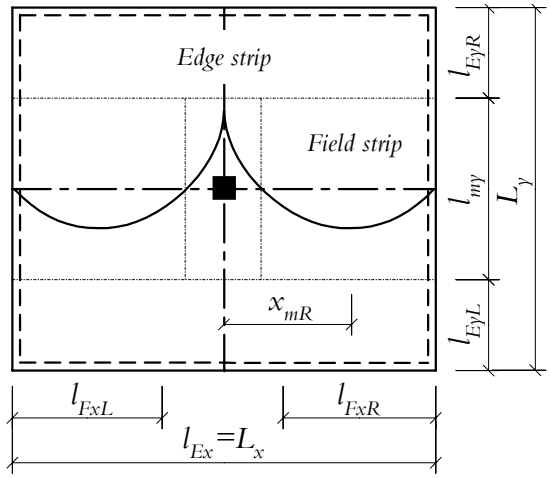

Figure C.2 Strips and distribution distances for the bottom reinforcement.

C.2 Determination of the distances and the reinforcement areas

C.2.1 Top reinforcement

The required top reinforcement A_{sxs} displays in x-direction without considering cracks, see *Figure* C.3, the distances c_{xR}, c_{xL} measures and

$$l_{cx} = c_{xL} + c_{xR} \qquad \text{C.1}$$

measures or calculates.

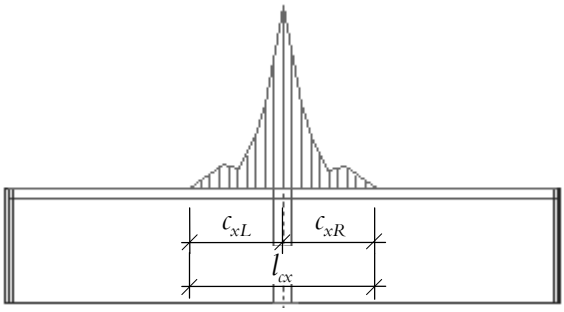

Figure C.3 The distances of the longitudinally distribution of the top reinforcement A_{sxs} in the column strips.

The required top reinforcement A_{sys} displays in y-direction, see *Figure* C.4, the distances c_{yR}, c_{yL} measures and

$$l_{cy} = c_{yL} + c_{yR} \qquad \text{C.2}$$

measures or calculates.

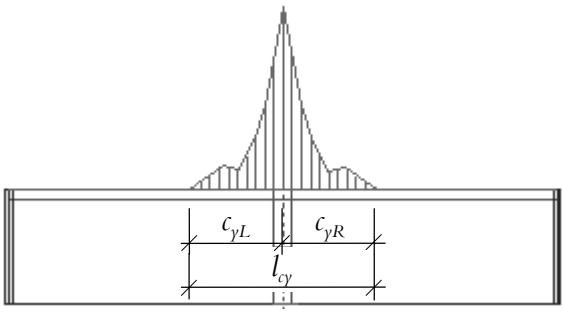

Figure C.4 The distances of the longitudinally distribution of the top reinforcement A_{sys} in the column strips.

The required top reinforcement A_{sxs} displays in y-direction with the option step equal to the distances $c_{yL} - b_c/2$ and $c_{yR} - b_c/2$, respectively, see *Figure* C.5. The distances l_{myL}, l_{myR} measures and

$$s_{yL} = l_{myL} - c_{yL} \qquad \text{C.3}$$

$$s_{yR} = l_{myR} - c_{yR} \qquad \text{C.4}$$

$$l_{my} = l_{myL} + l_{myR} \qquad \text{C.5}$$

measures or calculates.
The reinforcement quantities and the longitudinal and lateral distribution determine according to *Table* C.1.

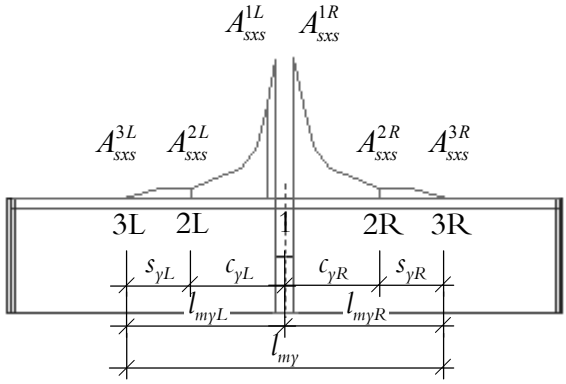

Figure C.5 The distances of the laterally distribution and the quantities of the top reinforcement A_{sxs} in the column and the side strips.

The required top reinforcement A_{sys} displays in x-direction with the option step equal to $c_{xL} - b_c/2$ and $c_{xR} - b_c/2$, respectively, see *Figure* C.6. The distances l_{mxL}, l_{mxR}, measures and

$$s_{xL} = l_{mxL} - c_{xL} \qquad \text{C.6}$$

$$s_{xR} = l_{mxR} - c_{xR} \qquad \text{C.7}$$

$$l_{mx} = l_{mxL} + l_{mxR} \qquad \text{C.8}$$

measures or calculates.

The reinforcement quantities in x-direction and the longitudinal and lateral distribution determine according to *Table* C.2.

Load or slab geometry	**Strip**	**Required top reinforcement**	**Longitudinal and lateral distribution**
Asymmetrical in y-direction	Left column	$A_{sxs}^{cL} = \frac{A_{sxs}^{1L} + A_{sxs}^{2L}}{2}$	$l_{cx} \times c_{yL}$
	Right column	$A_{sxs}^{cR} = \frac{A_{sxs}^{1R} + A_{sxs}^{2R}}{2}$	$l_{cx} \times c_{yR}$
Symmetrical	Column	$A_{sxs}^{c} = \frac{A_{sxs}^{1L} + A_{sxs}^{2L} + A_{sxs}^{1R} + A_{sxs}^{2R}}{4}$	$l_{cx} \times l_{cy}$
Symmetrical and asymmetrical	Left side	$A_{sxs}^{sL} = \frac{A_{sxs}^{2L} + A_{sxs}^{3L}}{2}$	$l_{cx} \times s_{yL}$
	Right side	$A_{sxs}^{sR} = \frac{A_{sxs}^{2R} + A_{sxs}^{3R}}{2}$	$l_{cx} \times s_{yR}$

Table C.1 The top reinforcement quantities in x-direction and its distribution depending on the load distribution and slab geometry.

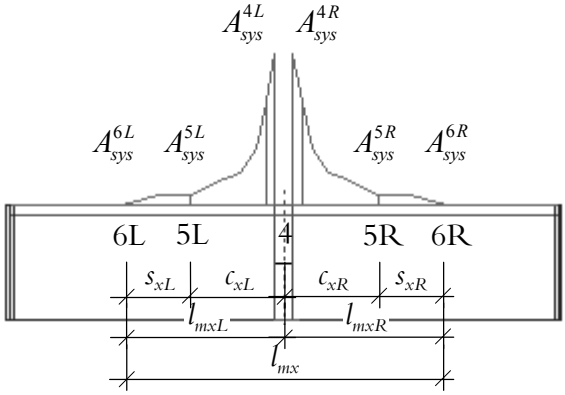

Figure C.6 The distances of the laterally distribution and the quantities of the top reinforcement A_{sys} in the column and the side strips.

Load or slab geometry	Strip	Required top reinforcement	Longitudinal and lateral distribution
Asymmetrical in x-direction	Left column	$A_{sys}^{cL} = \frac{A_{sys}^{4L} + A_{sys}^{5L}}{2}$	$l_{cy} \times c_{xL}$
	Right column	$A_{sys}^{cR} = \frac{A_{sys}^{4R} + A_{sys}^{5R}}{2}$	$l_{cy} \times c_{xR}$
Symmetrical	Column	$A_{sys}^{c} = \frac{A_{sys}^{4L} + A_{sys}^{5L} + A_{sys}^{4R} + A_{sys}^{5R}}{4}$	$l_{cy} \times l_{cx}$
Symmetrical and asymmetrical	Left side	$A_{sys}^{sL} = \frac{A_{sys}^{5L} + A_{sys}^{6L}}{2}$	$l_{cy} \times s_{xL}$
	Right side	$A_{sys}^{sR} = \frac{A_{sys}^{5R} + A_{sys}^{6R}}{2}$	$l_{cy} \times s_{xR}$

Table C.2 The top reinforcement quantities in y-direction and its distribution depending on the load distribution and slab geometry.

C.2.2 Bottom reinforcement

The required bottom reinforcement A_{sxf} in x-direction displays, see *Figure* C.7, and the distances x_{mL}, x_{mR}, l_{FxL} and l_{FxR} measures.

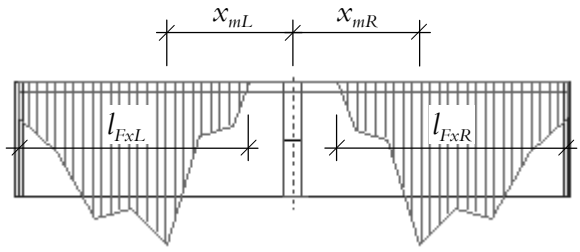

Figure C.7 The distances to the maximum required bottom reinforcement and the distances of the longitudinal distribution of A_{sxf} in the field strips.

A help line in y-direction draws at the distances x_{mL}, x_{mR} and the required bottom reinforcement A_{sxf} displays in y-direction with the option step equal to l_{myL} and l_{myR}, respectively, see *Figure* C.8, and

$$l_{EyL} = L_{yL} - l_{myL} \qquad \text{C.9}$$

$$l_{EyR} = L_{yR} - l_{myR} \qquad \text{C.10}$$

measures or calculates.

The reinforcement quantities in x-direction and the longitudinal and lateral distribution determine according to *Table* C.3. If not symmetry exists between the *left* and *right strips* in x-direction according to *Figure* C.7 the procedure is repeated which means that the bottom reinforcements in the edge strips are jointed across the column centre line in y-direction. If it should become just a small difference between the two strips the same quantity is applied in both strips. Generally, the required reinforcement quantities for the edge strips will become equal to the minimum reinforcement.

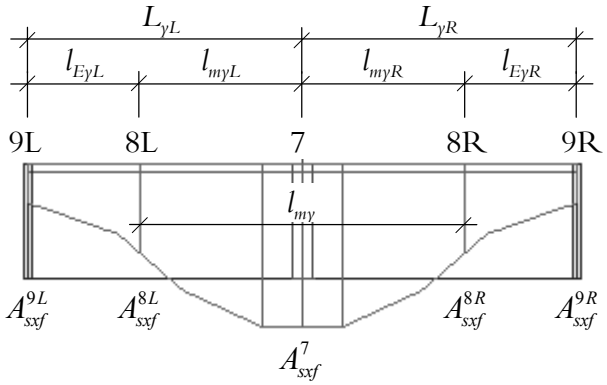

Figure C.8 The distances of the laterally distribution and the quantities of the bottom reinforcement A_{sxf} in the field and the edge strips.

The required bottom reinforcement A_{syf} displays in y-direction, see *Figure* C.9, and the distances γ_{mL}, γ_{mR}, l_{FyL} and l_{FyR} measures.

A help line in x-direction draws and the required bottom reinforcement A_{syf} displays in x-direction with the option step equal to l_{mxL} and l_{mxR}, respectively, see *Figure* C.10, and

$$l_{ExL} = L_{xL} - l_{mxL} \qquad \text{C.11}$$

$$l_{ExR} = L_{xR} - l_{mxR} \qquad \text{C.12}$$

measures or calculates.

Load or slab geometry	**Strip**	**Required bottom reinforcement**	**Longitudinal and lateral distribution**
Asymmetrical in y-direction and symmetrical in x-direction	Left field	$A_{sxf}^{FL} = \frac{A_{sxf}^{7} + A_{sxf}^{8L}}{2}$	$l_{FxL} = l_{FxR} \times l_{myL}$
	Right field	$A_{sxf}^{FR} = \frac{A_{sxf}^{7} + A_{sxf}^{8R}}{2}$	$l_{FxL} = l_{FxR} \times l_{myR}$
	Left edge	$A_{sxf}^{EL} = \frac{A_{sxf}^{8L} + A_{sxf}^{9L}}{2}$	$L_{xL} = L_{xR} \times l_{EyL}$
	Right edge	$A_{sxf}^{ER} = \frac{A_{sxf}^{8R} + A_{sxf}^{9R}}{2}$	$L_{xL} = L_{xR} \times l_{EyR}$
Asymmetrical in x-direction and symmetrical in y-direction	Left field	$A_{sxf}^{FL} = \frac{A_{sxf}^{7} + A_{sxf}^{8L}}{2}$	$l_{FxL} \neq l_{FxR} \times l_{myL}$
	Right field	$A_{sxf}^{FR} = \frac{A_{sxf}^{7} + A_{sxf}^{8R}}{2}$	$l_{FxL} \neq l_{FxR} \times l_{myR}$
	Left edge	$A_{sxf}^{EL} = \frac{A_{sxf}^{8L} + A_{sxf}^{9L}}{2}$	$L_{xL} \neq L_{xR} \times l_{EyL}$
	Right edge	$A_{sxf}^{ER} = \frac{A_{sxf}^{8R} + A_{sxf}^{9R}}{2}$	$L_{xL} \neq L_{xR} \times l_{EyR}$
Symmetrical in all directions	Field	$A_{sxf}^{F} = \frac{A_{sxf}^{8L} + A_{sxf}^{7} + A_{sxf}^{8R}}{3}$	$l_{FxL} = l_{FxR} \times l_{myL} = l_{myR}$
	Edge	$A_{sxf}^{E} = \frac{A_{sxf}^{8} + A_{sxf}^{9}}{2}$	$L_{xL} = L_{xR} \times l_{EyR} = l_{EyL}$

Table C.3 The bottom reinforcement quantities in x-direction and its distribution depending on the load distribution and slab geometry.

The reinforcement quantities in x-direction and the longitudinal and lateral distribution determine according to *Table* C.4. Like at the distribution of bottom reinforcement in x-direction the procedure is repeated if the *left* and *right strip* in y-direction according to *Figure* C.9 are non-symmetrically, which means that the bottom reinforcements in the *edge strips* are jointed across the column centre line in x-direction.

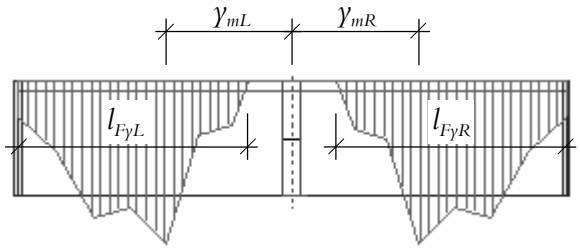

Figure C.9 *The distances to the maximum required bottom reinforcement and the distances of the longitudinal distribution of A_{syf} in the field strips.*

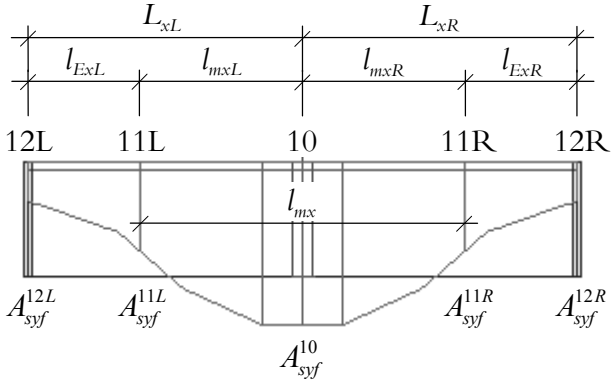

Figure C.10 *The distances of the laterally distribution and the quantities of the bottom reinforcement A_{syf} in the field and the edge strips.*

Load or slab geometry	**Strip**	**Required bottom reinforcement**	**Longitudinal and lateral distribution**
Asymmetrical in x-direction and symmetrical in y-direction	Left field	$A_{syf}^{FL} = \frac{A_{syf}^{10} + A_{syf}^{11L}}{2}$	$l_{FyL} = l_{FyR} \times l_{mxL}$
	Right field	$A_{syf}^{FR} = \frac{A_{syf}^{10} + A_{syf}^{11R}}{2}$	$l_{FyL} = l_{FyR} \times l_{mxR}$
	Left edge	$A_{syf}^{EL} = \frac{A_{syf}^{11L} + A_{syf}^{12L}}{2}$	$L_{yL} = L_{yR} \times l_{ExL}$
	Right edge	$A_{syf}^{ER} = \frac{A_{syf}^{11R} + A_{syf}^{12R}}{2}$	$L_{yL} = L_{yR} \times l_{ExR}$
Asymmetrical in y-direction and symmetrical in x-direction	Left field	$A_{syf}^{FL} = \frac{A_{syf}^{10} + A_{syf}^{11L}}{2}$	$l_{FyL} \neq l_{FyR} \times l_{mxL}$
	Right field	$A_{syf}^{FR} = \frac{A_{syf}^{10} + A_{syf}^{11R}}{2}$	$l_{FyL} \neq l_{FyR} \times l_{mxR}$
	Left edge	$A_{syf}^{EL} = \frac{A_{syf}^{11L} + A_{syf}^{12L}}{2}$	$L_{yL} \neq L_{yR} \times l_{ExL}$
	Right edge	$A_{syf}^{ER} = \frac{A_{syf}^{11R} + A_{syf}^{12R}}{2}$	$L_{yL} \neq L_{yR} \times l_{ExR}$
Symmetrical in all directions	Field	$A_{syf}^{F} = \frac{A_{syf}^{11L} + A_{syf}^{10} + A_{syf}^{11R}}{3}$	$l_{FyL} = l_{FyR} \times l_{mxL} = l_{mxR}$
	Edge	$A_{syf}^{E} = \frac{A_{syf}^{11} + A_{syf}^{12}}{2}$	$L_{yL} = L_{yR} \times l_{ExR} = l_{ExL}$

Table C.4 The bottom reinforcement quantities in y-direction and its distribution depending on the load distribution and slab geometry.